CALIFORNIA INSTITUTE OF TECHNOLOGY

EARTHQUAKE ENGINEERING RESEARCH LABORATORY

A STRAIN-SPACE PLASTICITY THEORY AND NUMERICAL IMPLEMENTATION

By

Paul Jerome Yoder

EERL 80-07

A Report on Research Conducted Under Grants
from the National Science Foundation

Pasadena, California
August, 1980

A STRAIN-SPACE PLASTICITY THEORY AND NUMERICAL IMPLEMENTATION

Thesis by

Paul Jerome Yoder

In Partial Fulfillment of the Requirements

for the Degree of

Doctor of Philosophy

California Institute of Technology

Pasadena, California

1981

(Submitted August 29, 1980)

ACKNOWLEDGEMENTS

I would like to express my sincere appreciation to Professor W. D. Iwan for providing guidance and unwavering encouragement throughout the course of this thesis project. Thanks are due also to Professor T.J.R. Hughes for making available his finite element programs and for offering advice on how to adapt them to this present investigation.

I am indebted, moreover, to Marty Cohen for the many times he put aside his own thesis work to help me ferret out errors from my computer programs, and Gloria Jackson deserves recognition for the fine job she did in typing a rather difficult manuscript.

This research was conducted under a grant from the National Science Foundation, whose financial support is hereby gratefully acknowledged.

ABSTRACT

This thesis sets forth an alternate version of plasticity which closely parallels the traditional theory but interchanges the roles of stress and strain. As a result, the new formulation gives stress as a functional of strain, rather than the reverse, and is thus attuned to the needs of the dynamicist.

In the case of a single loading surface, the two versions of plasticity are shown to be equivalent when the model parameters are appropriately selected. A similar though less satisfying result is obtained for formulations involving a plurality of loading surfaces.

The strain-space formulation is coded for numerical solution, with provision for a variable number of loading surfaces. The numerical algorithm is tested for accuracy in the handling of perfect plasticity, and the results are compared with those given by three commonly-used stress-space algorithms. The new algorithm is then interfaced with a finite element code and used to study the response of a foundation resting on an elastoplastic half-space.

TABLE OF CONTENTS

TABLE OF CONTENTS (CONTINUED)

TABLE OF CONTENTS (CONTINUED)

CHAPTER I

INTRODUCTION

Many materials respond elastically when loaded up to a certain level and then start to accumulate additional, permanent deformations as further loads are applied. Within the elastic regime, the strain depends linearly upon the applied stress and disappears completely when this stress is removed. However, when the stress exceeds the elastic limit, internal slipping occurs within the material, and as a result some of the induced deformation lingers even after the loads are taken away. This latter type of response is described by the theory of plasticity.

Originally patterned after the behavior of lead, the concept of plasticity was soon applied to other metals including steel. More recently it has been adapted to describe soils, albeit with somewhat less success. The model may also be applied to civil engineering structures, such as buildings and bridges, to describe their response to severe loads.

In any of these applications, the role of plasticity theory is to provide a mathematical model for the relationship between stress and strain. There is, of course, a vast gulf between developing a stress-strain law on the one hand and designing a die to stamp out automobile fenders on the other. To put the theory of plasticity to practical use, one has to be able to solve boundary-value problems involving elasto-plastic media. If the boundary conditions are fairly simple and the

stress-strain law is manageable, an analytical solution may be possible. Otherwise one resorts to numerical techniques.

The usual approach to solving dynamics problems analytically is to let the displacements be the independent variables of the problem. Toward this end, one eliminates stress from the equation of motion in favor of strain and then expresses strain in terms of displacement, as indicated in Figure 1.1. Similar manipulations are carried out, if need be, upon the boundary conditions. A solution may then be sought by any of the standard techniques, such as separation of variables or integral transforms. Out of this brief discussion emerges one significant point concerning the stress-strain law: A displacement formulation will be possible only if stress is expressible as a functional of strain.

$$\sigma_{ji,j} + b_i = \rho \ddot{u}_i \qquad \text{Cauchy's equation of motion}$$

$$\underset{\sim}{\sigma} = \underset{\sim}{\underset{\sim}{F}}\{\underset{\sim}{\varepsilon}\} \qquad \text{constitutive law}$$

$$\underset{\sim}{\varepsilon} = \frac{1}{2}\left[\Delta \underset{\sim}{u} + (\Delta \underset{\sim}{u})^T\right] \qquad \text{strain-displacement relation}$$

Figure 1.1 The displacement formulation of a continuum dynamics problem.

- From the displacement $\underset{\sim}{d}_n$, $\Delta \underset{\sim}{d}_n$, compute the strain $\underset{\sim}{\varepsilon}_n$, $\Delta \underset{\sim}{\varepsilon}_n$.
- Calculate the stress increment corresponding to $\Delta \underset{\sim}{\varepsilon}_n$, and find the new stress $\underset{\sim}{\sigma}_n$.
- Invoke Newton's second law to find the new displacement increment $\Delta \underset{\sim}{d}_{n+1}$.
- Start again from the top for the next time step.

Figure 1.2 A typical explicit algorithm for the dynamics of a continuous medium.

Numerical techniques for continuum dynamics are not quite so demanding in this respect, but nevertheless they simplify considerably when stress can be represented as a functional of strain. To illustrate the point, Figure 1.2 outlines a typical explicit algorithm, so called because the displacement increments are found directly — or explicitly — from Newton's second law. Observe that for each time step the strain increment is obtained first, and then the stress is updated accordingly. It will obviously be helpful in this case to have an analytical expression for stress in terms of strain and strain history. A similar conclusion holds for implicit algorithms, which construct a global stiffness based upon the current strain and then solve a matrix equation involving this stiffness to obtain the displacement increments. The process of forming the stiffness begins on the local level, and it is at this stage that the constitutive law enters in. So long as the law gives stress as a functional of strain, the required local stiffness can readily be extracted.

Plasticity, however, has traditionally been formulated in just the opposite manner. The classical theory treats the current stress and stress increment as independent variables and based on these computes the corresponding strain increment. From the standpoint of numerical implementation, this poses two difficulties. First, the material response at any given instant depends upon the very quantities one is trying to solve for. Thus, Joyner [1] uses at each stage of the calculation the stress data from the preceding time step. Others, including Hughes and Prévost [2] and Kalev and Gluck [3], estimate the

current stress increment on the basis of the previous elastoplastic stiffness. Either way, the estimated response will be considerably in error for those parts of the domain which have just turned plastic or just reverted to elastic behavior. Moreover, both approaches entail additional storage, and both require that all the stresses be computed whether or not they are of physical interest.

A second difficulty arises from the fact that conventional plasticity gives the response in terms of a compliance instead of a stiffness. Thus, after deciding whether the behavior is to be elastic or plastic, one still has to invert a matrix in order to find the stress increments corresponding to the given strain increments. Joyner's approach is to use Gaussian elimination, while Prévost [4] opts for an analytical inversion.

Looking beyond considerations of accuracy and computational efficiency, the procedures described above possess a more basic defect. They are piecemeal in nature and tend to obscure the essential simplicity of the theory of plasticity. It is easier conceptually to make a fresh start and seek out directly a law expressing stress as a functional of strain. Such a law comes about naturally if one develops plasticity theory with reference to strain space instead of stress space.

The traditional version of plasticity divides stress space into two regions separated by a yield surface. So long as the stress lies inside the yield surface, incremental deformations proceed elastically. The additional strains characteristic of plastic slip arise whenever the stress state lies instantaneously on the surface and, in addition, the stress

increment is directed outward from it. In this event, when loading is said to occur, the surface moves out to meet the new stress state. All of these ideas can readily be carried over to strain space, as shown in Chapter II. The result is a constitutive law expressing stress as a functional of strain, rather than the reverse.

The current interest in multilinear plasticity lends added significance to the strain-space formulation. Whereas traditional plasticity allows for only a bilinear stress-strain curve, a more general, multilinear response is obtained by introducing a plurality of yield surfaces. Iwan [5] reached this conclusion after studying the multilinear one-dimensional models of Figure 1.3. He noted in particular that the series-parallel model generalizes readily to the continuum case because it resembles traditional plasticity in one key respect: It gives strain as a functional of stress. Each spring-and-slider assembly carries the full stress and contributes independently to the inelastic strain. Thus, the series-parallel model leads to a stress-space formulation featuring several yield surfaces. By simply including a plurality of surfaces, one obtains a much more versatile constitutive law.

However, the difficulties associated with stress-space plasticity become even more vexing in the multilinear case. Suppose that the last available stress state happens to lie at the intersection of m yield surfaces. Then, without knowing the stress increment, it is impossible to say which of these surfaces are active and which are inactive. There are 2^m cases in all, and each gives a different candidate for the elasto-plastic stiffness. The only way to proceed is by trial and error. For each stiffness one would have to compute the corresponding stress

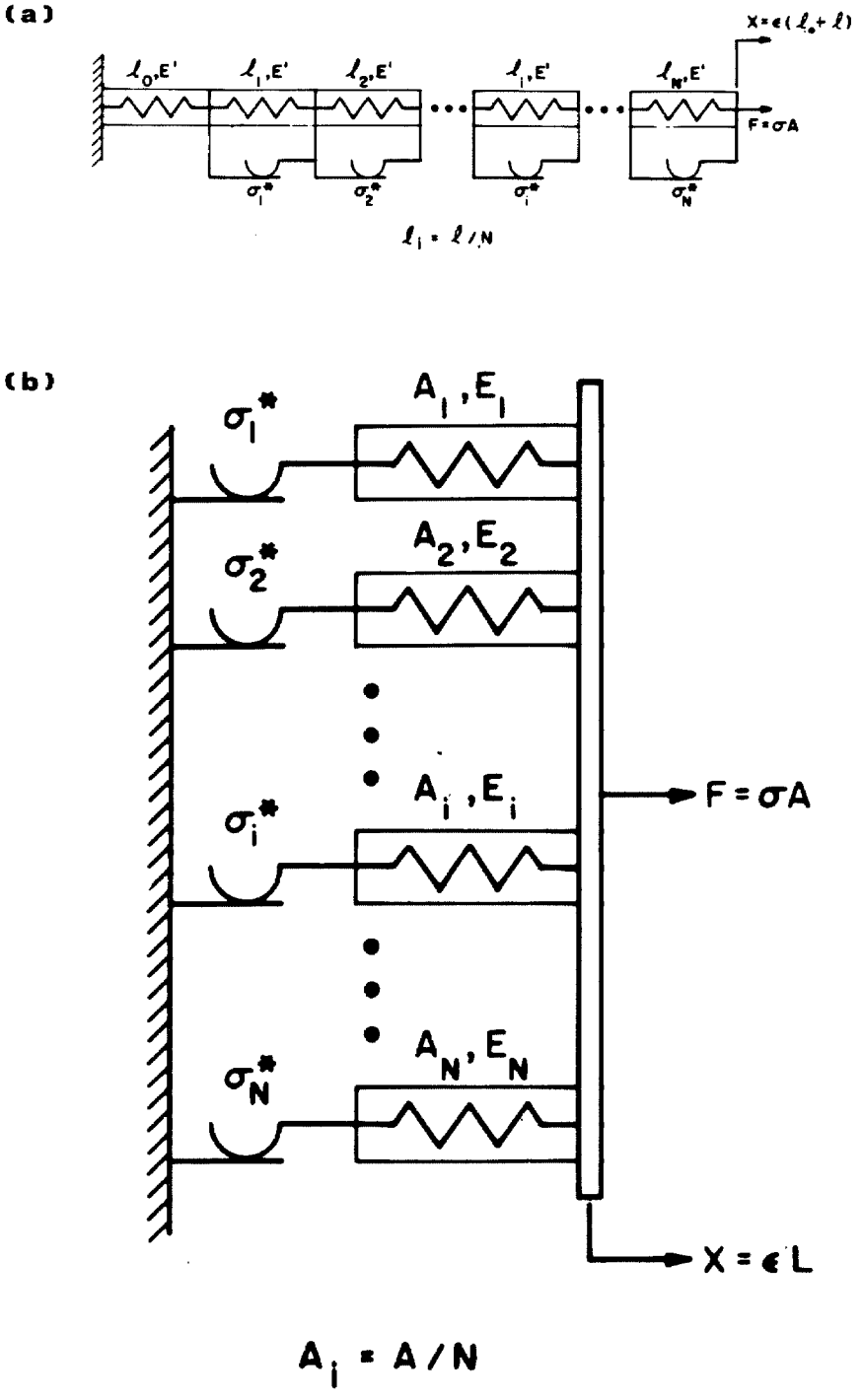

Figure 1.3 (a) The series-parallel model.
(b) The parallel-series model.

increment and then invoke the loading criteria to see whether the surfaces which were assumed to be active actually were. There could conceivably be several "correct" answers in some instances, or perhaps none at all. It is little wonder that Mróz [6] and Prevost [4] sidestep the issue by forcing the surfaces to nest tangentially whenever they intersect. This assures that if one surface is active, they will all be active. The number of possible cases is cut from 2^m to just 2. In the process, Mroz and Prevost abandon Prager's kinematic hardening law, which specifies that a surface translate in the direction of its normal at the point of loading. In its place they introduce a new law which involves not only the position of the surface being loaded, but also that of next surface out from it. One side effect of this change is to complicate the algebra.

An alternative set forth in this thesis, which avoids the inversion problem altogether, is to use strain-space surfaces. In this way one can construct a three-dimensional analog to the parallel-series model. In contrast to the series-parallel model considered earlier, each spring-and-slider pair in this case undergoes the full strain, and each contributes independently to the stress. This suggests a version of plasticity with multiple, strain-space surfaces. Interestingly enough, Drucker remarked about this possibility as early as 1950 [7]. He did not, however, work out the details of a strain-space formulation.

Other investigators have approached plasticity from a strain-space perspective. Lenskii [8] developed a model for permanently deforming media, which has since been applied to soils [9]. The model avoids

the use of yield surfaces, though, and bears little resemblance to traditional plasticity. In work much more akin to this thesis, Naghdi [10,11] showed that many of the familiar features of stress-space plasticity can be carried over to strain space. Naghdi did not, however, establish equivalence between stress- and strain-space loading criteria. Equally important, he did not pursue the possibility of expressing stress as a functional of strain.

Accordingly, Chapter II deals anew with the constitutive models discussed by Naghdi. Borrowing heavily from traditional derivations, the chapter develops in detail a version of plasticity which involves one yield surface in strain space. This analysis leads to an equation giving the stress increment as a function of the strain and strain increment. The chapter closes with a proof that for bilinear plasticity, the stress- and strain-space versions can be made equivalent.

Chapter III discusses multiple-surface models in a similar vein. The most straightforward approach is to let the loading surfaces behave independently of one another. Unfortunately, the stress- and strain-space models obtained in this way cannot be made equivalent to each other. To establish equivalence, one must allow for a bizarre sort of coupling between the surfaces in each model. This leads to analytical problems, which are discussed at some length. The chapter closes with an equivalence theorem for the multilinear case.

Chapter IV reports on a numerical implementation of strain-space plasticity. The coded algorithm is first examined to see how accurately it handles the case of perfect plasticity. Then it is interfaced with a

finite element program and used to study the response of a two-dimensional foundation on an elastoplastic half-space.

CHAPTER II

BILINEAR ELASTOPLASTIC MODELS

In the traditional formulation of plasticity stress plays the leading role. Both stress and strain enter into the formulation, but the stress state determines when yielding will occur and also governs the direction of plastic flow. The stresses act as independent variables; the strains, as dependent.

These roles can, however, be reversed. In Section 2.1 a version of plasticity is developed which views the strains as independent variables. The chapter also presents a proof that this strain-space formulation can be made equivalent to the traditional one in stress space.

2.1 A Strain-Space Formulation of Plasticity

2.1.1 Motivation

To appreciate the underlying difference between a strain-space and stress-space plasticity formulation, consider a simple, one-dimensional example. Let the mechanical response of the system considered be bilinear, as suggested by the stress-strain diagram of Figure 2.1(a). The steeper parts of the diagram are said to exhibit incrementally elastic behavior; the rest, plastic. To characterize the response mathematically, one must delineate at each stage along the curve (i) a criterion for determining whether the next increment will be elastic or plastic; and (ii) a scheme for relating the stress and strain to one another once the nonlinear effects have begun to accumulate.

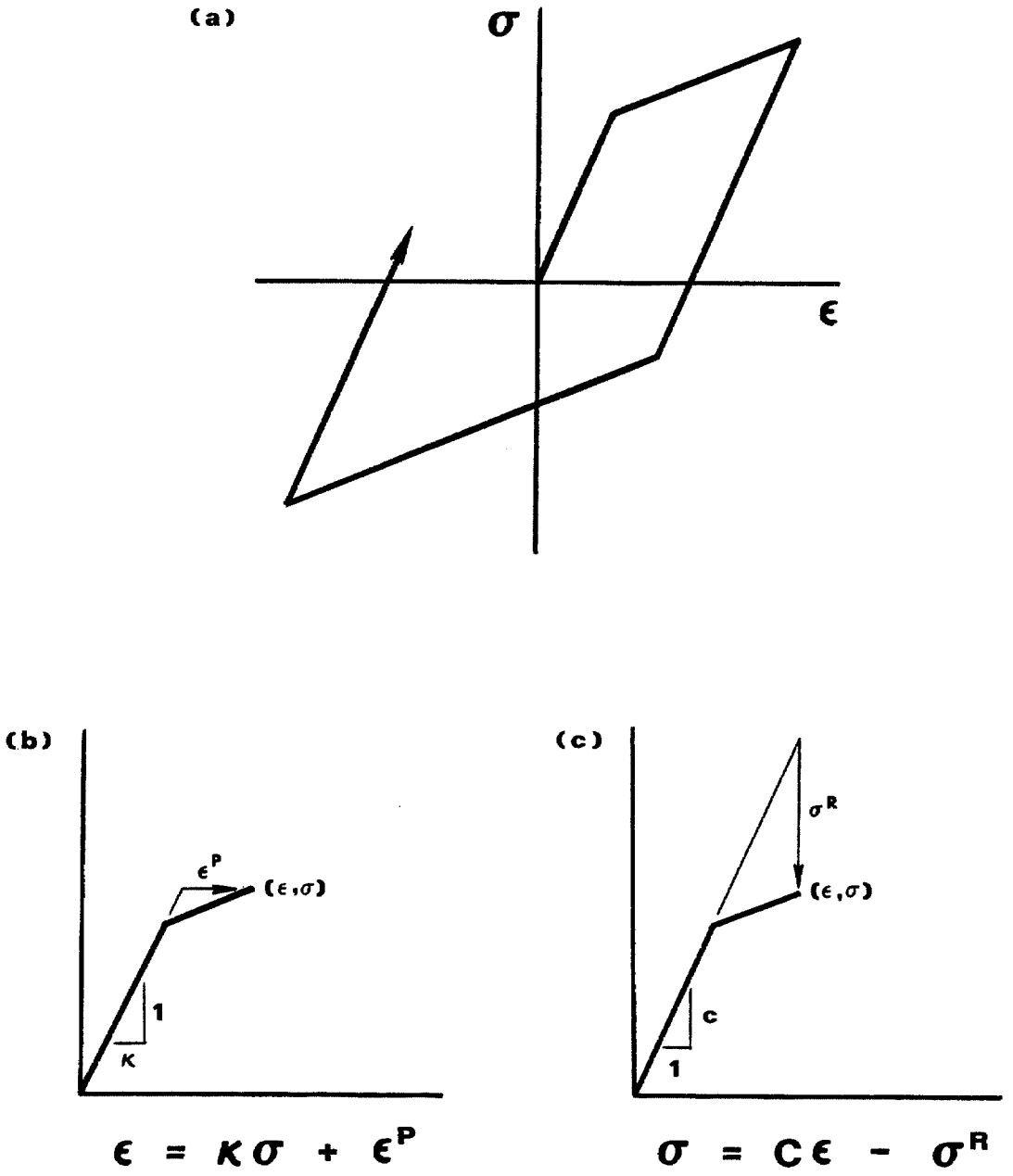

Figure 2.1 A one-dimensional bilinear system. To describe the material state at some point along the curve, we may use either (b) the traditional scheme; or (c) its strain-space counterpart.

In the traditional formulation of plasticity, the stress plays the dominant role. At any given point of the loading history, there is a range of stress within which the incremental behavior is elastic. Plastic response is possible only if the stress lies on the boundary of this interval and if the stress increment extends outward from it. At each point along the curve the stress σ is taken as an independent variable. The total strain is found by computing the strain which would arise elastically from the given stress and adding a plastic strain ε^P, as indicated in Figure 2.1(b). Thus

$$\varepsilon = \kappa\sigma + \varepsilon^P \tag{2.1}$$

An alternative approach would be to define an elastic interval along the strain axis such that yielding will occur only if the strain lies on the boundary of this interval and if the strain increment is directed outward from it. Then, the strain is taken as an independent variable in describing the material state. To find the stress it is necessary first to compute that stress which would result elastically from the current strain ε and then subtract the amount by which the stress has been relaxed on account of plastic effects. This is shown in Figure 2.1(c). In this approach

$$\sigma = c\varepsilon - \sigma^R \tag{2.2}$$

Equations (2.1) and (2.2) are identical in form except for a minus sign. In a similar way the whole framework of stress-space plasticity may be made to carry over to a strain-space formulation.

2.1.2 Definition of Relaxation Surface

Turning to the case of three-dimensional loading, let the elastic behavior be characterized by a Young's modulus E and a Poisson's ratio ν. Recall that in the last section it was convenient to use both c and κ, the slope of the loading curve and its reciprocal. Requiring that

$$E > 0 \quad \text{and} \quad -1 < \nu < \frac{1}{2} \tag{2.3}$$

will assure that Hooke's law can be inverted in the present case as well. Thus, for elastic deformation increments let

$$\begin{aligned} d\sigma_{ij} &= c_{ijk\ell}\, d\varepsilon_{k\ell} \\ d\varepsilon_{ij} &= \kappa_{ijk\ell}\, d\sigma_{k\ell} \end{aligned} \tag{2.4}$$

where

$$\begin{aligned} c_{ijk\ell} &= \frac{E}{1+\nu}\left[\delta_{ik}\delta_{j\ell} + \frac{\nu}{1-2\nu}\,\delta_{ij}\delta_{k\ell}\right], \\ \kappa_{ijk\ell} &= \frac{1}{E}\left[(1+\nu)\delta_{ik}\delta_{j\ell} - \nu\delta_{ij}\delta_{k\ell}\right]. \end{aligned} \tag{2.5}$$

It should be understood here and throughout the remainder of this thesis that $\underset{\sim}{\delta}$ denotes the Kronecker delta.

Once the loading becomes plastic, the strain $\underset{\sim}{\varepsilon}$ will be taken as the independent variable, by analogy to the scalar case of the last section. The stress will then be found by subtracting the stress relaxation $\underset{\sim}{\sigma}^R$ from the stress which would arise elastically from the current strain. That is,

$$\underset{\sim}{\sigma} = \underset{\sim\sim}{c}\underset{\sim}{\varepsilon} - \underset{\sim}{\sigma}^R \ . \tag{2.6}$$

In some contexts it is useful to keep track not only of the cumulative stress relaxation but also of some measure of how much relaxation (of whatever sign) has occurred throughout the history of the material sample. Accordingly, let

$$L = \int \left\{ \frac{2}{3} \, d\sigma^R_{ij} d\sigma^R_{ij} \right\}^{1/2} \tag{2.7}$$

where the integration is to be carried out over the entire stress history.

By analogy to the one-dimensional case, one expects the incremental elastic equations (2.4) to prevail in some simply-connected region of strain space which, in the course of time, may undergo translation and/or distortion. The instantaneous strain state always lies either within the region or on its boundary. This region may be defined by a function $\hat{F}$ such that at all times

$$\hat{F}(\underset{\sim}{\varepsilon}, \underset{\sim}{\sigma}^R, L) \leq 0 \quad . \tag{2.8}$$

Stress relaxation is possible only if

$$\hat{F}(\underset{\sim}{\varepsilon}, \underset{\sim}{\sigma}^R, L) = 0 \quad ; \tag{2.9}$$

otherwise equation (2.4) holds. For this reason the boundary, given by (2.9), is called the relaxation surface.

Since $\underset{\sim}{\varepsilon}$ is symmetric, there is no loss of generality in setting

$$\hat{F}(\underset{\sim}{x}, \underset{\sim}{y}, z) = \hat{F}(\underset{\sim}{x}^T, \underset{\sim}{y}, z) \qquad \text{on} \qquad \text{lin}(\mathbb{R}^3) \times \text{lin}(\mathbb{R}^3) \times \mathbb{R} \quad . \tag{2.10}$$

To verify this, consider a relaxation surface characterized by a function $\hat{G}$ which does not satisfy (2.10). Then, the function

$$\hat{F}(\underset{\sim}{x},\underset{\sim}{y},z) = \frac{1}{2}\left[\hat{G}(\underset{\sim}{x},\underset{\sim}{y},z) + \hat{G}(\underset{\sim}{x}^T,\underset{\sim}{y},z)\right] \quad \text{on} \quad \text{lin}(\mathbb{R}^3) \times \text{lin}(\mathbb{R}^3) \times \mathbb{R}$$

would satisfy (2.10) and, moreover, provide an equivalent description of the surface since

$$\hat{F}(\underset{\sim}{x},\underset{\sim}{y},z) = \hat{G}(\underset{\sim}{x},\underset{\sim}{y},z) \quad \text{on} \quad \text{sym}(\mathbb{R}^3) \times \text{lin}(\mathbb{R}^3) \times \mathbb{R} \ .$$

Owing to the symmetry of $\underset{\sim}{\sigma}^R$, a requirement analogous to (2.10) may also be imposed upon the second argument of $\hat{F}$. These stipulations, together with some smoothness assumptions, are collected below for future reference:

$$\left.\begin{aligned}
&\text{(a)} \quad \hat{F}(\underset{\sim}{x},\underset{\sim}{y},z) = \hat{F}(\underset{\sim}{x}^T,\underset{\sim}{y},z) = \hat{F}(\underset{\sim}{x},\underset{\sim}{y}^T,z) \ , \\
&\text{(b)} \quad \frac{\partial\hat{F}}{\partial x_{ij}} \ , \ \frac{\partial\hat{F}}{\partial y_{ij}} \ , \ \frac{\partial\hat{F}}{\partial z} \ \text{exist and are continuous,} \\
&\text{(c)} \quad \frac{\partial\hat{F}}{\partial x_{ij}} \ \frac{\partial\hat{F}}{\partial x_{ij}} > 0 \ , \ \text{and} \\
&\text{(d)} \quad \frac{\partial\hat{F}}{\partial x_{ij}} = \frac{\partial\hat{F}}{\partial x_{ji}} \ , \quad \frac{\partial\hat{F}}{\partial y_{ij}} = \frac{\partial\hat{F}}{\partial y_{ji}} \\
&\qquad \forall(\underset{\sim}{x},\underset{\sim}{y},z) \in \text{lin}(\mathbb{R}^3) \times \text{lin}(\mathbb{R}^3) \times \mathbb{R} \ .
\end{aligned}\right\} \qquad (2.11)$$

Relations (2.11d) clearly follow from (2.11a) and (2.11b).

2.1.3 Normality and Convexity

Thus far the extension from one dimension to three has been straightforward. Now, though, there arises a more troublesome question which has no one-dimensional counterpart: In what direction does the tensor $d\underset{\sim}{\sigma}^R$ point? This cannot be resolved without some further postulates about how stresses relax. To this end, consider a scenario inspired by the work of Drucker [12].

Suppose that the instantaneous state of strain, $\underset{\sim}{\varepsilon}^*$, lies within the incrementally elastic region, as indicated in Figure 2.2. Let an external agency vary the strain, following an arbitrary path within this region, until the system reaches the relaxation surface (at $\underset{\sim}{\varepsilon}$). Only elastic changes have taken place so far. Now, suppose a very small strain increment $d\underset{\sim}{\varepsilon}$ is supplied which produces an increment of permanent stress relaxation, $d\underset{\sim}{\sigma}^R$, as well as an elastic increment. Let the system then be brought back to $\underset{\sim}{\varepsilon}$, and from there to $\underset{\sim}{\varepsilon}^*$. Intuition suggests the following three postulates:

1. A small strain increment gives rise to a stress relaxation increment of the same order.

$$\max_{i,j}|d\varepsilon_{ij}| = O(\delta) \Rightarrow \max_{i,j}|d\sigma^R_{ij}| = O(\delta) \quad \text{as} \quad \delta \to 0 \tag{2.12}$$

2. The increment of stress relaxation $d\underset{\sim}{\sigma}^R$ does not depend upon $\underset{\sim}{\varepsilon}^*$.

$$d\underset{\sim}{\sigma}^R \neq \underset{\sim}{f}(\underset{\sim}{\varepsilon}^*) \tag{2.13}$$

3. The work done per unit volume by the external agency over the cycle is nonnegative for all $\underset{\sim}{\varepsilon}^*$.

In view of (2.6) and (2.12) (see Figure 2.3), the work done is given by

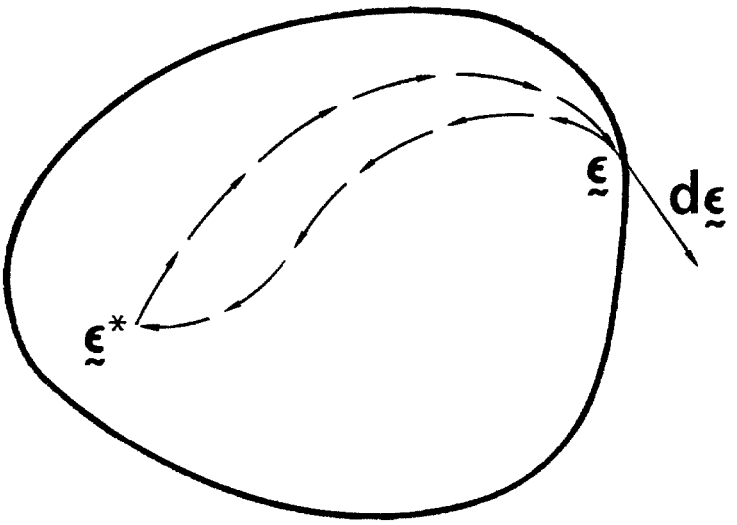

Figure 2.2 An excursion in strain space.

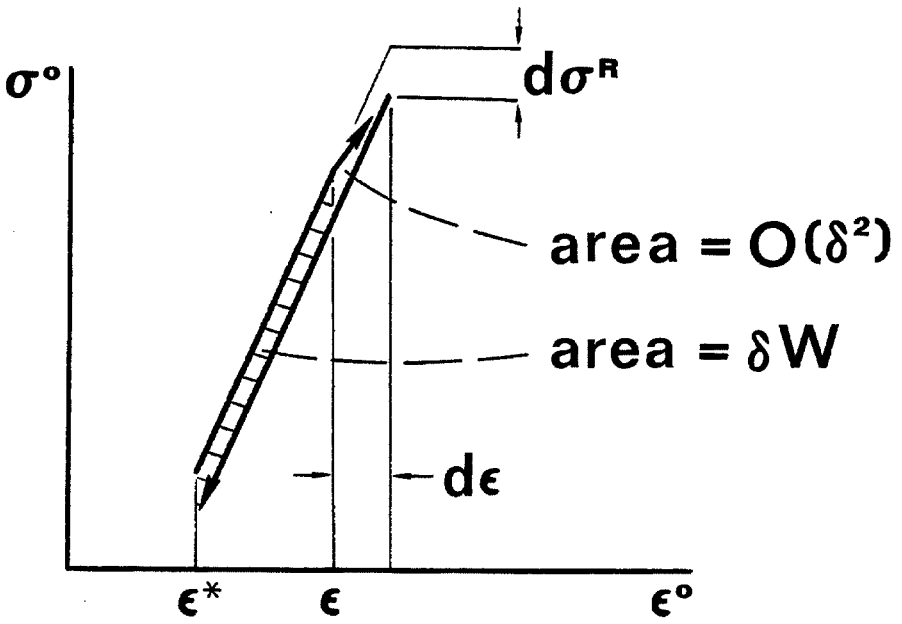

Figure 2.3 The work done <u>during</u> the plastic step is negligible, being $O(\delta^2)$.

$$\delta W = \int_{\underset{\sim}{\varepsilon}^*}^{\underset{\sim}{\varepsilon}} + \int_{\underset{\sim}{\varepsilon}}^{\underset{\sim}{\varepsilon}+d\underset{\sim}{\varepsilon}} + \int_{\underset{\sim}{\varepsilon}+d\underset{\sim}{\varepsilon}}^{\underset{\sim}{\varepsilon}} + \int_{\underset{\sim}{\varepsilon}}^{\underset{\sim}{\varepsilon}^*} \sigma_{ij}(\underset{\sim}{\varepsilon}^\circ)d\varepsilon^\circ_{ij} = \int_{\underset{\sim}{\varepsilon}^*}^{\underset{\sim}{\varepsilon}} \left[c_{ijk\ell}\varepsilon^\circ_{k\ell} - \sigma^R_{ij} \right] d\varepsilon^\circ_{ij}$$

$$+ \int_{\underset{\sim}{\varepsilon}}^{\underset{\sim}{\varepsilon}^*} \left[c_{ijk\ell}\varepsilon^\circ_{k\ell} - \sigma^R_{ij} - d\sigma^R_{ij} \right] d\varepsilon^\circ_{ij} + O(\delta^2) \qquad \text{as } \delta \to 0$$

Thus, the third postulate yields

$$(\varepsilon_{ij} - \varepsilon^*_{ij})d\sigma^R_{ij} + O(\delta^2) \geq 0 \qquad \text{as } \delta \to 0 \tag{2.14}$$

In words, this equation states that the increment of stress relaxation has a non-negative component in the direction of $(\underset{\sim}{\varepsilon}-\underset{\sim}{\varepsilon}^*)$.

The significance of the above postulates can readily be seen if one takes the liberty of representing two-tensors by two-dimensional arrows. As before, let the strain $\underset{\sim}{\varepsilon}$ lie on the relaxation surface, and let $d\underset{\sim}{\varepsilon}$ be an increment of strain pointing out into the plastic region from $\underset{\sim}{\varepsilon}$. According to postulate (2.13), the corresponding stress relaxation increment is independent of the strain path leading up to $\underset{\sim}{\varepsilon}$, so long as the recent history is elastic. So, consider three particular choices for $\underset{\sim}{\varepsilon}^*$, as suggested in Figure 2.4. For the first two cases, let $\underset{\sim}{\varepsilon}^*$ lie just inside the relaxation surface, on opposite sides of $\underset{\sim}{\varepsilon}$. For the third case, let $(\underset{\sim}{\varepsilon}-\underset{\sim}{\varepsilon}^*)$ point normally outward. Corresponding to each case, statement (2.14) defines a range of allowable directions for $d\underset{\sim}{\sigma}^R$, and these too are shown in the figure. Since $d\underset{\sim}{\sigma}^R$ must actually lie within all three ranges, it must point in the outward normal direction:

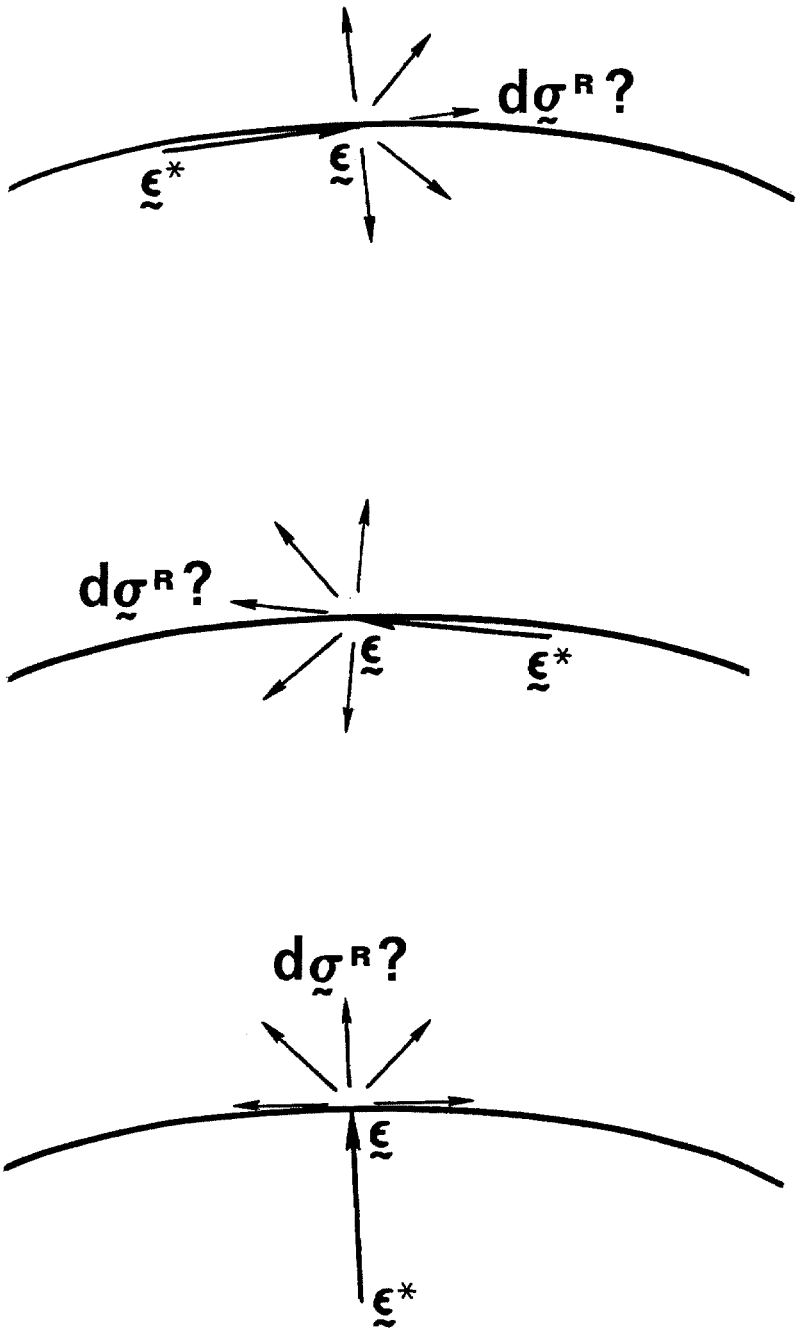

Figure 2.4 Three particular choices for $\underset{\sim}{\epsilon}^*$, and the corresponding ranges of allowable directions for $d\underset{\sim}{\sigma}^R$.

$$d\sigma^R_{ij} = d\ell \frac{\partial \hat{F}}{\partial \varepsilon_{ij}} \quad , \quad d\ell > 0 \quad . \tag{2.15}$$

This result may be established more rigorously through recourse to the implicit function theorem. For details, see Appendix I.

That a normality rule should hold in strain space may come as a surprise, particularly since its stress-space analog no longer commands universal acceptance. In the current literature a material which does satisfy normality in the sense of (2.15) is said to follow an "associative flow rule" and is regarded as a special case [13]. Nonassociative flow rules are routinely summoned to model soils and other materials which undergo permanent volume changes. Now, the experimental evidence does indicate a breakdown in normality for these materials, so some generalization of plasticity theory is necessary in order to accommodate them. Any such generalization, though, should incorporate a fundamental reworking of the notion of a relaxation surface (or yield surface, in the case of a stress-space theory). The second postulate of this section, in particular, seems suspect; the plastic increment evidently must depend upon the recent elastic history. And so the resulting theory will differ substantially from conventional plasticity. By opting for traditional loading surfaces, this present exposition must necessarily embrace a normality rule as well.

What is more, convexity of the relaxation surface also follows. Plotting the appropriate components of $d\underset{\sim}{\sigma}^R$ as a vector in principal strain space, the foregoing implies that this vector will point in the outward normal direction at $\underset{\sim}{\varepsilon}$. Statement (2.14), which now reduces to

a simple vector inner product, implies that the angle between this outward normal and $(\underset{\sim}{\varepsilon}^*-\underset{\sim}{\varepsilon})$ is between 0 and $\pi/2$. But (2.14) holds for every $\underset{\sim}{\varepsilon}^*$ within the incrementally elastic region. So, as indicated by Figure 2.5, the relaxation surface must be convex, as viewed in principal strain space.

2.1.4 Permanent Dilatation

Many materials respond linearly to a wide range of hydrostatic pressure, their volumetric strain showing little or no hysteresis. Not only is this true of structural metals [14], but it also applies to fully saturated clay so long as the pressure remains high [4,15]. Therefore, it seems appropriate to follow the usual practice in plasticity and rule out inelastic changes in volume.

In assessing the ramifications of this assumption, it is helpful to visualize the relaxation surface in principal strain space. Evidently, so long as the strain state moves parallel to the dilatational axis $\varepsilon_1 = \varepsilon_2 = \varepsilon_3$, the response will not be plastic. This can be true only if the relaxation surface is made up of lines parallel to the dilatational axis. The surface must therefore be a cylinder cutting at right angles through the plane of zero dilatation, $\varepsilon_1+\varepsilon_2+\varepsilon_3 = 0$. The locus of intersection will be called hereafter the relaxation curve. Once its shape is specified, the geometry of the entire relaxation surface will be fully determined. All that is known so far about the relaxation curve, though, is that it is closed and convex.

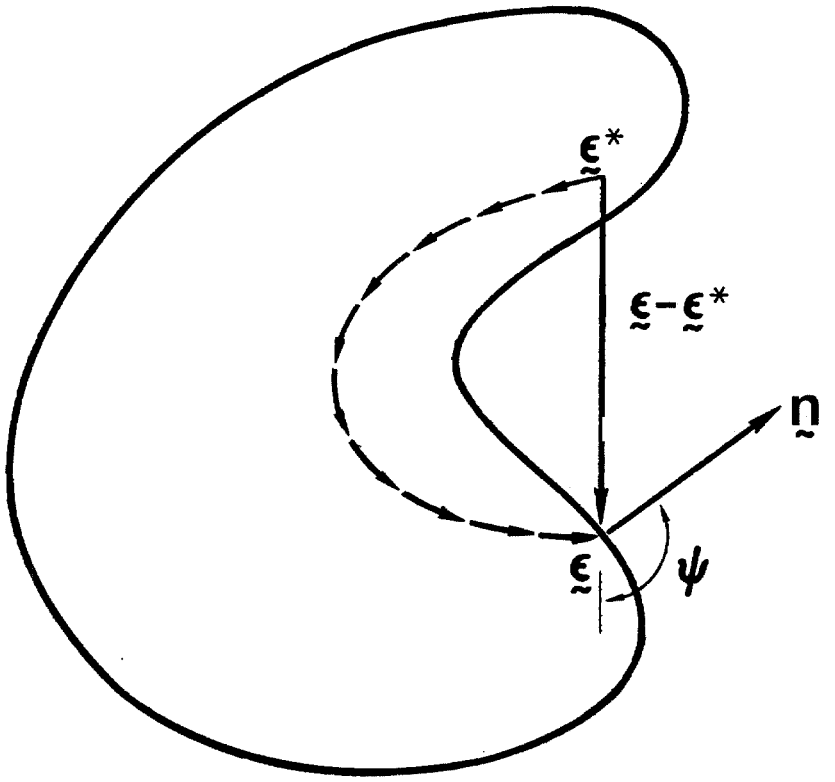

Figure 2.5 The angle ψ must be between 0 and $\pi/2$ for every interior $\underset{\sim}{\epsilon}^*$. This rules out concave surfaces like the one shown above.

2.1.5 Symmetries of the Relaxation Curve

Further restrictions on the relaxation curve emerge if one requires the criterion for plastic response to be isotropic for the virgin material. To clarify the assumptions being made in this case, consider an interchange of the x_2- and x_3-axes within the physical domain, along with a reversal of the x_1 direction, so as to retain right-handedness. Isotropy, in this context, means that such changes will not affect the criterion for stress relaxation. Therefore, the relaxation curve must be symmetric about the projection of the ε_1-axis onto the plane $\varepsilon_1+\varepsilon_2+\varepsilon_3 = 0$. This line is designated L_1 in Figure 2.6(a). Similarly, the projections of the ε_2- and ε_3-axes will also be lines of symmetry.

Further symmetries arise if one equates the compressive and extensional elastic limits. Let the point Q lie on the relaxation curve, as shown in Figure 2.6(a). Then, reversing the signs of all the strain components associated with Q will lead to a point Q′ lying an equal distance to the opposite side of the origin. According to hypothesis, Q′ is also on the relaxation curve, but then so is Q″, its reflection in the line L_1. It follows that the curve has symmetry about the line perpendicular to L_1 and passing through the origin; and, by the same token, about the perpendiculars to L_2 and L_3. Thus, the relaxation curve has twelve equally spaced rays of symmetry, as indicated in Figure 2.6(b).

This fact, along with convexity, leads to inner and outer bounds on the relaxation curve. Let A lie on the curve, as shown in Figure 2.6(b). Then by symmetry so do B and C. The innermost convex curve

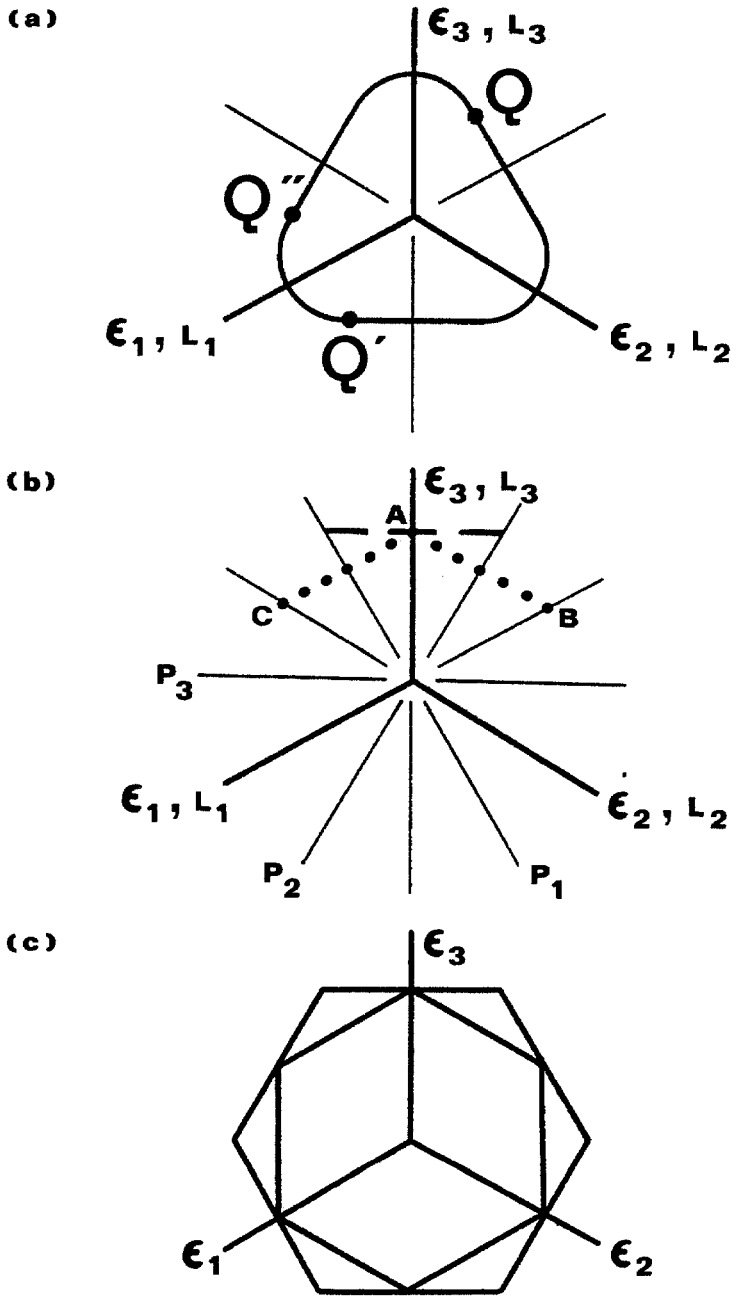

Figure 2.6 (a) Lines of symmetry L_1, L_2, and L_3 emerge from the virgin material's isotropy.

(b) Lines of symmetry P_1, P_2, and P_3 arise if the extensional and compressive elastic limits are equal.

(c) All possible relaxation curves lie between the hexagons shown.

passing through these points is drawn in dots. And the outermost curve passing through A, convex and symmetric about the ε_3-axes, appears as a dashed line. Dealing similarly with the other lines of symmetry, one ultimately concludes that any admissible relaxation curve will be between the hexagonal cylinders shown in Figure 2.6(c).

2.1.6 Consistency; and the Elastoplastic Constitutive Laws (Strain-Space Version)

Since the results of the last section follow from assumed properties of the virgin material, they really apply only to the initial configuration of the relaxation surface. How does the surface evolve as the material undergoes plastic deformation? A number of answers to this, all somewhat arbitrary, have found their way into the stress-space literature, but two stand out on account of their widespread acceptance. For isotropic plasticity the surface expands uniformly like a balloon (or shrinks, as the case may be). For kinematic plasticity the surface translates parallel to the instantaneous normal at the point of loading. In the absence of any compelling rationale on how to handle the strain-space problem, it seems reasonable to incorporate analogs of these two schemes. Accordingly, assume that with each increment $d\underset{\sim}{\sigma}^R$, the relaxation surface translates a distance $cd\underset{\sim}{\sigma}^R$ in strain space and simultaneously grows larger or smaller through the influence of the parameter L, defined in equation (2.7). Let c also depend upon L, in the interest of further generality, and thus set

$$\hat{F}(\underset{\sim}{\varepsilon},\underset{\sim}{\sigma}^R,L) = F\left(\left[\underset{\sim}{\varepsilon} - c(L)\underset{\sim}{\sigma}^R\right]'\right) - k^2(L) \quad ,$$

where $$F \in C^1(\mathbb{R}^9) \quad , \quad c \text{ and } k \in C^1(\mathbb{R}) \quad , \qquad (2.16)$$

$$\text{and } k > 0 \text{ on } \mathbb{R} \quad .$$

The prime is used here to signify a deviatoric component. It will be understood throughout the remainder of the thesis that

$$x'_{ij} = x_{ij} - \frac{1}{3} x_{kk}\delta_{ij} \quad \forall \underset{\sim}{x} \in \text{lin}(\mathbb{R}) \qquad (2.17)$$

The full elastoplastic constitutive law follows readily now; all that remains is to impose the so-called consistency condition. In words, this says that during stress relaxation each strain increment leads from one plastic state to another, equation (2.9) holding both before and after. Thus

$$0 = d\hat{F}(\underset{\sim}{\varepsilon},\underset{\sim}{\sigma}^R,L) = \frac{\partial \hat{F}}{\partial \varepsilon_{ij}} d\varepsilon_{ij} - c \frac{\partial \hat{F}}{\partial \varepsilon_{ij}} d\sigma^R_{ij} - \frac{\partial \hat{F}}{\partial \varepsilon_{ij}} \sigma^R_{ij} \frac{dc}{dL} dL - 2k \frac{dk}{dL} dL \, .$$

In view of (2.7) and (2.15a),

$$\frac{\partial \hat{F}}{\partial \varepsilon_{ij}} d\varepsilon_{ij} = c \frac{\partial \hat{F}}{\partial \varepsilon_{ij}} d\sigma^R_{ij} + \left\{ \frac{\partial \hat{F}}{\partial \varepsilon_{ij}} \sigma^R_{ij} \frac{dc}{dL} + 2k\frac{dk}{dL} \right\} \sqrt{\frac{2}{3} d\sigma^R_{k\ell} d\sigma^R_{k\ell}} = d\ell \, D \quad ,$$

where

$$D = c \frac{\partial \hat{F}}{\partial \varepsilon_{ij}} \frac{\partial \hat{F}}{\partial \varepsilon_{ij}} + \left\{ \frac{\partial \hat{F}}{\partial \varepsilon_{ij}} \sigma^R_{ij} \frac{dc}{dL} + 2k\frac{dk}{dL} \right\} \sqrt{\frac{2}{3} \frac{\partial \hat{F}}{\partial \varepsilon_{k\ell}} \frac{\partial \hat{F}}{\partial \varepsilon_{k\ell}}} \quad . \qquad (2.18a)$$

Assume that

$$D \in (0,\infty) \quad ; \qquad (2.18b)$$

then

$$d\ell = \frac{\frac{\partial \hat{F}}{\partial \varepsilon_{ij}} d\varepsilon_{ij}}{D} \tag{2.19}$$

and, in light of (2.15a),

$$d\sigma^R_{ij} = \frac{\partial \hat{F}}{\partial \varepsilon_{ij}} \frac{\frac{\partial \hat{F}}{\partial \varepsilon_{mn}} d\varepsilon_{mn}}{D} \tag{2.20}$$

The physical significance of assumption (2.18b) becomes evident upon comparing (2.19) with (2.15b). Ruling out negative values for D assures that during stress relaxation

$$\frac{\partial \hat{F}}{\partial \varepsilon_{ij}} d\varepsilon_{ij} > 0 \quad . \tag{2.21}$$

This means that during plastic deformations each strain increment takes a step into the current relaxation surface. The size of D governs the extent to which plastic effects dominate, as suggested in Figure 2.7. For D positive but tending to zero, a small increment of strain beyond the relaxation surface leads to an enormous jump in stress relaxation, in view of (2.20). Thus the surface becomes nearly an immovable barrier in strain space. On the other hand, as $D \to \infty$ one can accommodate a great deal of strain — and correspondingly a large amount of elastic stress — with minimal stress relaxation. In this limit, therefore, the material reverts to Hookean linearity.

Consider now a lemma which will serve to simplify the form of (2.16a).

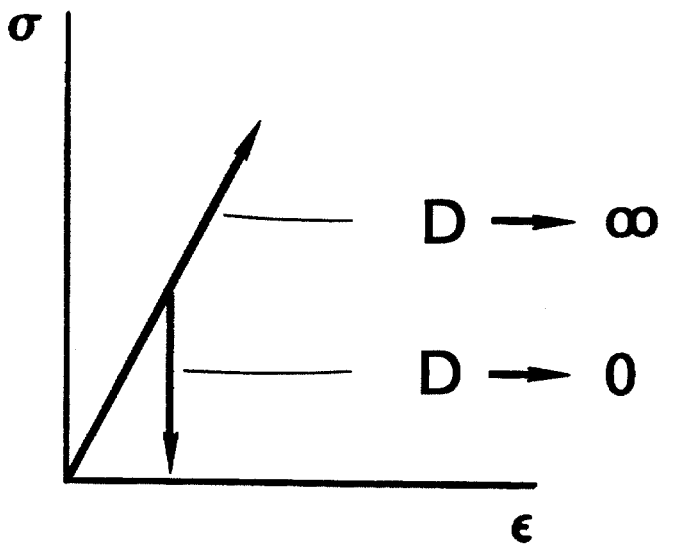

Figure 2.7 Effect of D upon the elastoplastic behavior (strain-space theory).

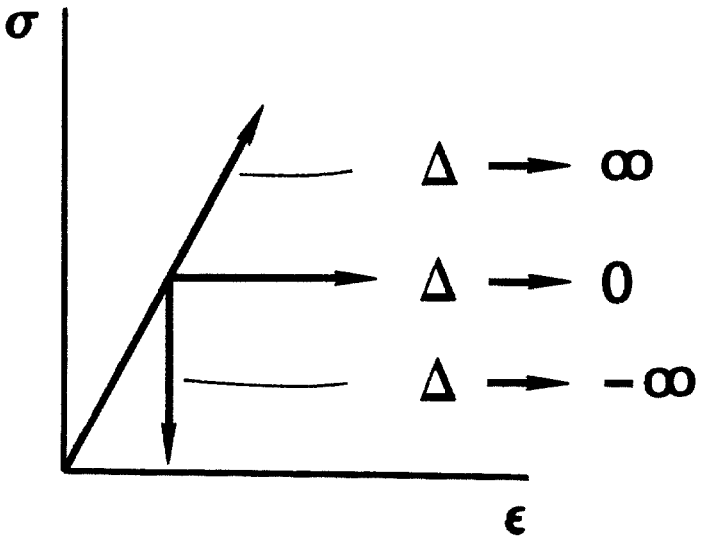

Figure 2.8 Effect of Δ upon the elastoplastic behavior (stress-space theories).

Lemma 2.1 Let Ψ be a differentiable function of $\underset{\sim}{x}$ and $\underset{\sim}{y}$, which are two-tensors, and of the scalar z. Suppose Ψ depends, in fact, only upon the deviatoric part of $\underset{\sim}{x}$. Then $\partial\Psi/\partial x_{ij}$ is purely deviatoric.

Proof: In the argument list of Ψ, replace $\underset{\sim}{x}$ by $\underset{\sim}{x}'$. Then invoke (2.17) and differentiate using the chain rule. Q.E.D.

According to (2.16), the function $\hat{F}$ meets the hypotheses of the lemma. Thus, by (2.20),

$$d\sigma^R_{ii} = 0 \quad .$$

Assume that for the virgin material

$$\underset{\sim}{\sigma}^R = \underset{\sim}{0} \; ; \tag{2.22}$$

then $\underset{\sim}{\sigma}^R$ will remain purely deviatoric, and the first of (2.16) simplifies to

$$\hat{F}(\underset{\sim}{\varepsilon},\underset{\sim}{\sigma}^R,L) = F(\underset{\sim}{\varepsilon}'-c(L)\underset{\sim}{\sigma}^R) - k^2(L) \quad . \tag{2.23}$$

Thus concludes the strain-space presentation of plasticity. Collecting statements (2.8), (2.9), (2.21), (2.20), and (2.6), one arrives at the following constitutive law:

$$
[C]\quad
\begin{cases}
\hat{F}(\underset{\sim}{\varepsilon},\underset{\sim}{\sigma}^{R},L) \le 0 \text{ always.} & \text{(a)}\\
\text{If}\quad \hat{F}(\underset{\sim}{\varepsilon},\underset{\sim}{\sigma}^{R},L) = 0 & \text{(b)}\\
\text{and}\quad \dfrac{\partial \hat{F}}{\partial \varepsilon_{ij}}\, d\varepsilon_{ij} > 0\ , & \text{(c)}\\
\text{then}\quad d\sigma_{ij} = c_{ijk\ell}\, d\varepsilon_{k\ell} - \dfrac{\partial \hat{F}}{\partial \varepsilon_{ij}} \dfrac{\dfrac{\partial \hat{F}}{\partial \varepsilon_{mn}}\, d\varepsilon_{mn}}{D}\ . & \text{(d)}\\
\text{If (b) or (c) is violated,} & \\
\text{then}\quad d\sigma_{ij} = c_{ijk\ell}\, d\varepsilon_{k\ell}. & \text{(e)}
\end{cases}
$$

Throughout the above, D and all derivatives of $\hat{F}$ are to be evaluated at the current values of $\underset{\sim}{\varepsilon}$, $\underset{\sim}{\sigma}^{R}$, and L.

2.2 The Elastoplastic Constitutive Relations (in Stress Space)

The analysis delineated in Section 2.1 parallels step by step the conventional, stress-space presentation of plasticity. This being true, there is little point in deriving here in detail the constitutive relations for the stress-space theory. Suffice it to note that the criteria for plastic flow are expressible in terms of a yield function

$$\hat{\Phi}\,(\underset{\sim}{\sigma},\underset{\sim}{\varepsilon}^{P},\Lambda) \;=\; \Phi(\underset{\sim}{\sigma}'-\gamma(\Lambda)\underset{\sim}{\varepsilon}^{P}) - \kappa^{2}(\Lambda)\ .$$

The roles played by $\hat{\Phi}$, Φ, $\underset{\sim}{\sigma}$, $\underset{\sim}{\varepsilon}^{P}$, Λ, γ, and κ correspond respectively to those of $\hat{F}$, F, $\underset{\sim}{\varepsilon}$, $\underset{\sim}{\sigma}^{R}$, L, c, and k. This analogy will receive more elaborate treatment in Lemma 2.3. For stress-space plasticity the analytical form of the constitutive law turns out to depend upon whether the scalar quantity

$$\Delta = \frac{\partial \hat{\Phi}}{\partial \sigma_{ij}} \frac{\partial \hat{\Phi}}{\partial \sigma_{ij}} + \left\{ \frac{\partial \hat{\Phi}}{\partial \sigma_{ij}} \varepsilon^{P}_{ij} \frac{d\gamma}{d\Lambda} + 2\kappa \frac{d\kappa}{d\Lambda} \right\} \sqrt{\frac{2}{3} \frac{\partial \hat{\Phi}}{\partial \sigma_{k\ell}} \frac{\partial \hat{\Phi}}{\partial \sigma_{k\ell}}}$$

is positive, zero, or negative. All three cases are of interest; they correspond respectively to strain hardening, "ideal" (or "perfect") plasticity, and strain softening. (See Figure 2.8 for a schematic indication of how Δ influences the elastoplastic behavior.)

The constitutive law for stress-space plasticity may be summarized as follows:

Strain hardening: $\Delta > 0$ (+)

[Γ+]

$\hat{\Phi}(\underset{\sim}{\sigma}, \underset{\sim}{\varepsilon}^{P}, \Lambda) \leq 0$ always . (α)

If $\hat{\Phi}(\underset{\sim}{\sigma}, \underset{\sim}{\varepsilon}^{P}, \Lambda) = 0$ (β)

and $\frac{\partial \hat{\Phi}}{\partial \sigma_{ij}} d\sigma_{ij} > 0$, (γ)

then $d\varepsilon_{ij} = \kappa_{ijk\ell} d\sigma_{k\ell} + \frac{\frac{\partial \hat{\Phi}}{\partial \sigma_{ij}} \frac{\partial \hat{\Phi}}{\partial \sigma_{mn}} d\sigma_{mn}}{\Delta}$. (δ)

If (β) or (γ) is violated,

then $d\varepsilon_{ij} = \kappa_{ijk\ell} d\sigma_{k\ell}$. (ε)

Ideal plasticity: $\Delta = 0$ (0)

$[\Gamma\circ]$

$\hat{\Phi}(\underset{\sim}{\sigma},\underset{\sim}{\varepsilon}^P,\Lambda) \leq 0$ always . (α)

If $\hat{\Phi}(\underset{\sim}{\sigma},\underset{\sim}{\varepsilon}^P,\Lambda) = 0$, (β)

then $\dfrac{\partial\hat{\Phi}}{\partial\sigma_{ij}}\, d\sigma_{ij} \leq 0$. (ϕ)

If (β) is true

and $\dfrac{\partial\hat{\Phi}}{\partial\sigma_{ij}}\, d\sigma_{ij} = 0$, ($\gamma\circ$)

then $d\varepsilon_{ij} = \kappa_{ijk\ell} d\sigma_{k\ell} + \lambda \dfrac{\partial\hat{\Phi}}{\partial\sigma_{ij}}$, $\lambda > 0$ ($\delta\circ$)

or $d\varepsilon_{ij} = \kappa_{ijk\ell} d\sigma_{k\ell}$. (ε)

If (β) or ($\gamma\circ$) is violated, then (ε) holds.

Strain softening: $\Delta < 0$ (-)

$[\Gamma-]$

$\hat{\Phi}(\underset{\sim}{\sigma},\underset{\sim}{\varepsilon}^P,\Lambda) \leq 0$ always . (α)

If $\hat{\Phi}(\underset{\sim}{\sigma},\underset{\sim}{\varepsilon}^P,\Lambda) = 0$ (β)

and $\dfrac{\partial\hat{\Phi}}{\partial\sigma_{ij}}\, d\varepsilon_{ij} > 0$, ($\gamma-$)

then $d\varepsilon_{ij} = \kappa_{ijk\ell} d\sigma_{k\ell} + \dfrac{\dfrac{\partial\hat{\Phi}}{\partial\sigma_{ij}} \dfrac{\partial\hat{\Phi}}{\partial\sigma_{mn}} d\sigma_{mn}}{\Delta}$. (δ)

If (β) or ($\gamma-$) is violated,

then $d\varepsilon_{ij} = \kappa_{ijk\ell} d\sigma_{k\ell}$. (ε)

In all of the above, Δ and the derivatives of $\hat{\Phi}$ are evaluated at the current values of $\underset{\sim}{\sigma}$, $\underset{\sim}{\varepsilon}^P$, and Λ.

2.3 Equivalence of the Stress- and Strain-Space Models

A cursory glance at constitutive laws [C] and [Γ+,$\circ$,-] will reveal that they are virtually identical in form. What is not so obvious is that they can actually be made equivalent. In fact the main difference between them is that they are formulated in terms of different sets of state variables. Hence, the first step toward establishing the relationship between the two formulations is to consider in detail these two schemes for describing the material state.

2.3.1 State Variables: Stress Space versus Strain Space

Note, as a preliminary, that under Hooke's law deviatoric stress and strain increments are simply proportional to one another. This useful if rather mundane result follows as a direct application of the following lemma.

Lemma 2.2 Let $\underset{\sim}{\alpha}'$ and $\underset{\sim}{\beta}'$ be the deviatoric parts of two-tensors $\underset{\sim}{\alpha}$ and $\underset{\sim}{\beta}$, respectively. Suppose (2.3) holds, and, with $\underset{\sim}{c}$ and $\underset{\sim}{\kappa}$ defined through (2.5),

$$\underset{\sim}{\alpha} = \underset{\sim}{c}\,\underset{\sim}{\beta} \quad \Leftrightarrow \quad \underset{\sim}{\beta} = \underset{\sim}{\kappa}\,\underset{\sim}{\alpha} \ .$$

Then

$$\underset{\sim}{\beta}' = \frac{1+\nu}{E}\,\underset{\sim}{\alpha}' \ .$$

Proof: Use (2.17) to express $\underset{\sim}{\beta}'$ in terms of $\underset{\sim}{\beta}$. Then replace $\underset{\sim}{\beta}$ by $\underset{\sim}{\kappa}\,\underset{\sim}{\alpha}$ and substitute from (2.5) for $\underset{\sim}{\kappa}$. The result follows upon simplifying. Q.E.D.

The path is now clear for a detailed presentation of the hypotheses and definitions underlying the stress- and strain-space formulations. In the process, $(\underset{\sim}{\sigma},\underset{\sim}{\varepsilon}^P,\Lambda)$ and $(\underset{\sim}{\varepsilon},\underset{\sim}{\sigma}^R,L)$ emerge as alternative sets of state variables, and Lemma 2.3 establishes the law of transformation between these two sets.

Lemma 2.3 Denote by $\underset{\sim}{\sigma}$ and $\underset{\sim}{\varepsilon}$ the current values of stress and strain, and assume that (2.3) holds, so that the elastic response and compliance tensors take the form indicated in (2.5):

$$\left.\begin{aligned} & E > 0 \quad , \qquad -1 < \nu < \tfrac{1}{2} \quad ; \\ c_{ijk\ell} &= \frac{E}{1+\nu}\left[\delta_{ik}\delta_{j\ell} + \frac{\nu}{1-2\nu}\,\delta_{ij}\delta_{k\ell}\right] , \\ \kappa_{ijk\ell} &= \frac{1}{E}\left[(1+\nu)\delta_{ik}\delta_{j\ell} - \nu\delta_{ij}\delta_{k\ell}\right] . \end{aligned}\right\} \quad (H1)$$

Consistent with (2.6), define $\underset{\sim}{\sigma}^R$ and $\underset{\sim}{\varepsilon}^P$ such that

$$\begin{aligned} \underset{\sim}{\sigma} &= \underset{\sim}{c}\,\underset{\sim}{\varepsilon} - \underset{\sim}{\sigma}^R \\ \underset{\sim}{\varepsilon} &= \underset{\sim}{\kappa}\,\underset{\sim}{\sigma} + \underset{\sim}{\varepsilon}^P \end{aligned} \quad (H2)$$

Assume, in conformity with (2.22), that

$$\underset{\sim}{\sigma}^R = \underset{\sim}{\varepsilon}^P = \underset{\sim}{0} \quad (H3)$$

for the virgin material. Define, consistent with (2.7),

$$\left.\begin{aligned} L &= \int \sqrt{\tfrac{2}{3}\, d\sigma^R_{ij}\, d\sigma^R_{ij}} \quad ; \quad \Lambda = \int \sqrt{\tfrac{2}{3}\, d\varepsilon^P_{ij}\, d\varepsilon^P_{ij}} \quad , \\ & \text{where both integrations are to be carried out over the entire} \\ & \text{deformation history.} \end{aligned}\right\} \quad (H4)$$

Let $\hat{F}(\underset{\sim}{\varepsilon},\underset{\sim}{\sigma}^R,L)$ and $\hat{\Phi}(\underset{\sim}{\sigma},\underset{\sim}{\varepsilon}^P,\Lambda)$ be scalar functions such that, in conformity with (2.11) and (2.16),

$$\left.\begin{aligned} \hat{F}(\underset{\sim}{\varepsilon},\underset{\sim}{\sigma}^R,L) &= F\left[\left[\underset{\sim}{\varepsilon} - c(L)\underset{\sim}{\sigma}^R\right]^{\cdot}\right] - k^2(L) \quad , \\ \hat{\Phi}(\underset{\sim}{\sigma},\underset{\sim}{\varepsilon}^P,\Lambda) &= \Phi\left[\left[\underset{\sim}{\sigma} - \gamma(\Lambda)\underset{\sim}{\varepsilon}^P\right]^{\cdot}\right] - \kappa^2(\Lambda) \quad ; \end{aligned}\right\} \text{(H5)}$$

where

$$\left.\begin{aligned} &F \in C^1(\mathbb{R}^9) \quad , \quad c \text{ and } k \in C^1(\mathbb{R}) \quad , \quad k > 0 \text{ on } \mathbb{R}, \\ &\Phi \in C^1(\mathbb{R}^9) \quad , \quad \gamma \text{ and } \kappa \in C^1(\mathbb{R}) \quad , \quad \kappa > 0 \text{ on } \mathbb{R}; \end{aligned}\right\}$$

and

$$\left.\begin{aligned} &\frac{\partial\hat{F}}{\partial\varepsilon_{ij}}\frac{\partial\hat{F}}{\partial\varepsilon_{ij}} > 0 \\ &\frac{\partial\hat{\Phi}}{\partial\sigma_{ij}}\frac{\partial\hat{\Phi}}{\partial\sigma_{ij}} > 0 \end{aligned}\right\} \text{ on } \mathrm{sym}\,(\mathbb{R}^3) \times \mathrm{sym}(\mathbb{R}^3) \times \mathbb{R}. \Bigg\} \text{(H6)}$$

Suppose

$$\left.\begin{aligned} &\text{Either} \quad \text{constitutive law [C]} \quad \text{holds} \\ &\text{or} \quad \text{constitutive laws } [\Gamma+,\circ,-] \text{ hold,} \end{aligned}\right\} \text{(H7)}$$

where, consistent with (2.18),

$$\left.\begin{aligned} D &= c\frac{\partial\hat{F}}{\partial\varepsilon_{ij}}\frac{\partial\hat{F}}{\partial\varepsilon_{ij}} + \left\{\frac{\partial\hat{F}}{\partial\varepsilon_{ij}}\sigma^R_{ij}\frac{dc}{dL} + 2k\frac{dk}{dL}\right\}\sqrt{\frac{2}{3}\frac{\partial\hat{F}}{\partial\varepsilon_{k\ell}}\frac{\partial\hat{F}}{\partial\varepsilon_{k\ell}}} \in (0,\infty) \\ \Delta &= \gamma\frac{\partial\hat{\Phi}}{\partial\sigma_{ij}}\frac{\partial\hat{\Phi}}{\partial\sigma_{ij}} + \left\{\frac{\partial\hat{\Phi}}{\partial\sigma_{ij}}\varepsilon^P_{ij}\frac{d\gamma}{d\Lambda} + 2\kappa\frac{d\kappa}{d\Lambda}\right\}\sqrt{\frac{2}{3}\frac{\partial\hat{\Phi}}{\partial\sigma_{k\ell}}\frac{\partial\hat{\Phi}}{\partial\sigma_{k\ell}}} \quad . \end{aligned}\right\} \text{(H8)}$$

Then,

$$\frac{\partial\hat{F}}{\partial\varepsilon_{kk}} = \frac{\partial\hat{\Phi}}{\partial\sigma_{kk}} = 0 \quad ; \tag{2.24}$$

$$\sigma^R_{kk} = \varepsilon^P_{kk} = 0 \quad . \tag{2.25}$$

The state of the material may equivalently be described by the state variables $(\underset{\sim}{\varepsilon}, \underset{\sim}{\sigma}^R, L)$ or $(\underset{\sim}{\sigma}, \underset{\sim}{\varepsilon}^P, \Lambda)$, and either set may be obtained from the other through the transformations

$$\left.\begin{aligned} \underset{\sim}{\varepsilon} &= \underset{\approx}{\kappa}\underset{\sim}{\sigma} + \underset{\sim}{\varepsilon}^P \\ \underset{\sim}{\sigma}^R &= \frac{E}{1+\nu}\,\underset{\sim}{\varepsilon}^P \\ L &= \frac{E}{1+\nu}\,\Lambda \end{aligned}\right] \Leftrightarrow \left[\begin{aligned} \underset{\sim}{\sigma} &= \underset{\approx}{c}\underset{\sim}{\varepsilon} - \underset{\sim}{\sigma}^R \\ \underset{\sim}{\varepsilon}^P &= \frac{1+\nu}{E}\,\underset{\sim}{\sigma}^R \\ \Lambda &= \frac{1+\nu}{E}\,L \end{aligned}\right. \tag{2.26}$$

Proof.

Re (2.24): In view of (H5) and (H6), Lemma 2.1 applies to both $\hat{F}$ and $\hat{\Phi}$. Thus (2.24) follows.

Re (2.25): Multiply through the first of (H2) by $\underset{\sim}{\kappa}$, and compare the result with the second of (H2). It follows, in view of Lemma 2.2 and (H1), that

$$\underset{\sim}{\varepsilon}^{P\prime} = \frac{1+\nu}{E}\,\underset{\sim}{\sigma}^{R\prime} \tag{i}$$

$$\varepsilon^P_{kk} = \frac{1-2\nu}{E}\,\sigma^R_{kk} \tag{ii}$$

Suppose [C] holds. Then (d) or (e) must be true. This implies, in light of (H2), that

$$d\sigma^R_{ij} = \begin{cases} d\ell\,\dfrac{\partial \hat{F}}{\partial \varepsilon_{ij}} \quad , & d\ell \in \mathbb{R} \\ \text{or } 0 \quad . \end{cases}$$

Then, (2.24) $\Rightarrow d\sigma^R_{kk} = 0$, so by virtue of (H3),

$$[C] \Rightarrow \sigma^R_{kk} = 0 \quad . \tag{iiia}$$

Alternatively, suppose [Γ+,∘,-] hold. Then (δ), (δ∘), or (ε) holds. Invoking (H2), (2.24), and (H3) as for the other case, one obtains

$$[\Gamma+,\circ,-] \Rightarrow \varepsilon^P_{kk} = 0 \quad . \tag{iiib}$$

Thus (H7), (iiia), (iiib), and (ii) ⇒ (2.25), as required.

Re 2.26: (2.25) $\Rightarrow \underset{\sim}{\varepsilon}^{P\prime} = \underset{\sim}{\varepsilon}^P$ and $\underset{\sim}{\sigma}^{R\prime} = \underset{\sim}{\sigma}^R$, so

$$(i) \Rightarrow \underset{\sim}{\varepsilon}^P = \frac{1+\nu}{E}\,\underset{\sim}{\sigma}^R \tag{iv}$$

Equation (iv) applies also to each increment of $\underset{\sim}{\varepsilon}^P$ and $\underset{\sim}{\sigma}^R$, so, invoking (H4),

$$\Lambda = \frac{1+\nu}{E}\,L \tag{v}$$

The transformations (2.26) follow immediately from (H2), (iv), and (v), with (H1) assuring the invertibility of Hooke's law. Q.E.D.

2.3.2 Relationships Between Corresponding Model Parameters

The constitutive models associated with [C] and [Γ+,∘,-], as outlined in the last lemma, will be equivalent only if the stress- and strain-space plastic parameters are properly related to one another. The appropriate relations, adopted as hypotheses (H9), (H10), and (H11), readily give rise to a number of important results.

Lemma 2.4 In addition to the hypotheses of Lemma 2.3, assume that

$$F(\underset{\sim}{x}') = \Phi\left(\frac{E}{1+\nu}\,\underset{\sim}{x}'\right) \quad \text{on} \quad \text{sym}(\mathbb{R}^3) \; ; \tag{H9}$$

$$c(x) = \frac{1+\nu}{E}\left[\frac{1+\nu}{E}\,\gamma\left(\frac{1+\nu}{E}\,x\right) + 1\right] \quad \text{on} \quad \mathbb{R} \; ; \tag{H10}$$

$$k(x) = \kappa\left(\frac{1+\nu}{E}\,x\right) \quad \text{on} \quad \mathbb{R} \; . \tag{H11}$$

Then

$$k(L) = \kappa(\Lambda) \tag{2.27}$$

$$c(L) = \frac{1+\nu}{E}\left[\frac{1+\nu}{E}\,\gamma(\Lambda) + 1\right] \; , \tag{2.28}$$

$$F\left([\underset{\sim}{\varepsilon} - c(L)\underset{\sim}{\sigma}^R]'\right) = \Phi\left([\underset{\sim}{\sigma} - \gamma(\Lambda)\underset{\sim}{\varepsilon}^P]'\right) \tag{2.29}$$

$$\hat{F}\left(\underset{\sim}{\varepsilon},\underset{\sim}{\sigma}^R,L\right) = \hat{\Phi}\left(\underset{\sim}{\sigma},\underset{\sim}{\varepsilon}^P,\Lambda\right) \; . \tag{2.30}$$

$$\frac{\partial \hat{F}}{\partial \varepsilon_{ij}}\left(\underset{\sim}{\varepsilon},\underset{\sim}{\sigma}^R,L\right) = \frac{E}{1+\nu}\,\frac{\partial \hat{\Phi}}{\partial \sigma_{ij}}\left(\underset{\sim}{\sigma},\underset{\sim}{\varepsilon}^P,\Lambda\right) \tag{2.31}$$

$$\frac{dk(L)}{dL} = \frac{1+\nu}{E}\,\frac{d\kappa(\Lambda)}{d\Lambda} \tag{2.32}$$

$$\frac{dc(L)}{dL} = \left(\frac{1+\nu}{E}\right)^3 \frac{d\gamma(\Lambda)}{d\Lambda} \; , \tag{2.33}$$

where it is understood that in each of the above, $(\underset{\sim}{\varepsilon},\underset{\sim}{\sigma}^R,L)$ is related to $(\underset{\sim}{\sigma},\underset{\sim}{\varepsilon}^P,\Lambda)$ through (2.26).

Proof.

Re (2.27): (H11) and (2.26) $\Rightarrow$ (2.27).

Re (2.28): (H10) and (2.26) $\Rightarrow$ (2.28).

Re (2.29): Invoking (2.26), Lemma 2.2, and then (2.28), one establishes that

$$[\underset{\sim}{\varepsilon} - c(L)\underset{\sim}{\sigma}^R]' = \frac{1+\nu}{E}[\underset{\sim}{\sigma} - \gamma(L)\underset{\sim}{\varepsilon}^P]' \quad .$$

This result and (H9) $\Rightarrow$ (2.29).

Re (2.30): (H5), (2.27), and (2.29) $\Rightarrow$ (2.30).

Re (2.31): In light of (H5) and (H6), it is possible to differentiate (2.30) through use of the chain rule. Statement (2.31) follows, then, upon invoking (2.26), (H1), (H5), Lemma 2.1 and Lemma 2.2.

Re (2.32): (H6), (2.27), and (2.26) $\Rightarrow$ (2.32).

Re (2.33): (H6), (2.28), and (2.26) $\Rightarrow$ (2.33). Q.E.D.

Equations (2.27) through (2.33) link a number of the quantities arising in the strain-space theory with their more familiar counterparts from stress space. Thus, while laying groundwork for the equivalence theorem, these results serve also to bridge the gap between the two formulations on an intuitive level.

2.3.3 Loading Criteria for the Stress- and Strain-Space Theories

The matter of a strain-space loading criterion has proved somewhat troublesome in the past and accordingly deserves careful attention here. Naghdi [10,11], for instance, in pioneering strain-space plasticity established most of the results of the last section but seemingly overlooked the possibility of setting up a strain-space loading rule equivalent to the traditional one in stress space. This makes Lemma 2.6 all the more significant.

A brief digression is in order first. Lemma 2.5 sets forth a basic result on the inner products of deviatoric tensors.

Lemma 2.5 Let $\underset{\sim}{\alpha}'$ and $\underset{\sim}{\beta}'$ be the deviatoric parts of two-tensors $\underset{\sim}{\alpha}$ and and $\underset{\sim}{\beta}$, respectively. Then

$$\alpha'_{ij}\,\beta_{ij} = \alpha'_{ij}\,\beta'_{ij}$$

Proof: The result follows readily from (2.17). Q.E.D.

Return now to the question of plastic loading. Without introducing any further hypotheses, Lemma 2.6 establishes the relationship between D and Δ and then deals with the inner products which serve as loading criteria for the stress- and strain-space theories.

Lemma 2.6 Under the hypotheses of Lemma 2.4,

$$D = \Delta + \frac{E}{1+\nu}\frac{\partial\hat{\Phi}}{\partial\sigma_{mn}}\frac{\partial\hat{\Phi}}{\partial\sigma_{mn}} = \Delta + \frac{1+\nu}{E}\frac{\partial\hat{F}}{\partial\varepsilon_{mn}}\frac{\partial\hat{F}}{\partial\varepsilon_{mn}} \quad . \tag{2.34}$$

Also,

$$(e) \text{ or } (\varepsilon) \Rightarrow \frac{\partial\hat{F}}{\partial\varepsilon_{k\ell}}\,d\varepsilon_{k\ell} = \frac{\partial\hat{\Phi}}{\partial\sigma_{k\ell}}\,d\sigma_{k\ell} \quad , \tag{2.35}$$

and if Δ, like D, is nonzero,

$$(d) \text{ or } (\delta) \Rightarrow \frac{\frac{\partial\hat{F}}{\partial\varepsilon_{k\ell}}\,d\varepsilon_{k\ell}}{D} = \frac{\frac{\partial\hat{\Phi}}{\partial\sigma_{k\ell}}\,d\sigma_{k\ell}}{\Delta} \tag{2.36}$$

In all of the above it is understood that D and $\frac{\partial\hat{F}}{\partial\varepsilon_{ij}}$ are evaluated at $(\underset{\sim}{\varepsilon},\underset{\sim}{\sigma}^R,L)$; Δ and $\frac{\partial\hat{\Phi}}{\partial\sigma_{ij}}$ are evaluated at $(\underset{\sim}{\sigma},\underset{\sim}{\varepsilon}^P,\Lambda)$; and $(\underset{\sim}{\varepsilon},\underset{\sim}{\sigma}^R,L)$ and $(\underset{\sim}{\sigma},\underset{\sim}{\varepsilon}^P,L)$ are related through equations (2.26).

Proof.

Re (2.34): Substitute from (2.28), (2.31), (2.26), (2.33), (2.27), and (2.32) into the expression for D given in (H8). Simplifying, one recognizes the corresponding expression for Δ. Thus, and invoking (2.31), the result follows.

Re (2.35): In view of Lemma 2.2 and (H1), either (ε) or (e) implies

$$d\underset{\sim}{\varepsilon}' = \frac{1+\nu}{E}\, d\underset{\sim}{\sigma}' \qquad \text{(i)}$$

To establish (2.35), invoke (2.24) together with Lemma 2.5, substitute from (i) and (2.31), and then use (2.24) and Lemma 2.5 once more.

Re (d) $\Rightarrow$ (2.36): It follows from (d) and (H2) that

$$D d\sigma_{ij}^R = \frac{\partial \hat{F}}{\partial \varepsilon_{ij}} \frac{\partial \hat{F}}{\partial \varepsilon_{mn}}\, d\varepsilon_{mn} \qquad \text{(ii)}$$

Starting with (ii), invoke (H2); (2.24) and Lemma 2.5; Lemma 2.2; (2.25); (2.26); (2.31); and again (2.24) and Lemma 2.5. In this way one obtains

$$D d\sigma_{ij}^R = \frac{E}{1+\nu} \frac{\partial \hat{\Phi}}{\partial \sigma_{ij}} \frac{\partial \hat{\Phi}}{\partial \sigma_{mn}} (d\sigma_{mn} + d\sigma_{mn}^R) \qquad \text{(iii)}$$

Multiply through (iii) by $\frac{\partial \hat{\Phi}}{\partial \sigma_{ij}}$ and sum over i and j. After some rearranging, invoke (2.34) to get

$$\Delta \frac{\partial \hat{\Phi}}{\partial \sigma_{mn}} d\sigma_{mn}^R = \frac{E}{1+\nu} \frac{\partial \hat{\Phi}}{\partial \sigma_{k\ell}} \frac{\partial \hat{\Phi}}{\partial \sigma_{k\ell}} \frac{\partial \hat{\Phi}}{\partial \sigma_{mn}}\, d\sigma_{mn}$$

Now multiply through (iii) by Δ and substitute from the above. Invoking (2.34) and (2.31), one finds that

$$\Delta D d\sigma^R_{ij} = \frac{\partial \hat{F}}{\partial \varepsilon_{ij}} \frac{\partial \hat{\Phi}}{\partial \sigma_{mn}} d\sigma_{mn} D \qquad \text{(iv)}$$

Recall that $D \neq 0$ by (H8) and that Δ is also assumed here to be nonzero. Moreover, recall from (H6) that the quantities $\frac{\partial \hat{F}}{\partial \varepsilon_{ij}}$ cannot all vanish at once. The desired result, therefore, follows from (ii) and (iv).

Re (δ) $\Rightarrow$ (2.36): Similar to above. Q.E.D.

To see the significance of Lemma 2.6, consider the case of strain hardening, for which Δ is positive as well as D. In light of (H7), statements (2.35) and (2.36) assure that $\frac{\partial \hat{F}}{\partial \varepsilon_{ij}} d\varepsilon_{ij}$ and $\frac{\partial \hat{\Phi}}{\partial \sigma_{ij}} d\sigma_{ij}$ will always take on the same sign. It makes no difference, therefore, which of these inner products is used as a loading criterion. This somewhat surprising result plays a key role in proving the equivalence theorem of the next section.

2.3.4 Equivalence Theorem

It was claimed at the beginning of Section 2.3 that constitutive laws [C] and [$\Gamma+, \circ, -$] can be made equivalent to one another. Theorem 2.1 will prove this assertion, making use of the foregoing lemmas.

Theorem 2.1. Under the hypotheses of Lemma 2.4, constitutive law [C] is equivalent to either [$\Gamma+$], [$\Gamma\circ$], or [$\Gamma-$], depending on whether Δ is positive, zero, or negative, respectively.

Proof.

Case I: $\Delta > 0$ (i)

Re $[C] \Rightarrow [\Gamma+]$:

By (2.30), (a) $\Rightarrow$ (α) , as required.

Also, (β) $\Leftrightarrow$ (b) (ii)

According to [C], either (d) or (e) holds. Because of (2.35), (2.36), (i), and (H8), therefore,

(γ) $\Leftrightarrow$ (c) (iii)

Thus,

(β) and (γ) $\Rightarrow$ (b) and (c) in view of (ii), (iii);
$\Rightarrow$ (d) by virtue of [C];
$\Rightarrow$ (δ)

The last line follows upon invoking (i) and (2.36); (H1); (2.24) and Lemma 2.2; and finally (2.31). Similarly,

not (β) or not (γ) $\Rightarrow$ not (b) or not (c) by (ii), (iii) ;
$\Rightarrow$ (e) by [C] ;
$\Rightarrow$ (ε) by (H1) .

Thus $[C] \Rightarrow [\Gamma+]$ when $\Delta > 0$.

Re $[\Gamma+] \Rightarrow [C]$: Similar to above.

Case II: $\Delta = 0$ (iv)

Re $[C] \Rightarrow [\Gamma_o]$:

By (2.30), (a) $\Rightarrow$ (α) , as required.

Also, (β) $\Leftrightarrow$ (b) . (v)

Say (β) is true. Then, to establish [$\Gamma\circ$], it remains to show that:

$$(\phi) \text{ is true} \tag{vi}$$

$$(\gamma\circ) \Rightarrow (\delta\circ) \text{ or } (\varepsilon) \tag{vii}$$

$$\text{and} \qquad \text{not } (\gamma\circ) \Rightarrow (\varepsilon) \tag{viii}$$

Re (β) $\Rightarrow$ (vi): Assuming [C] and (β) to hold and recalling (H1), it follows from (v) that

$$(c) \Rightarrow (d) \ , \tag{ix}$$

$$\text{not } (c) \Rightarrow (e) \Rightarrow (\varepsilon) \ . \tag{x}$$

To track down the ramifications of (d), multiply through it by $\frac{\partial\hat{\Phi}}{\partial\sigma_{ij}}$ and sum over i and j. Then invoke (H1), (2.24), and Lemma 2.2; (2.31); and finally (2.34) and (iv). In this way one determines that

$$(d) \Rightarrow (\gamma\circ) \tag{xi}$$

Now,

$$\text{not } (c) \Rightarrow (\phi) \ , \tag{xii}$$

which may be verified by invoking (2.24) and Lemma 2.5; (ε); Lemma 2.2; (2.31); and, once more,(2.24) and Lemma 2.5. Statements (ix), (xi), and (xii) establish (vi), as required.

Re (β) $\Rightarrow$ (vii): The main challenge is to show that

$$(c) \Rightarrow (\delta\circ) \ . \tag{xiii}$$

Toward this end, invoke (ix) and then multiply through (d) by $\underset{\sim}{\kappa}$, in conformity with (H1). Statement (xiii) follows in light of (2.24) and

Lemma 2.2; (2.31); and (c) and (H8). The required result, (vii), follows trivially from (x) and (xiii).

Re $(\beta) \Rightarrow$ (viii): (xi), (ix), and (x) $\Rightarrow$ (viii).

These results establish the validity of $[\Gamma\circ]$ in the case where (β) is true.

Now say (β) is false. To establish $[\Gamma\circ]$, it suffices to show that (ε) holds. By (v),

$$\begin{aligned} \text{not } (\beta) \Rightarrow \text{not } (b) &\Rightarrow (e) \quad \text{by} \quad [C] \\ &\Rightarrow (\varepsilon) \quad \text{by} \quad (H1) \end{aligned}$$

This completes the proof that $[C] \Rightarrow [\Gamma\circ]$ when $\Delta = 0$.

Re $[\Gamma\circ] \Rightarrow [C]$:

$$\begin{aligned} &\text{By (2.30)} \quad (\alpha) \Rightarrow (a) \ , \ \text{as required.} \\ &\text{Also,} \quad\quad (b) \Leftrightarrow (\beta) \ . \end{aligned} \tag{xiv}$$

Say (b) is true. Then, to establish [C] it remains to show that:

$$(c) \Rightarrow (d) \tag{xv}$$

$$\text{and} \quad \text{not } (c) \Rightarrow (e) \tag{xvi}$$

Toward this end, substitute for $d\underset{\sim}{\varepsilon}$, using alternatively $(\delta\circ)$ and (ε). Then invoke (2.24), (H1), and Lemma 2.2; make use of (2.31); and note, in view of $[\Gamma\circ]$, that $(\delta\circ) \Rightarrow (\gamma\circ)$. In this way, one deduces that

$$\frac{\partial \hat{F}}{\partial \varepsilon_{ij}} d\varepsilon_{ij} = \begin{cases} \lambda \left(\frac{1+\nu}{E}\right) \frac{\partial \hat{F}}{\partial \varepsilon_{ij}} \frac{\partial \hat{F}}{\partial \varepsilon_{ij}} & \text{if } (\delta\circ) \text{ holds} \ , \\ \frac{\partial \hat{\Phi}}{\partial \sigma_{ij}} d\sigma_{ij} & \text{if } (\varepsilon) \text{ holds} \end{cases} \tag{xvii}$$

Now, in view of (xiv), (b) and $[\Gamma\circ]$ $\Rightarrow$ (ϕ). Noting, in addition, (H1) and (2.15b), it follows from (xvii) that

$$(\delta\circ) \Rightarrow (c)$$
$$(\varepsilon) \Rightarrow \text{not } (c)$$

But $[\Gamma^{\circ}]$ assures that $(\varepsilon) \Leftrightarrow$ not $(\delta\circ)$, so

$$(c) \Rightarrow (\delta\circ) \qquad \text{(xviii)}$$
$$\text{not } (c) \Rightarrow (\varepsilon) \qquad \text{(xix)}$$

Statement (xv) follows readily now. Multiply through $(\delta\circ)$ by $\underset{\sim}{c}$ and simplify using (H1), invoke (2.24) and Lemma 2.2, and apply (2.31). Then substitute for λ from (xvii), and invoke (2.34) and (iv). Thus, one establishes that

$$(\delta\circ) \Rightarrow (d)$$

This result, in conjunction with (xviii), implies (xv), as required.

Similarly, (xix) $\Rightarrow$ (xvi) in light of (H1). This establishes that [C] holds in the case where (b) is true.

Now say (b) is false. To establish [C], it suffices to show that (e) holds. By virtue of (xiv), $[\Gamma\circ]$, and (H1),

$$\text{not } (b) \Rightarrow \text{not } (\beta) \Rightarrow (\varepsilon) \Rightarrow (e)$$

This completes the proof that $[\Gamma\circ] \Rightarrow$ [C] when $\Delta = 0$.

Case III: $\Delta < 0$. Similar to Case I Q.E.D.

2.3.5 Remarks and Observations

The analysis for bilinear, elastoplastic models is now complete, but some of the results deserve comment. To begin with, consider again hypothesis (H9). For a given constitutive behavior, the stress- and strain-space models will evidently feature loading surfaces that differ only in scale. Thus the strain-space counterpart of the Tresca yield surface is a regular hexagonal cylinder centered along the line $\varepsilon_1=\varepsilon_2=\varepsilon_3$; and similarly for the von Mises surface. These strain-space relaxation surfaces should therefore seem quite natural to anyone who has worked with conventional plasticity.

Note the versatility of the strain-space formulation. The conventional theory requires one set of constitutive relations for strain hardening, another for ideal plasticity, and yet another for strain softening. In strain space, on the other hand, just one set can accommodate all three cases. This simplification could be of some import in computer applications.

Some final comments center upon the hardening laws and stem from hypotheses (H10) and (H11). For isotropic hardening/softening (in stress space), $\gamma = 0$ and κ grows or shrinks as the plastic deformations proceed. Corresponding to this, $c = \frac{1+\nu}{E}$ and k fluctuates like κ, so the loading surface in strain space translates as well as changing size. In a similar way, the strain space models equivalent to kinematic hardening/softening and to perfect plasticity feature translating relaxation surfaces. This may seem bizarre in the case of perfect plasticity, but it is in fact fortunate. In stress-space computer codes for ideal plasticity, the stress point tends under loading to follow the local

tangent and inevitably winds up outside the surface on account of convexity. Accordingly, Krieg and Krieg [16] discuss and evaluate three common schemes for returning the stress point to the yield surface. The best way to handle the problem, though, may well be to circumvent it — by working in strain space. More will be said about this in Chapter IV.

CHAPTER III

MODELS WITH MULTIPLE LOADING SURFACES

The constitutive models of Chapter II allow for only a bilinear approximation to the observed relationship between stress and strain. Accordingly, a number of authors [5,6,7] have suggested extending plasticity theory to incorporate several loading surfaces. If the surfaces behave like those of the last chapter and their respective plastic contributions are summed, the resulting stress-strain law will be multilinear. This is true whether stress- or strain-space surfaces are used. In light of Chapter II, one might expect the two alternatives to yield equivalent formulations, but such is not the case. It will be shown that for equivalence to hold, there must be coupling between the surfaces. This gives rise to some analytical complications.

Section 3.1 contains a detailed discussion of multiple-yield-surface models. Section 3.2 then presents an equivalence theorem.

3.1 Multiple-Yield-Surface Models

This section lays out side by side the stress- and strain-space models which will ultimately figure in the equivalence theorem. Each model features N loading surfaces, with coupling arising through the hardening laws.

3.1.1 Incrementally Elastic Behavior

Suppose that incrementally elastic deformations are governed by response and compliance tensors of the form

$$c_{ijk\ell} = \frac{E}{1+\nu}\left[\delta_{ik}\delta_{j\ell} + \frac{\nu}{1-2\nu}\,\delta_{ij}\delta_{k\ell}\right]$$

$$\kappa_{ijk\ell} = \frac{1}{E}\left[(1+\nu)\delta_{ik}\delta_{j\ell} - \nu\delta_{ij}\delta_{k\ell}\right]; \qquad \text{(H1)}$$

$$\text{where } E > 0 \quad \text{and} \quad -1 < \nu < \frac{1}{2} \ ;$$

and that deviations from Hookean linearity are accounted for either by subtracting stress relaxations or by adding plastic strains. That is,

EITHER

$$[C] \qquad \underset{\sim}{\sigma} = \underset{\sim\sim}{c}\underset{\sim}{\varepsilon} - \sum_{\phi\in N} \underset{\sim}{\sigma}^{R}_{\phi}$$

OR

$$[\Gamma] \qquad \underset{\sim}{\varepsilon} = \underset{\sim\sim}{\kappa}\underset{\sim}{\sigma} + \sum_{\phi\in N} \underset{\sim}{\varepsilon}^{P}_{\phi} \qquad \text{(H2)}^{1}$$

where

$$N = \{1,2,3,\ldots N\} \qquad \text{(H3)}$$

Assume that the material behaves elastically at the outset of loading. Thus,

$$\underset{\sim}{\sigma}^{R}_{\phi} = \underset{\sim}{\varepsilon}^{P}_{\phi} = \underset{\sim}{0} \qquad \forall\phi \in N \ , \ \text{initially} \qquad \text{(H4)}$$

After loading, some plastic effects will have set in. As a measure of the influence of these effects, define

$$L^{\phi} = \int \sqrt{\frac{2}{3}\, d\sigma^{R}_{ij\phi} d\sigma^{R}_{ij\phi}} \ , \quad \Lambda^{\phi} = \int \sqrt{\frac{2}{3}\, d\varepsilon^{P}_{ij\phi} d\varepsilon^{P}_{ij\phi}} \quad \forall\phi \in N \qquad \text{(H5)}$$

where the integrations are to be carried out over the entire history of the deformation;

and

---

[1] The summation convention will apply only to Latin indices. Whenever there is summation over a Greek index, this will be indicated explicitly.

$$\underset{\sim}{S}^{\phi} = \sum_{\substack{\psi \in N \\ \psi \neq \phi}} \underset{\sim}{\sigma}^{R}_{\psi} \quad , \qquad \underset{\sim}{E}^{\phi} = \sum_{\substack{\psi \in N \\ \psi \neq \phi}} \underset{\sim}{\varepsilon}^{P}_{\psi} \qquad \forall \phi \in N \ . \tag{H6}$$

For each constitutive model, there are N loading surfaces, and the current value of strain (or stress, for the stress-space theory) can never lie outside any of these surfaces. Thus,

$$\left.\begin{aligned} \hat{F}^{\phi}(\underset{\sim}{\varepsilon}, \underset{\sim}{S}^{\phi}, \underset{\sim}{\sigma}^{R}_{\phi}, L^{\phi}) \leq 0 \\ \hat{\Phi}^{\phi}(\underset{\sim}{\sigma}, \underset{\sim}{E}^{\phi}, \underset{\sim}{\varepsilon}^{P}_{\phi}, \Lambda^{\phi}) \leq 0 \end{aligned}\right\} \ \forall \phi \in N \ . \tag{H7}$$

At any given instant the ϕ^{th} surface can contribute to the mechanical response only if $\phi \in W$ (or Ω), where

$$\begin{aligned} W &= \left\{ \phi \,|\, \phi \in N \quad \text{and} \quad \hat{F}^{\phi}(\underset{\sim}{\varepsilon}, \underset{\sim}{S}^{\phi}, \underset{\sim}{\sigma}^{R}_{\phi}, L^{\phi}) = 0 \right\} \\ \Omega &= \left\{ \phi \,|\, \phi \in N \quad \text{and} \quad \hat{\Phi}^{\phi}(\underset{\sim}{\sigma}, \underset{\sim}{E}^{\phi}, \underset{\sim}{\varepsilon}^{P}_{\phi}, \Lambda^{\phi}) = 0 \right\} \end{aligned} \tag{H8}$$

If the instantaneous strain (or stress) happens to lie inside all N surfaces, Hooke's law will prevail incrementally.

3.1.2 The Hardening Law

In order to satisfy (H7), the loading surfaces must in general move during plastic deformations. To prescribe these motions — and thus set down the so-called hardening law — it suffices to assume an analytical form for the functions $\hat{F}^{\phi}$ (or $\hat{\Phi}^{\phi}$). Accordingly, set

$$\begin{aligned} \hat{F}^{\phi}(\underset{\sim}{\varepsilon}, \underset{\sim}{S}^{\phi}, \underset{\sim}{\sigma}^{R}_{\phi}, L^{\phi}) &\equiv F(\underset{\sim}{\varepsilon} - b\underset{\sim}{S}^{\phi} - c\underset{\sim}{\sigma}^{R}_{\phi}) - [k^{\phi}(L^{\phi})]^2 \\ \hat{\Phi}^{\phi}(\underset{\sim}{\sigma}, \underset{\sim}{E}^{\phi}, \underset{\sim}{\varepsilon}^{P}_{\phi}, \Lambda^{\phi}) &\equiv \Phi(\underset{\sim}{\sigma} - \beta\underset{\sim}{E}^{\phi} - \gamma\underset{\sim}{\varepsilon}^{P}_{\phi}) - [\kappa^{\phi}(\Lambda^{\phi})]^2 \end{aligned} \qquad \forall \phi \in N \ . \tag{H9}$$

where

$$\left.\begin{aligned} F(\underset{\sim}{x}) &= F(\underset{\sim}{x}') = F(\underset{\sim}{x}^T) \\ \Phi(\underset{\sim}{x}) &= \Phi(\underset{\sim}{x}') = \Phi(\underset{\sim}{x}^T) \end{aligned}\right\} \quad \forall \underset{\sim}{x} \in \text{lin}\,(\mathbb{R}^3) \quad ,$$

$$F,\ \Phi \in C^1\,(\text{lin}(\mathbb{R}^3)) \quad ,$$

$$\frac{\partial F}{\partial x_{ij}}\frac{\partial F}{\partial x_{ij}} > 0 \quad , \quad \frac{\partial \Phi}{\partial x_{ij}}\frac{\partial \Phi}{\partial x_{ij}} > 0 \qquad \forall \underset{\sim}{x} \in \text{lin}\,(\mathbb{R}^3) \quad , \tag{H10}$$

$$\left.\begin{aligned} k^\phi &: \mathbb{R} \to (0,\infty) \ , \ k^\phi \in C^1 \\ \kappa^\phi &: \mathbb{R} \to (0,\infty) \ , \ \kappa^\phi \in C^1 \end{aligned}\right\} \quad \forall \phi \in N$$

Hypothesis (H9) can accommodate either isotropic or kinematic plasticity, or, for that matter, any linear combination of the two. What is more, through parameters b and β, it allows for coupling amongst the surfaces. Suppose, for example, that the innermost surface produces an increment of stress relaxation, causing it to translate under the influence of c. The other surfaces will likewise move, on account of b, even though they are not being loaded.

This coupling can, of course, be overridden. If β is set equal to zero, the yield surfaces function independently of one another. In this case, once the stress increment is known, the surfaces can be examined one by one to determine their individual contributions to the overall compliance. If, in addition, the κ^ϕ are chosen to be constants, this model reduces to one proposed by Iwan [5] and implemented by Joyner [1].

In a similar way, the strain-space models obtained by setting b to zero lend themselves readily to the calculation of elastoplastic stiffness. For this reason the computer program described in Chapter IV is based upon a formulation of this sort.

3.1.3 Normality

Under the influence of parameters c and γ, each loading surface tends to move in the direction of the plastic increment associated with it. But how, in turn, are these increments directed? In the case of single-surface models, the stress relaxation increment always points along the outward normal to the surface that produced it. This rule follows mathematically from more elementary postulates, as shown in Section 2.1.3 and Appendix I. The derivation given there breaks down, though, when there is a plurality of loading surfaces. Accordingly, in this case, normality itself will be taken as a postulate:

$$d\sigma^R_{ij\phi} = \begin{cases} \dfrac{x^\phi H(x^\phi)}{\sqrt{D^\phi}} \dfrac{\partial \hat{F}^\phi}{\partial \varepsilon_{ij}} & \forall\phi \in W \\ 0 & \forall\phi \in N\text{-}W \end{cases} ; \qquad (H11)$$

$$d\varepsilon^P_{ij\phi} = \begin{cases} \dfrac{\xi^\phi H(\xi^\phi)}{\sqrt{\Delta^\phi}} \dfrac{\partial \hat{\Phi}^\phi}{\partial \sigma_{ij}} & \forall\phi \in \Omega \\ 0 & \forall\phi \in N\text{-}\Omega \end{cases}$$

where H is the Heaviside step function, and

$$
\begin{aligned}
D^{\phi} &= c\,\frac{\partial \hat{F}^{\phi}}{\partial \varepsilon_{ij}}\,\frac{\partial \hat{F}^{\phi}}{\partial \varepsilon_{ij}} + 2k^{\phi}(L^{\phi})k^{\phi'}(L^{\phi})\sqrt{\frac{2}{3}\,\frac{\partial \hat{F}^{\phi}}{\partial \varepsilon_{ij}}\,\frac{\partial \hat{F}^{\phi}}{\partial \varepsilon_{ij}}} \\
&\geq C\,\frac{\partial \hat{F}^{\phi}}{\partial \varepsilon_{ij}}\,\frac{\partial \hat{F}^{\phi}}{\partial \varepsilon_{ij}} \quad , \quad C > 0 \quad ; \\
\Delta^{\phi} &= \gamma\,\frac{\partial \hat{\Phi}^{\phi}}{\partial \sigma_{ij}}\,\frac{\partial \hat{\phi}^{\phi}}{\partial \sigma_{ij}} + 2\kappa^{\phi}(\Lambda^{\phi})\kappa^{\phi'}(\Lambda^{\phi})\sqrt{\frac{2}{3}\,\frac{\partial \hat{\Phi}^{\phi}}{\partial \sigma_{ij}}\,\frac{\partial \hat{\Phi}^{\phi}}{\partial \sigma_{ij}}} \\
&\geq \Gamma\,\frac{\partial \hat{\Phi}^{\phi}}{\partial \sigma_{ij}}\,\frac{\partial \hat{\phi}^{\phi}}{\partial \sigma_{ij}} \quad , \quad \Gamma > 0 \quad ; \qquad \text{(H12)} \\
&\qquad\qquad \forall \phi \in N \quad .
\end{aligned}
$$

Throughout Chapter III it is understood that

$$
\begin{aligned}
&\frac{\partial \hat{F}^{\phi}}{\partial \varepsilon_{ij}} \text{ is evaluated at } (\underset{\sim}{\varepsilon}, \underset{\sim}{S}^{\phi}, \underset{\sim}{\sigma}^{R}_{\phi}, L^{\phi}), \text{ holding } \underset{\sim}{S}^{\phi},\ \underset{\sim}{\sigma}^{R}_{\phi}, \\
&\qquad\qquad\qquad\qquad\qquad\qquad \text{and } L^{\phi} \text{ constant;} \\
&\frac{\partial \hat{\Phi}^{\phi}}{\partial \sigma_{ij}} \text{ is evaluated at } (\underset{\sim}{\sigma}, \underset{\sim}{E}^{\phi}, \underset{\sim}{\varepsilon}^{P}_{\phi}, \Lambda^{\phi}), \text{ holding } \underset{\sim}{E}^{\phi},\ \underset{\sim}{\varepsilon}^{P}_{\phi}, \\
&\qquad\qquad\qquad\qquad\qquad\qquad \text{and } \Lambda^{\phi} \text{ constant.}
\end{aligned}
\qquad \text{(H13)}
$$

3.1.4 Volumetric Strains

In the constitutive models of Chapter II the loading surfaces were deliberately designed to rule out any plastic influence upon the volumetric component of strain. Since the loading functions introduced above are almost identical in form to those of the last chapter, one might expect a similar rule to prevail in this case as well. This question is explored in the following lemma.

Lemma 3.1 In view of (H4), (H9), (H10), and (H11),

$$
\sigma^{R}_{ii\phi} = \varepsilon^{P}_{ii\phi} = 0 \qquad \forall \phi \in N
$$

Proof. In light of (H9) and (H10), one can invoke Lemma 2.1. The result follows, then, on account of (H11) and (H4). Q.E.D.

Thus the plastic increments will again be purely deviatoric.

3.1.5 Consistency and Loading Criteria

The quantities D^{ϕ} and Δ^{ϕ}, introduced somewhat arbitrarily above, arise as in the one-surface models upon invoking the principle of consistency. For brevity's sake the discussion will focus, both here and throughout the balance of Section 3.1, upon the strain-space theory. The analysis in stress space proceeds similarly.

Suppose the strain point lies at some instant on the ϕ^{th} relaxation surface. Then, during the next strain increment this surface will undergo either

$$\text{unloading} \Leftrightarrow d\hat{F}^{\phi} \leq 0 \quad \text{and} \quad d\underset{\sim}{\sigma}^{R}_{\phi} = \underset{\sim}{0}; \text{ or} \tag{3.1}$$

$$\text{loading} \Leftrightarrow d\hat{F}^{\phi} = 0 \quad \text{and} \quad d\underset{\sim}{\sigma}^{R}_{\phi} \neq \underset{\sim}{0}. \tag{3.2}$$

In either case, $d\hat{F}^{\phi}$ denotes the change occurring in $\hat{F}^{\phi}$ as a result of a strain increment. Thus, applying the chain rule with reference to (H9), (H5), and (H6), substituting from (H11), and invoking (H12), one concludes that

$$\frac{d\hat{F}^{\phi}}{\sqrt{D^{\phi}}} = \frac{\frac{\partial \hat{F}^{\phi}}{\partial \varepsilon_{ij}} d\varepsilon_{ij}}{\sqrt{D^{\phi}}} - b \sum_{\substack{\psi \in W \\ \psi \neq \phi}} \frac{\frac{\partial \hat{F}^{\phi}}{\partial \varepsilon_{ij}} \frac{\partial \hat{F}^{\psi}}{\partial \varepsilon_{ij}}}{\sqrt{D^{\phi} D^{\psi}}} x^{\psi} H(x^{\psi}) - x^{\phi} H(x^{\phi})$$

Comparing the above and (H11) with (3.1) and (3.2), one concludes that the ϕ^{th} surface will experience either unloading or loading, according to the following conditions:

$$\text{unloading} \Leftrightarrow \begin{cases} \dfrac{\dfrac{\partial \hat{F}^{\phi}}{\partial \varepsilon_{ij}} d\varepsilon_{ij}}{\sqrt{D^{\phi}}} - b \sum\limits_{\substack{\psi \in N \\ \psi \neq \phi}} \dfrac{\dfrac{\partial \hat{F}^{\phi}}{\partial \varepsilon_{ij}} \dfrac{\partial \hat{F}^{\psi}}{\partial \varepsilon_{ij}}}{\sqrt{D^{\phi} D^{\psi}}} x^{\psi} H(x^{\psi}) \leq 0 & (3.3a) \\ \text{and } x^{\phi} \leq 0 \quad ; \quad \text{or} & (3.3b) \end{cases}$$

$$\text{loading} \Leftrightarrow \begin{cases} \dfrac{\dfrac{\partial \hat{F}^{\phi}}{\partial \varepsilon_{ij}} d\varepsilon_{ij}}{\sqrt{D^{\phi}}} - b \sum\limits_{\substack{\psi \in N \\ \psi \neq \phi}} \dfrac{\dfrac{\partial \hat{F}^{\phi}}{\partial \varepsilon_{ij}} \dfrac{\partial \hat{F}^{\psi}}{\partial \varepsilon_{ij}}}{\sqrt{D^{\phi} D^{\psi}}} x^{\psi} H(x^{\psi}) > 0 & (3.4a) \\ \text{and} & \\ x^{\phi} = \dfrac{\dfrac{\partial \hat{F}^{\phi}}{\partial \varepsilon_{ij}} d\varepsilon_{ij}}{\sqrt{D^{\phi}}} - b \sum\limits_{\substack{\psi \in N \\ \psi \neq \phi}} \dfrac{\dfrac{\partial \hat{F}^{\phi}}{\partial \varepsilon_{ij}} \dfrac{\partial \hat{F}^{\psi}}{\partial \varepsilon_{ij}}}{\sqrt{D^{\phi} D^{\psi}}} x^{\psi} H(x^{\psi}) & (3.4b) \end{cases}$$

In a corresponding way, all of the other surfaces upon which the strain point lies will likewise fall into one of the categories listed above.

How does one apply this analysis? If there is just one relaxation surface, or if b equals zero, the strategy is simple. Refer to statements (3.3a) and (3.4a) to determine which of the surfaces are in fact being loaded. Then invoke (3.4b) in each instance of loading to find x^{ϕ}, and substitute back into (H11) to obtain the corresponding increment of stress relaxation.

In the general case, on the other hand, to apply the loading test to any one surface, one needs to know already the stress relaxation increments generated by all the other surfaces. This coupling makes the present case hard to deal with. As a matter of fact, it is by no means self-evident whether the problem is even well-posed. To show that it is, one must establish: (i) that there always exists at least one set of x^{ϕ} such that, for each $\phi \in W$, either statements (3.3) or (3.4) hold; and (ii) that if there are multiple solution sets, they all yield the same stress relaxation increments when substituted into (H11). These issues will be dealt with in turn by Sections 3.1.6 and 3.1.7.

Both questions, as it turns out, are obscured by the fact that in general the set $\{x^{\phi}\}$ is not itself unique. For all, equation (3.4b) holds sway only over those $\phi \in W$ for which (3.4) is true — that is, over some subset $X \subset W$ which, incidentally, is unknown a priori. For those $\phi \in W\text{-}X$, the x^{ϕ} are nonpositive but otherwise unspecified.

3.1.6 Existence

Consider now in detail the question of existence. Since the nonpositive x^{ϕ} may be chosen arbitrarily, it is permissible to let them also satisfy (3.4b). Thus, to guarantee existence it will suffice to find a set of x^{ϕ} satisfying

$$x^{\phi} = \frac{\frac{\partial \hat{F}^{\phi}}{\partial \varepsilon_{ij}} d\varepsilon_{ij}}{\sqrt{D^{\phi}}} - b \sum_{\substack{\psi \in W \\ \psi \neq \phi}} \frac{\frac{\partial \hat{F}^{\phi}}{\partial \varepsilon_{ij}} \frac{\partial \hat{F}^{\psi}}{\partial \varepsilon_{ij}}}{\sqrt{D^{\phi} D^{\psi}}} x^{\psi} H(x^{\psi}) \quad \forall \phi \in W ,$$

$$\xi^{\phi} = \frac{\frac{\partial \hat{\Phi}^{\phi}}{\partial \sigma_{ij}} d\sigma_{ij}}{\sqrt{\Delta^{\phi}}} - \beta \sum_{\substack{\psi \in \Omega \\ \psi \neq \phi}} \frac{\frac{\partial \hat{\Phi}^{\phi}}{\partial \sigma_{ij}} \frac{\partial \hat{\Phi}^{\psi}}{\partial \sigma_{ij}}}{\sqrt{\Delta^{\phi} \Delta^{\psi}}} \xi^{\psi} H(\xi^{\psi}) \quad \forall \phi \in \Omega \tag{H14}$$

Once this is accomplished, define X to be $\{\phi | \phi \in W \text{ and } x^{\phi} > 0\}$. Statements (3.4) will hold for all $\phi \in X$, while the rest of the surfaces undergo unloading, in accordance with (3.3). All that remains is to show that (H14) possesses solutions. Lemma 3.2 establishes that it does, provided (H15) holds. The physical significance of (H15) will be discussed in Section 3.2.4.

Lemma 3.2 In addition to hypotheses (H3), (H5), (H6), H(8) - (H10), H(12), and (H13) suppose that

$$\text{(N-1)} \quad \left|\frac{b}{C}\right| < 1 \quad ,$$

$$\text{(N-1)} \quad \left|\frac{\beta}{\Gamma}\right| < 1 \tag{H15}$$

Then there exist solutions to equations (H14).

Proof.

Re: Strain-space model. The proof below follows a Picard iteration scheme. Accordingly, consider the sequence

$$\overset{\circ}{x}{}^{\phi} = 0 \qquad \forall \phi \in W \; ; \qquad \text{(i)}$$

$$\overset{\pi+1}{x}{}^{\phi} = \frac{\frac{\partial \hat{F}^{\phi}}{\partial \varepsilon_{ij}} d\varepsilon_{ij}}{\sqrt{D^{\phi}}} - b \sum_{\substack{\psi \in W \\ \psi \neq \phi}} \frac{\frac{\partial \hat{F}^{\phi}}{\partial \varepsilon_{ij}} \frac{\partial \hat{F}^{\psi}}{\partial \varepsilon_{ij}}}{\sqrt{D^{\phi} D^{\psi}}} \overset{\pi}{x}{}^{\psi} H\left(\overset{\pi}{x}{}^{\psi}\right) \qquad \forall \phi \in W \; , \qquad \text{(ii)}$$

$$\pi = 0,1,2,\ldots$$

Clearly,

$$\overset{\rho}{x}{}^{\phi} = \sum_{\pi=0}^{\rho-1} \overset{\pi+1}{x}{}^{\phi} - \overset{\pi}{x}{}^{\phi} \qquad \forall \phi \in W \; , \quad \rho = 1,2,3,\ldots \qquad \text{(iii)}$$

(H12), (H10) $\Rightarrow \exists M < \infty \ni$ for any given $d\underset{\sim}{\varepsilon}$

$$M = \max_{\phi \in W} \left| \frac{\frac{\partial \hat{F}^{\phi}}{\partial \varepsilon_{ij}} d\varepsilon_{ij}}{\sqrt{D^{\phi}}} \right| \qquad \text{(iv)}$$

Then,

$$\left| \overset{\pi+1}{x}{}^{\phi} - \overset{\pi}{x}{}^{\phi} \right| \leq \left[(N-1) \left| \frac{b}{C} \right| \right]^{\pi} M \qquad \forall \phi \in W \; , \qquad \text{(v)}$$

$$\pi = 0,1,2,\ldots$$

Statement (v) is proven by induction.

I. Re: $\pi = 0$. (v) follows immediately from (i), (ii), and (iv), when $\pi = 0$.

II. Re: (v) holds for $\pi = \tau \Rightarrow$ (v) holds for $\pi = \tau + 1$, $\tau = 0,1,2,\ldots$ For all $\phi \in W$, (ii) $\Rightarrow$

$$ {}^{\tau+2}x^{\phi} - {}^{\tau+1}x^{\phi} = -b \sum_{\substack{\psi \in W \\ \psi \neq \phi}} \frac{\frac{\partial \hat{F}^{\phi}}{\partial \varepsilon_{ij}} \frac{\partial \hat{F}^{\psi}}{\partial \varepsilon_{ij}}}{\sqrt{D^{\phi} D^{\psi}}} \left\{ {}^{\tau+1}x^{\psi} H\left({}^{\tau+1}x^{\psi}\right) - {}^{\tau}x^{\psi}\left(H\, {}^{\tau}x^{\psi}\right) \right\} $$

Thus, invoking (H12) and the triangle inequality, applying (v) for the case $\pi = \tau$, and making use of (H8) and (H3), one establishes (v) for the case $\pi = \tau + 1$, as required. In view of (v) and (H15), the series in (iii) converges geometrically as $\rho \to \infty$. Thus there exist

$$ x^{\phi} \equiv \lim_{\pi \to \infty} {}^{\pi}x^{\phi} \qquad \forall \phi \in W $$

Comparing (ii) with the first of (H14), it is clear that the x^{ϕ} constitute a solution, and the result follows.

Re: Stress-space model. Similar to above. Q.E.D.

The foregoing lemma does more than simply prove that there exist solutions to (H14). It provides as well a workable scheme for constructing such solutions. Indeed, Picard iteration lends itself to computer applications. Once a solution to (H14) has been found, the corresponding plastic increments can be found by substituting back into (H11).

3.1.7 Uniqueness

As already noted, there may well be more than one set of x^ϕ meeting the requirement that either (3.3) or (3.4) prevail for all $\phi \in W$. Accordingly, suppose for the strain-space model that

$$\left.\begin{aligned} &\exists \{x_1^\phi \,,\ \phi \in W\} \quad \text{and} \quad \{x_2^\phi \,,\ \phi \in W\} \ni \\ x_\rho^\phi \;=\; &\frac{\frac{\partial \hat{F}^\phi}{\partial \varepsilon_{ij}}\, d\varepsilon_{ij}}{\sqrt{D^\phi}} - b \sum_{\substack{\psi \in W \\ \psi \neq \phi}} \frac{\frac{\partial \hat{F}^\phi}{\partial \varepsilon_{ij}} \frac{\partial \hat{F}^\psi}{\partial \varepsilon_{ij}}}{\sqrt{D^\phi\, D^\psi}}\, x_\rho^\psi\, H\left(x_\rho^\psi\right) \quad \forall \phi \in X_\rho \,, \\ &\frac{\frac{\partial \hat{F}^\phi}{\partial \varepsilon_{ij}}\, d\varepsilon_{ij}}{\sqrt{D^\phi}} \le b \sum_{\substack{\psi \in W \\ \psi \neq \phi}} \frac{\frac{\partial \hat{F}^\phi}{\partial \varepsilon_{ij}} \frac{\partial \hat{F}^\psi}{\partial \varepsilon_{ij}}}{\sqrt{D^\phi\, D^\psi}}\, x_\rho^\psi\, H\left(x_\rho^\psi\right) \quad \forall \phi \in W - X_\rho \,; \\ &X_\rho \;=\; \{\phi \,|\, \phi \in W \quad \text{and} \quad x_\rho^\phi > 0\} \,, \quad \rho = 1,2. \end{aligned}\right\} \tag{3.5a}$$

For the stress-space model, suppose that

$$\left.\begin{aligned} &\exists \{\xi_1^\phi \,,\ \phi \in \Omega\} \quad \text{and} \quad \{\xi_2^\phi \,,\ \phi \in \Omega\} \ni \\ \xi_\rho^\phi \;=\; &\frac{\frac{\partial \hat{\Phi}^\phi}{\partial \sigma_{ij}}\, d\sigma_{ij}}{\sqrt{\Delta^\phi}} - \beta \sum_{\substack{\psi \in \Omega \\ \psi \neq \phi}} \frac{\frac{\partial \hat{\Phi}^\phi}{\partial \sigma_{ij}} \frac{\partial \hat{\Phi}^\psi}{\partial \sigma_{ij}}}{\sqrt{\Delta^\phi\, \Delta^\psi}}\, \xi_\rho^\psi\, H\left(\xi_\rho^\psi\right) \quad \forall \phi \in \Xi_\rho \,, \\ &\frac{\frac{\partial \hat{\Phi}^\phi}{\partial \sigma_{ij}}\, d\sigma_{ij}}{\sqrt{\Delta^\phi}} \le \beta \sum_{\substack{\psi \in \Omega \\ \psi \neq \phi}} \frac{\frac{\partial \hat{\Phi}^\phi}{\partial \sigma_{ij}} \frac{\partial \hat{\Phi}^\psi}{\partial \sigma_{ij}}}{\sqrt{\Delta^\phi\, \Delta^\psi}}\, \xi_\rho^\psi\, H\left(\xi_\rho^\psi\right) \quad \forall \phi \in \Omega - \Xi_\rho \,; \\ &\Xi_\rho \;=\; \{\phi \,|\, \phi \in \Omega \quad \text{and} \quad \xi_\rho^\phi > 0\}, \quad \rho = 1,2. \end{aligned}\right\} \tag{3.5b}$$

The plastic increment will still be uniquely determined through (H11) if

$$\begin{aligned} x_1^\phi \, H(x_1^\phi) &= x_2^\phi \, H(x_2^\phi) \qquad \forall \phi \in W \ , \\ \xi_1^\phi \, H(\xi_1^\phi) &= \xi_2^\phi \, H(\xi_2^\phi) \qquad \forall \phi \in \Omega \ . \end{aligned} \tag{3.6}$$

The following lemma establishes sufficient conditions for (3.6) to hold.

Lemma 3.3 In addition to the hypotheses of Lemma 3.2, suppose that statements (3.5) hold. Then (3.6) follows.

Proof.

Re strain-space model: Considering separately the cases $\phi \notin X_1 \cup X_2$, $\phi \in X_1 - X_2$, $\phi \in X_2 - X_1$, and $\phi \in X_1 \cap X_2$, one concludes from (3.5a) that for all $\phi \in W$,

$$\begin{aligned} &\left| x_1^\phi \, H(x_1^\phi) - x_2^\phi \, H(x_2^\phi) \right| \\ &\qquad \leq \left| b \sum_{\substack{\psi \in W \\ \psi \neq \phi}} \frac{\frac{\partial \hat{F}^\phi}{\partial \varepsilon_{ij}} \frac{\partial \hat{F}^\psi}{\partial \varepsilon_{ij}}}{\sqrt{D^\phi \, D^\psi}} \left\{ x_1^\psi \, H(x_1^\psi) - x_2^\psi \, H(x_2^\psi) \right\} \right| \\ &\qquad \leq (N-1) \left| \frac{b}{C} \right| \max_{\psi \in W} \left| x_1^\psi \, H(x_1^\psi) - x_2^\psi \, H(x_2^\psi) \right| , \end{aligned}$$

in view of the triangle inequality, (H12), (H8), and (H3). The foregoing holds for all $\phi \in W$, so in particular it holds for that ϕ which maximizes the left-hand side.

In view of (H15), the first of (3.6) follows.

Re stress-space model: Similar to above. Q.E.D.

In light of this lemma, no matter what solution of (3.5) is substituted into (H11), the same plastic increment will result. In cases where the surfaces are uncoupled, it may be possible to solve (3.5) by inspection. If not, one can always fall back on the Picard iteration scheme of Lemma 3.2. Thus, the lemmas not only establish the existence and uniqueness of the plastic increment but also provide a way to carry out the actual computations. This being true, the formulation for these models may now be considered complete.

3.2 Equivalence of the Strain- and Stress-Space Models

As in Chapter II, constitutive relations [C] and [Γ] will be equivalent to one another if the corresponding model parameters are appropriately interrelated. Accordingly, let

$$F(\underset{\sim}{x}) = \Phi\left(\frac{E}{1+\nu}\,\underset{\sim}{x}\right) \qquad \forall x \in \mathrm{lin}\,(\mathbb{R}^3) \quad ; \tag{H16}$$

$$b = \frac{1+\nu}{E}\left(\frac{1+\nu}{E}\,\beta + 1\right) \quad ; \tag{H17}$$

$$c = \frac{1+\nu}{E}\left(\frac{1+\nu}{E}\,\gamma + 1\right) \quad ; \tag{H18}$$

$$k^{\phi}(x) = \kappa^{\phi}\left(\frac{1+\nu}{E}\,x\right) \quad \forall x \in \mathbb{R}\ ,\ \forall \phi \in N \tag{H19}$$

Invoking these hypotheses, the next two sections unveil a number of results which prevail whenever

$$\left.\begin{aligned} \underset{\sim}{\sigma}^{R}_{\phi} &= \frac{E}{1+\nu}\,\underset{\sim}{\varepsilon}^{P}_{\phi} \\ L^{\phi} &= \frac{E}{1+\nu}\,\Lambda^{\phi} \end{aligned}\right\} \quad \forall \phi \in N \tag{3.7}$$

Then, since (3.7) holds for the virgin state, these results lead in turn to the equivalence theorem.

3.2.1 Relationships Between Corresponding Model Parameters

By themselves, hypotheses (H16) through (H19) prove rather fruitless, but when (3.7) is also assumed to hold, several important relationships emerge between corresponding parameters of the stress- and strain-space models.

Lemma 3.4. Assume, in addition to hypotheses (H1) - (H19), that (3.7) holds at some instant.

Then, at that same instant, $\forall \phi \in N$,

$$k^{\phi}(L^{\phi}) = \kappa^{\phi}(\Lambda^{\phi}) \quad , \tag{3.8}$$

$$\underset{\sim}{\varepsilon} - b\underset{\sim}{S}^{\phi} - c\underset{\sim}{\sigma}^{R}_{\phi} = \kappa(\underset{\sim}{\sigma} - \beta\underset{\sim}{E}^{\phi} - \gamma\underset{\sim}{\varepsilon}^{P}_{\phi}) \quad , \tag{3.9}$$

$$\hat{F}^{\phi}(\underset{\sim}{\varepsilon},\underset{\sim}{S}^{\phi},\underset{\sim}{\sigma}^{R}_{\phi},L^{\phi}) = \hat{\Phi}^{\phi}(\underset{\sim}{\sigma},\underset{\sim}{E}^{\phi},\underset{\sim}{\varepsilon}^{P}_{\phi},\Lambda^{\phi}) \quad , \tag{3.10}$$

$$W = \Omega \quad , \tag{3.11}$$

$$k^{\phi\prime}(L^{\phi}) = \frac{1+\nu}{E}\kappa^{\phi\prime}(\Lambda^{\phi}) \quad , \tag{3.12}$$

$$\frac{\partial \hat{F}^{\phi}}{\partial \varepsilon_{ij}} = \frac{E}{1+\nu}\frac{\partial \hat{\Phi}^{\phi}}{\partial \sigma_{ij}} \quad , \tag{3.13}$$

$$D^{\phi} = \Delta^{\phi} + \frac{\partial \hat{F}^{\phi}}{\partial \varepsilon_{ij}}\frac{\partial \hat{\Phi}^{\phi}}{\partial \sigma_{ij}} \quad . \tag{3.14}$$

where the derivatives in (3.13) and (3.14) are understood in the sense of (H13).

Proof.

Re (3.8): Substitute from (3.7) into (H19).

Re (3.9): In view of (H1) and Lemmas 3.1 and 2.2, [C] $\Rightarrow$ [Γ] when (3.7) holds. Therefore, because of (H2), [Γ] holds whenever (3.7) does. The result follows upon invoking [Γ]; (3.7) and (H6); Lemmas 3.1 and 2.2, and finally (H17) and (H18).

Re (3.10): For all $\phi \in N$,

$$\left.\begin{aligned} \underset{\sim}{z} - b\underset{\sim}{S}^{\phi} - c\underset{\sim}{\sigma}^{R}_{\phi} \equiv \underset{\sim}{\kappa}\left(\underset{\sim}{\zeta} - \beta\underset{\sim}{E}^{\phi} - \gamma\underset{\sim}{\varepsilon}^{P}_{\phi}\right) \in \text{lin}\,(\mathbb{R}^3) \\ \Rightarrow F\left(\underset{\sim}{z} - b\underset{\sim}{S}^{\phi} - c\underset{\sim}{\sigma}^{R}_{\phi}\right) \equiv \Phi\left(\underset{\sim}{\zeta} - \beta\underset{\sim}{E}^{\phi} - \gamma\underset{\sim}{\varepsilon}^{P}_{\phi}\right), \end{aligned}\right\} \quad \text{(i)}$$

by virtue of Lemma 2.2, (H16), and (H10). In light of (i) and (H9), (3.8) and (3.9) $\Rightarrow$ (3.10).

Re (3.11): (H8) and (3.10) $\Rightarrow$ (3.11).

Re (3.12): (H19) $\Rightarrow k^{\phi'}(z) = \frac{1+\nu}{E}\kappa^{\phi'}(\zeta) \quad \forall \phi \in N$

whenever $\zeta = \frac{1+\nu}{E} z \in \mathbb{R}$.

In view of (3.7), the result follows.

Re (3.13): (i) and (H1) $\Rightarrow$

$$\frac{\partial F}{\partial z_{ij}}\left(\underset{\sim}{z}-b\underset{\sim}{S}^{\phi}-c\underset{\sim}{\sigma}^{R}_{\phi}\right) = c_{ijk\ell}\,\frac{\partial \Phi}{\partial \zeta_{k\ell}}\left(\underset{\sim}{\zeta}-\beta\underset{\sim}{E}^{\phi}-\gamma\underset{\sim}{\varepsilon}^{P}_{\phi}\right) \quad \forall \phi \in N$$

$$\text{whenever } \underset{\sim}{\zeta}-\beta\underset{\sim}{E}^{\phi}-\gamma\underset{\sim}{\varepsilon}^{P}_{\phi} = \underset{\sim}{c}\left(\underset{\sim}{z}-b\underset{\sim}{S}^{\phi}-c\underset{\sim}{\sigma}^{R}_{\phi}\right) \in \text{lin}\,(\mathbb{R}^3).$$

In view of (3.9) and (H1), the foregoing holds with $\underset{\sim}{z}$ replaced by $\underset{\sim}{\varepsilon}$ and $\underset{\sim}{\zeta}$ by $\underset{\sim}{\sigma}$, whenever (3.7) is valid. Invoking (H10) and Lemmas 2.1 and 2.2, and then (H9), one obtains (3.13).

Re (3.14): Into the expression for D^{ϕ} given in (H12), substitute (H18), (3.13), (3.8), and (3.12). Upon simplifying, one recognizes the expression for Δ^{ϕ} given in (H12). Invoke (3.13) once more to obtain (3.14). Q.E.D.

It should be borne in mind that (3.8) through (3.14) are valid only at those moments when (3.7) happens to hold. Accordingly, their most important application is in proving the lemma of the next section.

3.2.2 Relationship Between the Plastic Increments

The results of the last section lead readily to Lemma 3.5. It will now be shown that whenever the plastic strain and the stress relaxation satisfy (3.7), the corresponding increments are similarly related.

Lemma 3.5. Suppose, in addition to hypotheses (H1) - (H19), that (3.7) holds at some instant. Then, at that same instant,

$$\left.\begin{aligned} d\underset{\sim}{\sigma}^{R}_{\phi} &= \frac{E}{1+\nu}\, d\underset{\sim}{\varepsilon}^{P}_{\phi} \\ dL^{\phi} &= \frac{E}{1+\nu}\, d\Lambda^{\phi} \end{aligned}\right\} \quad \forall \phi \in N \ . \tag{3.15}$$

Proof. Evidently, equations (3.8)-(3.14) are all valid at the moment in question. Moreover, according to (H2), either [C] or [Γ] holds.

Re [C] $\Rightarrow$ (3.15a): Let the x^{ϕ}, $\phi \in W$, be a solution of the first of (H14), at the instant when (3.7) prevails. Invoking (H12); [C] and (H1); (3.13); Lemma 2.1, (H1), and Lemma 2.2; (H17); (3.14); (H11); (3.13); and (H12); one establishes that the first of (H14) is equivalent to

$$\sqrt{\frac{\Delta^\phi}{D^\phi}}\, x^\phi = \begin{cases} \dfrac{\frac{\partial \hat{\Phi}^\phi}{\partial \sigma_{ij}}\, d\sigma_{ij}}{\sqrt{\Delta^\phi}} - \beta \sum\limits_{\substack{\psi \in W \\ \psi \neq \phi}} \dfrac{\frac{\partial \hat{\Phi}^\phi}{\partial \sigma_{ij}} \frac{\partial \hat{\Phi}^\psi}{\partial \sigma_{ij}}}{\sqrt{\Delta^\phi\ \Delta^\psi}} \sqrt{\frac{\Delta^\psi}{D^\psi}}\, x^\psi H\left(\sqrt{\frac{\Delta^\psi}{D^\psi}}\, x^\psi\right) \\ \qquad\qquad \forall \phi \in W \ni x^\phi > 0 \quad ; \\ \\ \dfrac{\Delta^\phi}{D^\phi}\left[\dfrac{\frac{\partial \hat{\Phi}^\phi}{\partial \sigma_{ij}}\, d\sigma_{ij}}{\sqrt{\Delta^\phi}} - \beta \sum\limits_{\substack{\psi \in W \\ \psi \neq \phi}} \dfrac{\frac{\partial \hat{\Phi}^\phi}{\partial \sigma_{ij}} \frac{\partial \hat{\Phi}^\psi}{\partial \sigma_{ij}}}{\sqrt{\Delta^\phi\ \Delta^\psi}} \sqrt{\frac{\Delta^\psi}{D^\psi}}\, x^\psi H\left(\sqrt{\frac{\Delta^\psi}{D^\psi}}\, x^\psi\right)\right] \\ \qquad\qquad \forall \phi \in W \ni x^\phi \leq 0 \end{cases}$$

In view of (3.11), the $\sqrt{\frac{\Delta^\phi}{D^\phi}}\, x^\phi$, $\phi \in \Omega$, satisfy (3.5b). Therefore, by Lemma 3.3

$$\sqrt{\frac{\Delta^\phi}{D^\phi}}\, x^\phi\, H\left(\sqrt{\frac{\Delta^\phi}{D^\phi}}\, x^\phi\right) = \xi^\phi H(\xi^\phi) \qquad \forall \phi \in \Omega\ ,$$

where the ξ^ϕ, $\phi \in \Omega$, are solutions to the second of (H14), at the instant when (3.7) holds. Invoking (H12) and (3.13),

$$\frac{x^\phi H(x^\phi)}{\sqrt{D^\phi}} \frac{\partial \hat{F}^\phi}{\partial \varepsilon_{ij}} = \frac{E}{1+\nu} \frac{\xi^\phi H(\xi^\phi)}{\sqrt{\Delta^\phi}} \frac{\partial \hat{\Phi}^\phi}{\partial \sigma_{ij}} \qquad \forall \phi \in \Omega\ .$$

By virtue of (3.11) and (H11), the above $\Rightarrow$ (3.15a).

Re [Γ] $\Rightarrow$ (3.15a): Similar to above.

Re (3.15b): The result follows from (H5) and (3.15a). Q.E.D.

Thus at any instant during the deformation, equations (3.7) imply (3.15).

3.2.3 Equivalence Theorem

It now follows readily that the stress- and strain-space models are equivalent.

Theorem 3.1 Under hypotheses (H1) through (H18), equations (3.7) hold throughout the history of the motion. Moreover, constitutive relations [C] and [Γ] are equivalent.

Proof.

Re (3.7): (H4), (H5) ⇒ (3.7) holds initially. By Lemma 3.5, so does (3.15).

Thus (3.7) holds at the next instant, and, continuing the argument, at all times.

Re [C] ⇒ [Γ]: Multiply through [C] by $\underset{\sim}{\kappa}$, invoking (H1). The result follows, then, through use of Lemmas 3.1 and 2.2, and finally (3.7).

Re [Γ] ⇒ [C]: Similar to above. Q.E.D.

3.2.4 Remarks and Observations

Now that an equivalence theorem has been established for multiple-surface models, two questions come to mind. How wide a range of stress-strain curves can the theorem accommodate, and how fruitful is the theorem in the realm of practical applications?

The first question focuses attention upon hypotheses (H12) and (H15). Statements (H12) require not only the D^{ϕ} but also the Δ^{ϕ} to take on positive values. Thus, upon setting N = 1, one can recover only the strain-hardening case of Theorem 2.1. When there are several surfaces, statements (H15) also come into play. In general, they bear in a rather

complicated way upon the question at hand. Accordingly, since models with uncoupled surfaces are of particular interest, they will be singled out for examination.

Consider a stress-space model with N uncoupled surfaces. Evidently, $\beta = 0$. In conformity with Theorem 3.1, the strain-space equivalent will feature coupling, with $b = (1+\nu)/E$, as dictated by (H17). To make this strain-space model well-behaved, one must impose (H15), whence

$$C > (N-1)\,\frac{1+\nu}{E} \quad .$$

For simplicity let the hardening be purely kinematic, so that $\kappa^{\phi'} = k^{\phi'} = 0$ for all ϕ. Then

$$c > (N-1)\,\frac{1+\nu}{E} \quad .$$

This requirement, in turn, places restrictions on the original stress-space model, through hypothesis (H18):

$$\gamma > (N-2)\,\frac{E}{1+\nu} \quad .$$

For a given model the greatest deviation from Hookean linearity occurs when all the surfaces are activated and all their normals point in the direction of $d\underset{\sim}{\sigma}'$. In this event,

$$d\underset{\sim}{\varepsilon}' = \frac{1+\nu}{E}\,d\underset{\sim}{\sigma}' + \frac{N}{\gamma}\,d\underset{\sim}{\sigma}' < \frac{2(N-1)}{N-2}\,\frac{1+\nu}{E}\,d\underset{\sim}{\sigma}' \quad .$$

As indicated in Figure 3.1, the ultimate deviatoric, elastoplastic stiffness is zero when N = 2 and tends toward half the elastic value as $N \to \infty$. Theorem 3.1, then, guarantees the existence of an equivalent strain-space model only if the original stress-space model conforms to these specifications.

The analysis proceeds similarly for models with uncoupled strain-space surfaces. Oddly enough, though, the results are different. So long as the constitutive law falls within the strain-hardening regime, Theorem 3.1 guarantees the existence of an equivalent model in stress space, no matter how many surfaces are involved. In light of this paradoxical asymmetry, Theorem 3.1 could likely be generalized to accommodate a relaxation of (H12) and/or (H15). It was decided, though, not to pursue the matter, for the analytical difficulties seem to outweigh the potential benefits.

This leads to the second question raised at the outset. From the standpoint of practical applications, Theorem 3.1 proves somewhat disappointing. The prospect of shifting from strain space to stress space or vice versa is considerably less appealing in the case of multiple-surface models than for the single-surface models of the last chapter. This is because the only models anyone would really want to use are those featuring uncoupled surfaces, and by virtue of (H17) these cannot be made equivalent to one another. To achieve, in stress space, constitutive behavior the same as that given by an uncoupled strain-space model, one must resort to coupling.

From a practical viewpoint, the main conclusion to be drawn from Theorem 3.1 is that, for multiple-surface models, it is no easy matter

$N = 2$

extreme case:

$d\underset{\sim}{\epsilon}' \longrightarrow \infty$

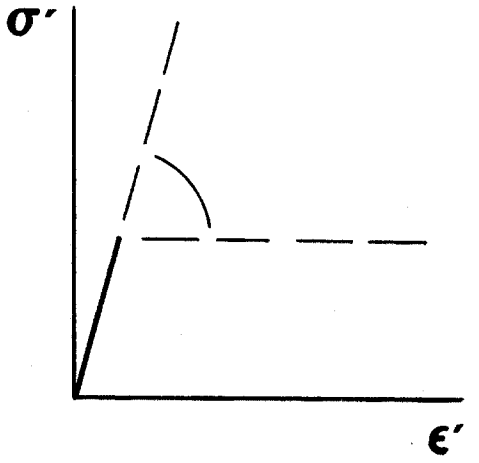

$N = 3$

extreme case:

$d\underset{\sim}{\epsilon}' = 4\left(\frac{1+\nu}{E}\right) d\underset{\sim}{\sigma}'$

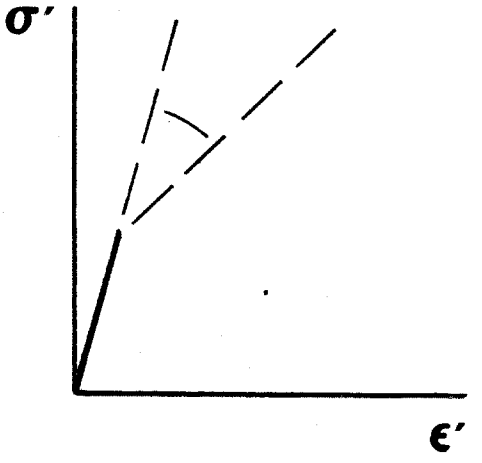

$N \longrightarrow \infty$

extreme case:

$d\underset{\sim}{\epsilon}' = 2\left(\frac{1+\nu}{E}\right) d\underset{\sim}{\sigma}'$

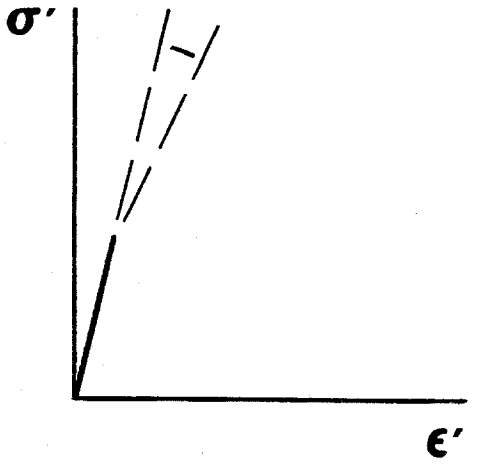

Figure 3.1 For the ranges of constitutive behavior indicated above, a stress-space model with uncoupled surfaces possesses a strain-space equivalent.

to invert elastoplastic stiffnesses and compliances. Since the uncoupled strain-space models give stiffnesses quite readily, they show the greatest promise for finite element applications. Accordingly, a model of this type was coded in Fortran, and the results are reported in Chapter IV.

CHAPTER IV

A NUMERICAL IMPLEMENTATION OF STRAIN-SPACE PLASTICITY

The analytical work of the last two chapters opens the door to a new approach for numerical plasticity. In exploring its merits, the starting point will be a finite element code for quasi-static plasticity written by Prévost and Hughes [15]. This program, named DIRT, incorporates a sophisticated stress-space model for soils plasticity. The constitutive behavior, as in most such programs, is more or less segregated from the main body of the finite element code. Thus, it is a relatively straightforward matter to interface this code with a new package of constitutive subroutines featuring loading surfaces in strain space. Section 4.1 details this package, and the remaining sections of Chapter IV are given over to working some representative boundary-value problems.

4.1 The Plasticity Algorithm

The model chosen for coding incorporates an arbitrary number of independent, strain-space loading surfaces of the von Mises type. In the language of Chapter III, b equals zero and N may be set to any non-negative integer. Thus the relaxation functions take the form

$$F^{\phi}(\underset{\sim}{\varepsilon},\underset{\sim}{S}^{\phi},\underset{\sim\phi}{\sigma}^{R},L^{\phi}) = \frac{3}{2}(\varepsilon'_{ij}-a^{\phi}_{ij})(\varepsilon'_{ij}-a^{\phi}_{ij}) - [k^{\phi}(L^{\phi})]^{2} \qquad (4.1)$$

where $\underset{\sim}{a}^{\phi} = c\,\underset{\sim\phi}{\sigma}^{R}$, for $\phi = 1,2,\ldots,N$.

When N equals zero, the model reverts to Hookean elasticity. With N equal to one, the response is bilinear, just like that given by traditional plasticity (Theorem 2.1). For N greater than one, the behavior is multilinear, allowing for a more exact modeling of empirical stress-strain diagrams.

Consider, for example, the experimental curves for 6061-T6 aluminum given by Christman et al. [17] and reproduced in Figure 4.1. Cyclic loading produces nearly stable hysteresis loops, so the hardening law is taken to be kinematic. Letting N equal three, one can adjust the constitutive subroutines so that they produce the behavior shown in Figure 4.2. With more surfaces, of course, a closer fit to the given curves could be obtained. This example should serve, though, to demonstrate the versatility of the strain-space package.

The balance of 4.1 will be given over to a discussion of this package. Section 4.1.1 describes how it fits into the finite element program. Section 4.1.2 details the algorithm for updating relaxation surfaces. And Section 4.1.3 deals with the question of accuracy.

4.1.1 An Overview of the Quasi-Static Analysis Program

For an overview of the quasi-static analysis program, examine the outline given in Figure 4.3. It will be noted that for each time step the program goes through two stages. The predictor stage uses the stiffness associated with the most recent displacement state to estimate the displacement increment which would result upon applying α times the next increment of load. The objective is to test the water, as it were, to see approximately what displacements can be expected midway

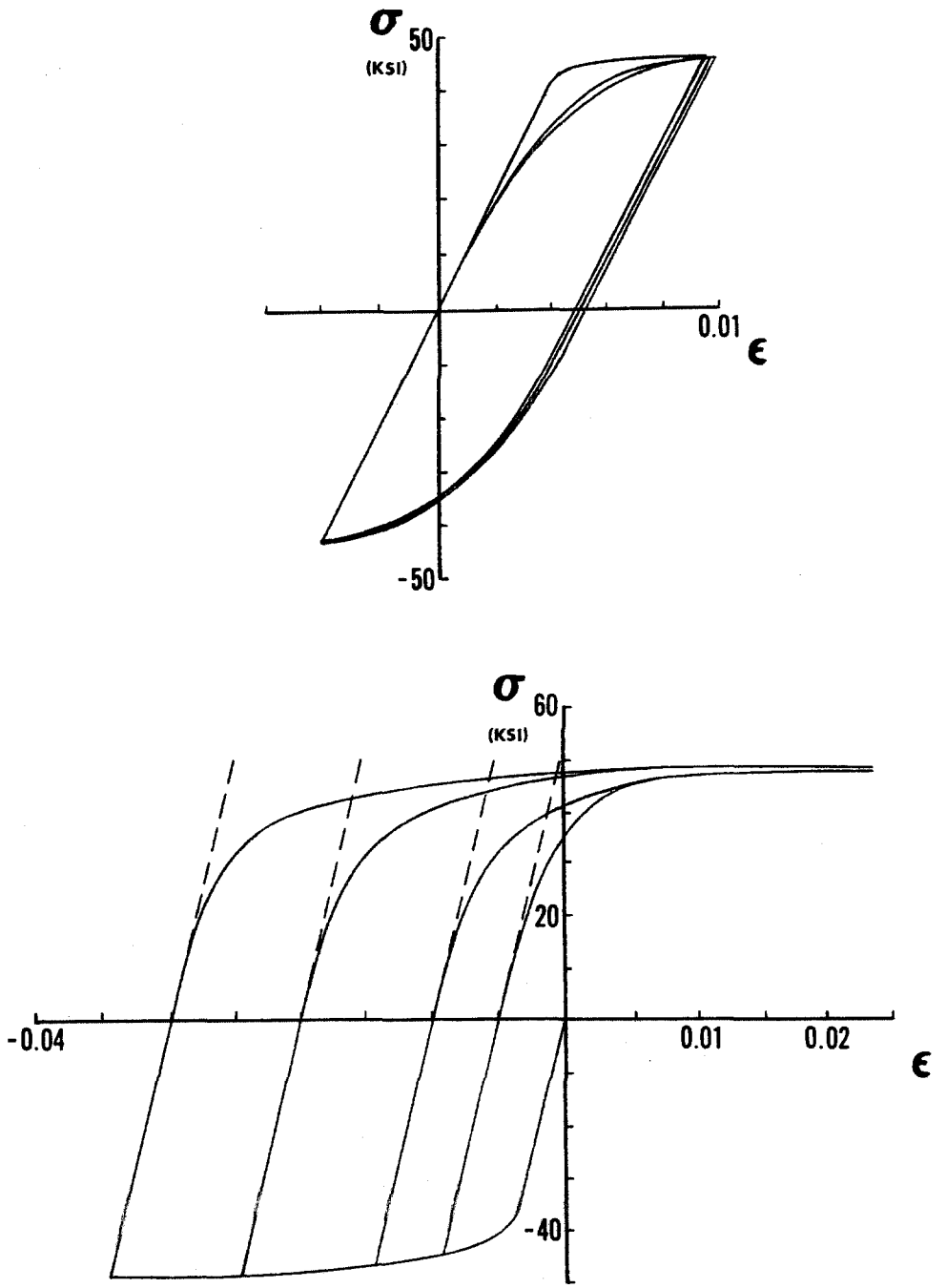

Figure 4.1 Experimental stress-strain curves for 6061-T6 aluminum, from Christman, et al. [17]. The top diagram shows results from a set of cyclic compression-tension tests. For the lower figure, specimens were loaded in compression to strains of 0.5 to 3.0 percent, unloaded to zero stress, and then immediately subjected to uniaxial tension.

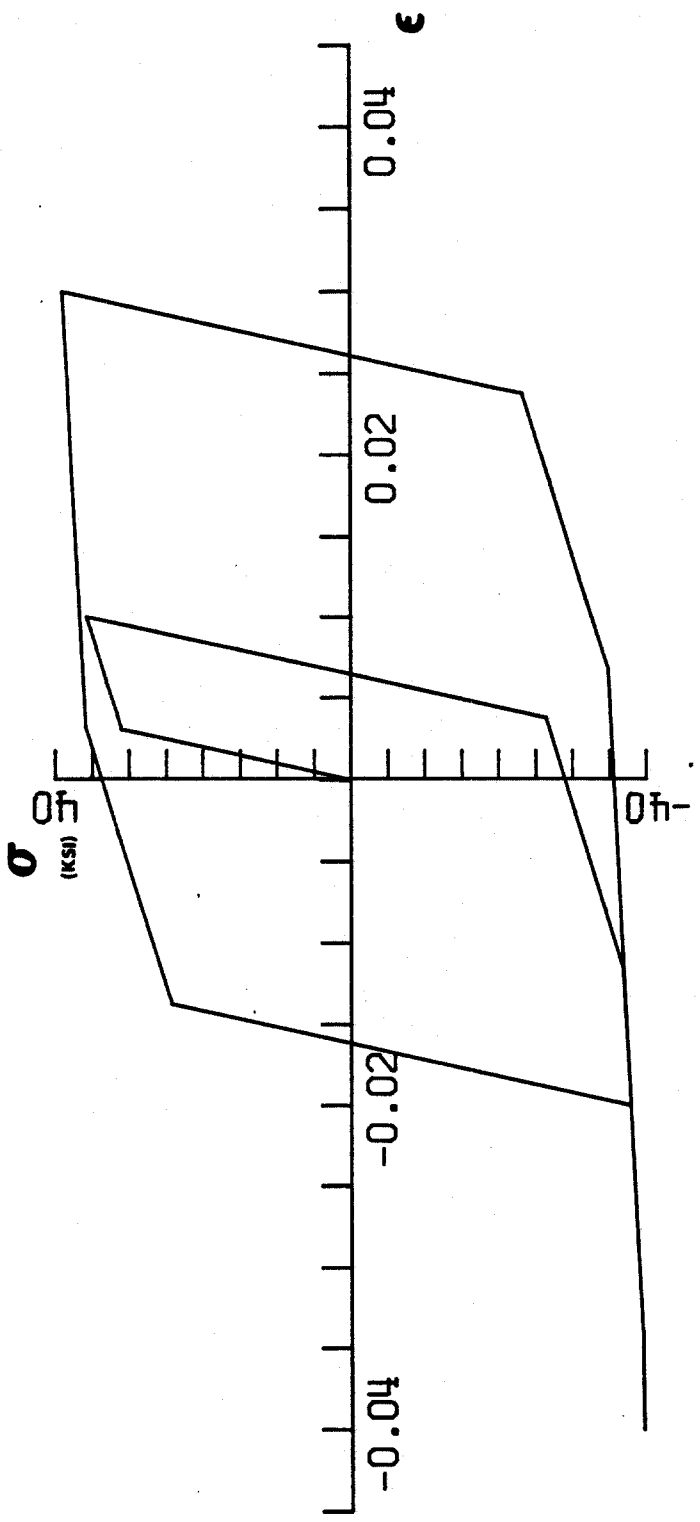

Figure 4.2 A strain-space plasticity model for 6061-T6 aluminum.

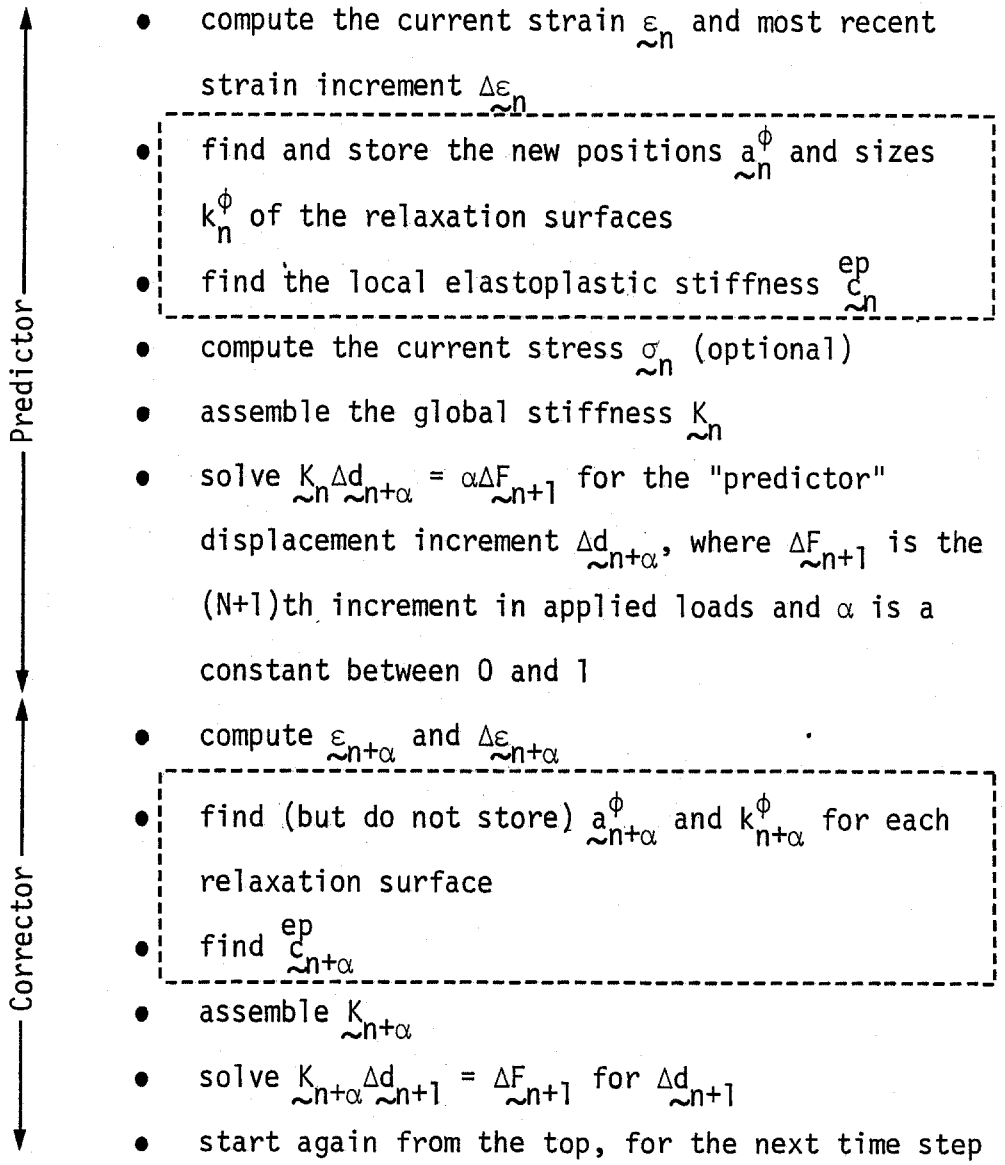

Figure 4.3 Outline of the algorithm for quasi-static analysis. The dashed boxes enclose those steps handled by the constitutive subroutine package.

through the next step. (The parameter α is normally set to $\frac{1}{2}$.) The corrector stage then uses the stiffness associated with these predicted displacements to compute the actual displacement increment. Because of this predictor/corrector feature, the constitutive subroutines need to be called twice for each time step.

Whenever the constitutive package is called, it performs two distinct functions. First, it adjusts the positions and/or sizes of the various relaxation surfaces in order to move them out to the new strain state. The algorithm for doing this will be discussed in Section 4.1.2. Second, the constitutive package constructs the local elastoplastic stiffness tensor, $\overset{ep}{\underset{\sim}{c}}$, corresponding to this strain state. This is done through recourse to the multiple-surface analog of $[\dot{C}](d)$, from Chapter II. Thus,

$$
\begin{aligned}
{}^{ep}c_{ijk\ell} &= c_{ijk\ell} - \sum_{\phi} \frac{\frac{\partial \hat{F}^{\phi}}{\partial \varepsilon_{ij}} \frac{\partial \hat{F}^{\phi}}{\partial \varepsilon_{k\ell}}}{D^{\phi}} \\
&= c_{ijk\ell} - \sum_{\phi} \frac{(\varepsilon'_{ij} - a^{\phi}_{ij})(\varepsilon'_{k\ell} - a^{\phi}_{k\ell})}{\left[c + \frac{2}{3}\frac{dk^{\phi}}{dL^{\phi}}\right](\varepsilon'_{mn} - a^{\phi}_{mn})(\varepsilon'_{mn} - a^{\phi}_{mn})}
\end{aligned}
\tag{4.2}
$$

where the summation is carried out over all active surfaces. The second equation in (4.2) follows from the first upon substituting (4.1) into (H12) of Chaper III.

Note that the stresses do not have to be computed unless they are wanted. This is one of the advantages of a strain-space formulation.

When they are in fact needed, they can be obtained through the relation

$$\underset{\sim}{\sigma} = \underset{\sim\sim}{\kappa\varepsilon} - \frac{1}{c} \sum_{\phi=1}^{N} \underset{\sim}{a}^{\phi} \quad , \tag{4.3}$$

which follows upon substituting (4.1) into [C] of Chapter III. Evidently, the positions of the relaxation surfaces, the $\underset{\sim}{a}^{\phi}$'s, play a key role in the overall strategy and should be updated with care.

4.1.2 Updating the Relaxation Surfaces

In determining how to update the position of a relaxation surface, the main question to be settled is what direction to assume for its motion. For a truly infinitesimal strain increment, the motion is parallel to the corresponding increment of stress relaxation and, thus, to the local normal. But as a matter of practicality in working boundary-value problems on the computer, it is hard to keep the strain increments uniformly small throughout the domain. In any case, one judges whether a strain increment is large or small by comparing it to the radius of the surface involved, and these radii may vary considerably across the domain, particularly if the hardening law admits some isotropic effects.

For these reasons it is important to investigate how a surface moves when subjected to a large strain increment. Figure 4.4 depicts a case in point and suggests one way to resolve the question. The strain increment is broken up into subincrements small enough that for each of them the surface will move roughly in the direction of its local normal.

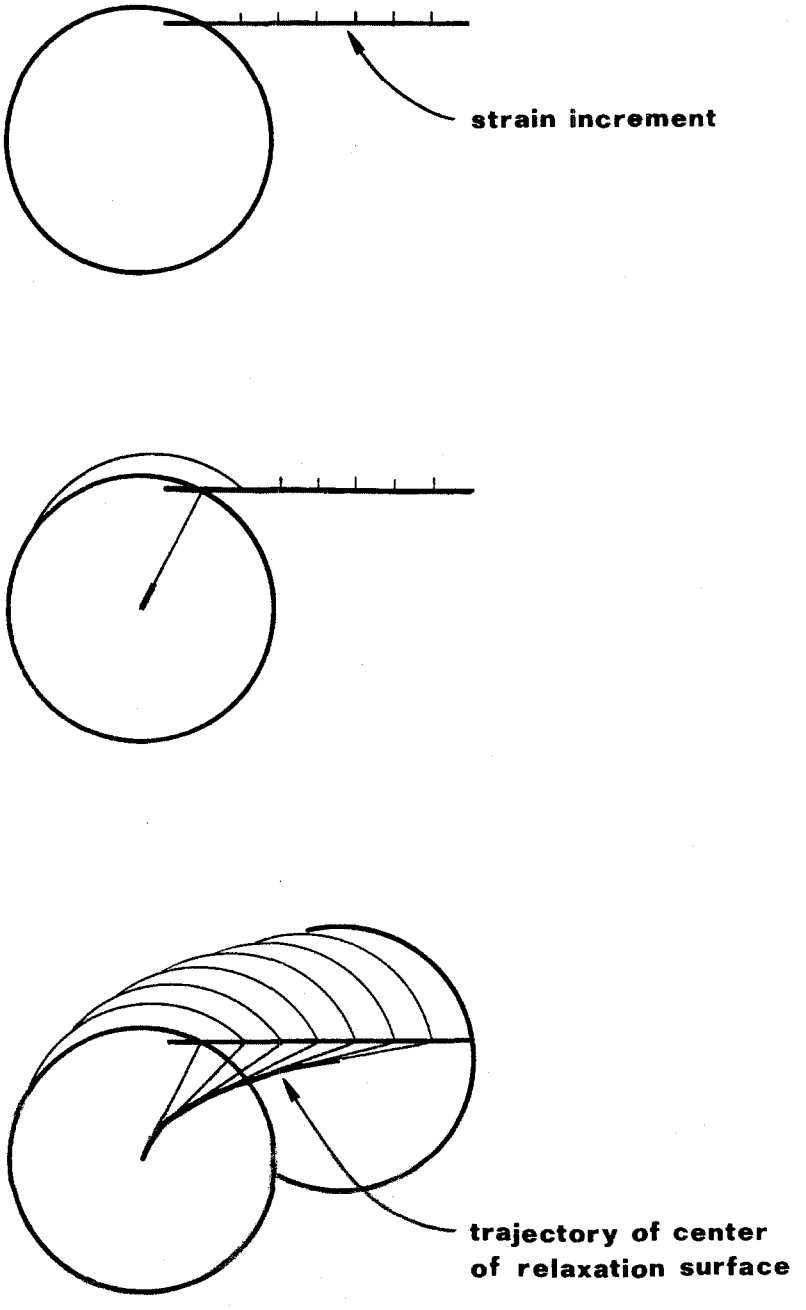

Figure 4.4 The trajectory of a surface responding to a large strain increment.

Evidently the trajectory starts off in the direction of the initial normal and then bends over to approach the strain increment as an asymptote. This conclusion is borne out by an analytical solution given by Krieg and Krieg [16] for the special case of perfect plasticity.

In the strain-space constitutive package, a simple and rather ad hoc approximation is used to describe the trajectory of a relaxation surface. If the strain increment protrudes less than one radius from the surface, then the new center is placed along a line running from the old center toward the midpoint of the protruding section. When the strain increment extends more than one radius beyond the surface, the trajectory is approximated by a line extending from the old center to a point half a radius back from the tip of the strain increment. These rules, depicted graphically in Figure 4.5, are discussed more fully in a separate report [18].

4.1.3 Accuracy

In view of (4.3), the adequacy of the above approximation for repositioning relaxation surfaces can be gauged by seeing how accurately the stress is updated. Attention focuses upon the case of perfect plasticity because it proves to be particularly troublesome for the traditional formulation. In theory, the stress state should follow the perimeter of the yield surface when loading occurs. In practice, though, since the surface is fixed and convex, the stress tends to stray outside. This phenomenon is illustrated schematically is Figure 4.6, which is reproduced from Maier [19]. Various steps can be taken to alleviate this problem.

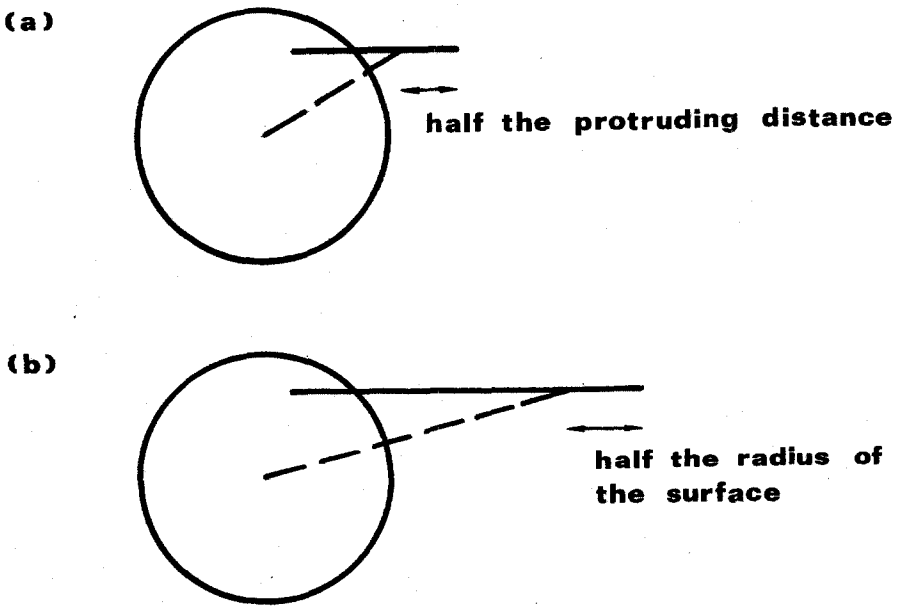

Figure 4.5 The dashed line shows the trajectory along which the relaxation surface is assumed to move in each of two cases:

(a) When the strain increment protrudes less than one radius beyond the surface; and

(b) When it protrudes more than one radius.

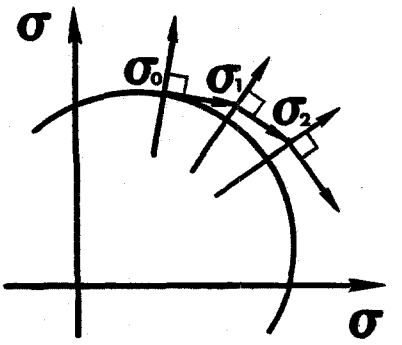

Figure 4.6 When perfect plasticity is implemented in the traditional way, the stress state tends to stray outside the surface. (See Maier [18]).

Krieg and Krieg [16] describe three ways to implement perfect plasticity in stress space. They then test for accuracy by picking an initial stress state and subjecting each algorithm to a variety of strain increments. Noting that higher derivatives of strain are not as a rule available to a constitutive subroutine, they take the strain rate to be constant. This enables them to obtain an analytical solution. Thus the final stresses given by each of the numerical methods can be compared to exact answers.

The first of the three schemes considered is called the tangent stiffness — radial return method. Letting $\underset{\sim}{\Delta\varepsilon}$ denote the strain increment and $\underset{\sim}{\sigma}_I$ the initial stress, the first step is to compute the trial state

$$\underset{\sim}{\sigma}_T' = \underset{\sim}{\sigma}_I' + \frac{E}{1+\nu}\underset{\sim}{\Delta\varepsilon}' \quad .$$

If $\underset{\sim}{\sigma}_T'$ lies within or on the yield surface, the trial state is also the final state. Otherwise, the contact point $\underset{\sim}{\sigma}_C'$ is found, as indicated in Figure 4.7(a), and the protruding part of the increment is resolved into components normal and tangential to the yield surface at $\underset{\sim}{\sigma}_C'$. To find the final state $\underset{\sim}{\sigma}_F'$, one subtracts the normal component from $\underset{\sim}{\sigma}_T'$ and then returns radially to the surface.

The second scheme is called the secant stiffness method. The trial state $\underset{\sim}{\sigma}_T'$ is found as before, and the contact stress $\underset{\sim}{\sigma}_C'$ is computed if necessary. This time an intermediate state

$$\underset{\sim}{\sigma}_M' = \frac{1}{2}\left(\underset{\sim}{\sigma}_C' + \underset{\sim}{\sigma}_T'\right)$$

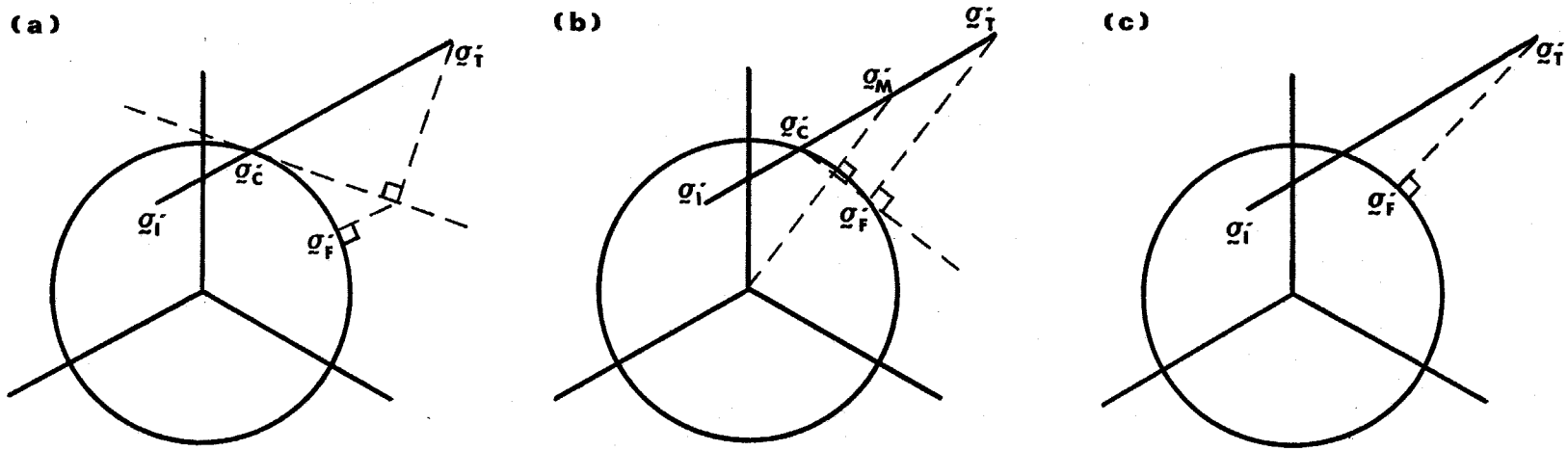

Tangent stiffness–radial return method. The component of $(\underline{\sigma}'_T - \underline{\sigma}'_C)$ parallel to $\underline{\sigma}'_C$ is subtracted from $\underline{\sigma}'_T$, and the result is pulled back radially to the surface.

Secant stiffness method. The component of $(\underline{\sigma}'_T - \underline{\sigma}'_C)$ parallel to $\underline{\sigma}'_M$ is subtracted from $\underline{\sigma}'_T$. Here, $\underline{\sigma}'_M$ is the midpoint of $(\underline{\sigma}'_T - \underline{\sigma}'_C)$.

Radial return method. The trial stress $\underline{\sigma}'_T$ is simply pulled back radially to the surface.

Figure 4.7 Three common algorithms for perfect plasticity, interpreted geometrically.

is found, and the portion of the increment extending beyond the yield surface is projected onto the line from $\underset{\sim}{0}$ to $\underset{\sim}{\sigma}'_M$. The result is subtracted from $\underset{\sim}{\sigma}'_T$ to obtain the final state $\underset{\sim}{\sigma}'_F$. It can be shown that this final state always lies exactly on the yield surface, as shown in Figure 4.7(b).

The third scheme is called the radial return method. The trial state $\underset{\sim}{\sigma}'_T$ is found as before, and, if necessary, it is pulled back to the yield surface by a simple reduction in magnitude. This is illustrated in Figure 4.7(c).

When given a partly elastic, partly plastic step, all three methods deal exactly with the elastic portion, and, for that matter, so does the strain-space constitutive package. It suffices, therefore, to compare accuracies for a purely plastic step, as pointed out by Krieg and Krieg. They take the strain increment to be of arbitrary magnitude but, for ease of comparison, limit it to the same principal directions as $\underset{\sim}{\sigma}'_I$.

This test will now be applied to the strain-space constitutive package. To allow for a fair comparison, the predictor/corrector feature is temporarily suspended, since the other three schemes are all single-step methods. The relaxation surface is centered at the origin of strain space, and an initial state

$$\underset{\sim}{\varepsilon}'_I \equiv \frac{1+\nu}{E} \underset{\sim}{\sigma}'_I$$

is placed rather arbitrarily on the surface.

The results for the strain-space package are presented in the same form used by Krieg and Krieg. The strain increment is resolved into

components $\Delta\varepsilon_r'$ and $\Delta\varepsilon_t'$, radial and tangential at the initial point of loading. For each ordered pair $(\Delta\varepsilon_t', \Delta\varepsilon_r')$, the package yields an approximation $\underset{\sim}{\sigma}_F'$ to the exact final stress $\underset{\sim}{\sigma}_E'$. The angle

$$\theta = \cos^{-1}\left(\frac{\sigma_{F\ ij}'\ \sigma_{E\ ij}'}{|\sigma_E'|^2}\right)$$

where

$$|\sigma_E'|^2 = \sigma_{E\ ij}'\ \sigma_{E\ ij}' \ ,$$

fully describes the error. If $\underset{\sim}{\sigma}_E'$ lies between $\underset{\sim}{\sigma}_I'$ and $\underset{\sim}{\sigma}_F'$, as shown in Figure 4.8, then θ is positive[1].

The contour plots in Figure 4.9 show how the angle of error θ varies for each of the four algorithms. On the whole, the error is smaller in absolute value for the strain-space scheme than for any of the others. Its closest competitor is the radial return method, the two contour maps resembling one another quite markedly. This resemblance is no mere coincidence. Implementing the equivalent of radial return in strain space would entail placing the surface's new center along a line joining the old center to the new, final strain. This rule is qualitatively similar to the one which was in fact coded. The strain-space scheme is better, though, not only because the angular errors are smaller in absolute value, but also because they vary in sign across the contour plot. Thus, after several time steps, they will tend to cancel one another out.

---

[1]This sign convention is different from the one described by Krieg and Krieg, but it seems to be the one they used in their contour plots.

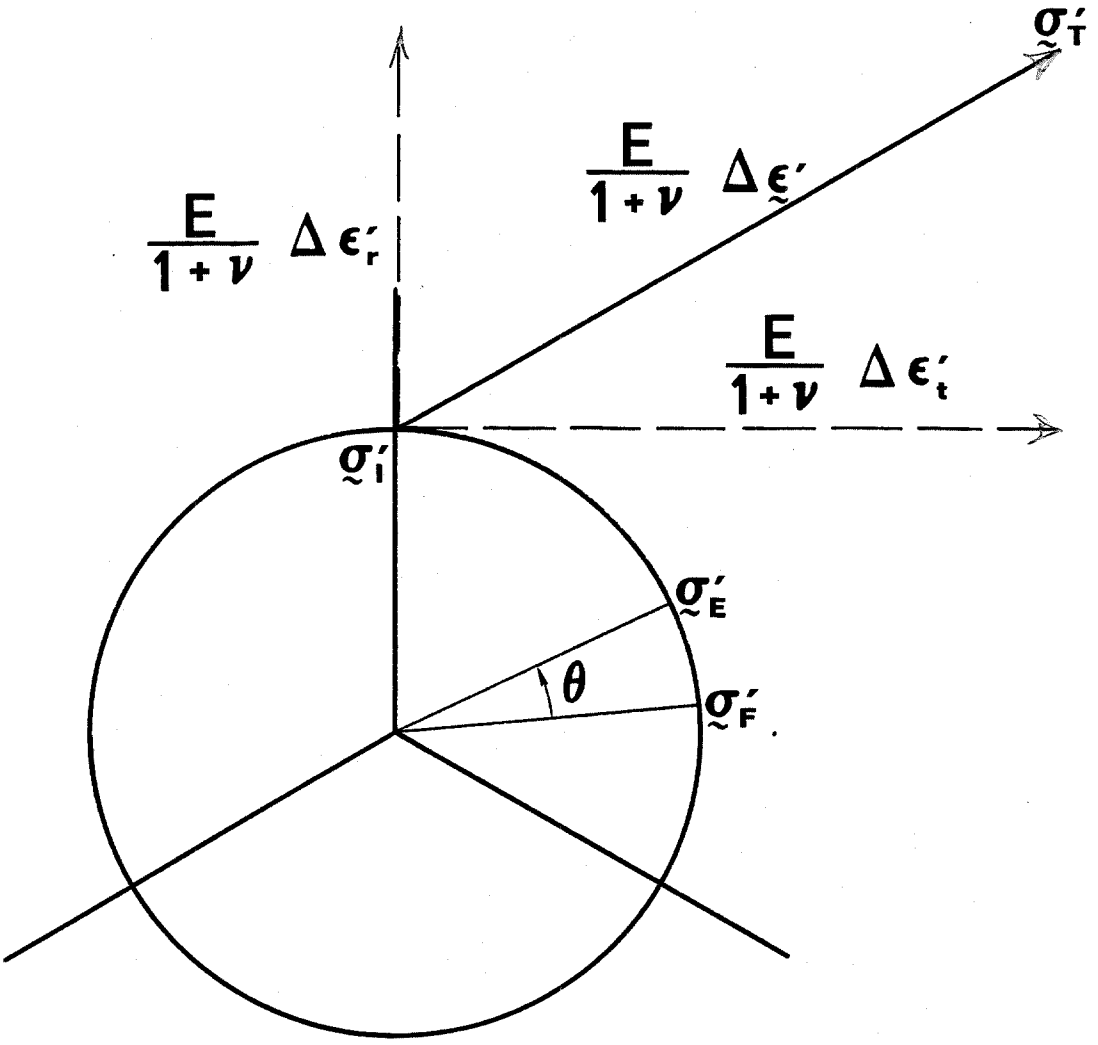

Figure 4.8 The strain increment is resolved into components $\Delta\epsilon'_r$ and $\Delta\epsilon'_t$. The angle θ between computed and exact stress, which is positive as shown, completely characterizes the error.

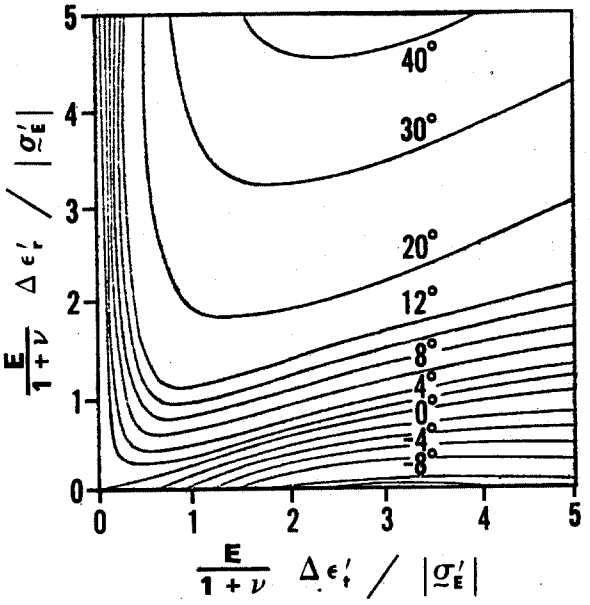

Tangent stiffness–radial return method

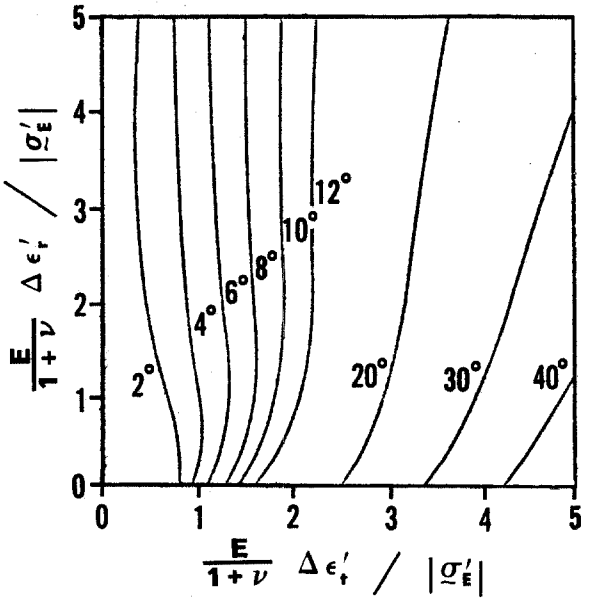

Secant stiffness method

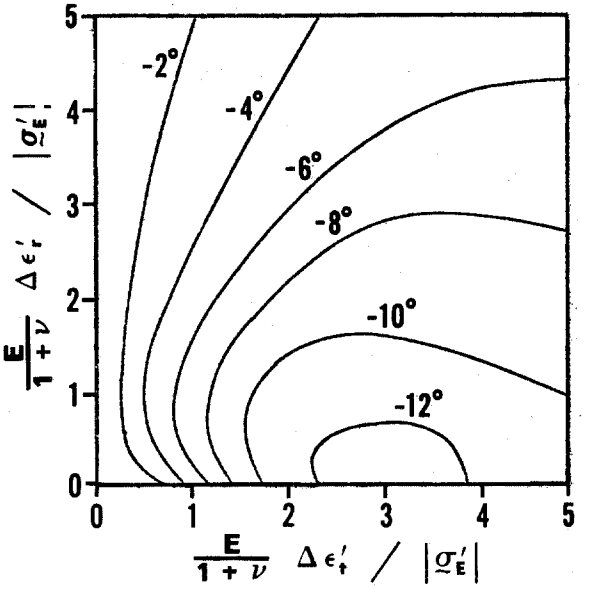

Radial return method

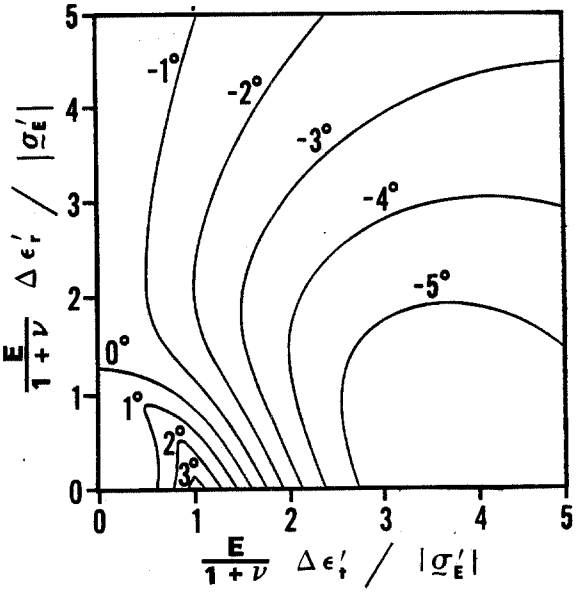

Strain–space method

Figure 4.9 Contours of θ, the angular error, are plotted for each method.

Bear in mind, too, that the rule tested here by no means exhausts the possibilities for working in strain space. It is remarkable that a rule which seems so ad hoc, even crude, nevertheless competes so well. Further improvement could be expected if one assumed quadratic instead of linear trajectories, or, barring that, if one merely allowed for a smoother transition from the case of small strain increments to the case of large ones.

Because shifting between stress and strain space is particularly easy for perfect plasticity, the rule reported on here could of course be implemented in stress space just as well. Extending it in stress space to accommodate hardening or softening would prove cumbersome, but possible once again. What, then, is so intriguing about strain-space plasticity? The answer is simple: Someone approaching the subject in the traditional way would never stumble upon such an algorithm. Strain-space plasticity opens the door to a whole range of possibilities.

4.2 Further Confirmation of the Strain-Space Algorithm: The Vertically Loaded Foundation

The results of the last section demonstrate that the strain-space constitutive package can indeed handle perfect plasticity, just as Theorem 2.1 had predicted. Through use of the finite element code DIRT, however, a more direct confirmation is possible. This is true because DIRT can now accommodate both a stress-space option and the strain-space package described herein. Thus it is possible to consider a representative boundary-value problem and see whether the two complementary constitutive models lead to the same solution.

4.2.1 Description of the Problem

The problem, as depicted in Figure 4.10, consists of a vertically loaded foundation resting on a semi-infinite half-space. The medium is taken to be incompressible and elastic — perfectly plastic, with a uniaxial limit stress κ = 1.3 pressure units and a Young's modulus E = 200 pressure units. For the sake of economy, conditions of plane strain are assumed to prevail. Thus the foundation has only one dimension, a width of 10 units. The problem may be thought of as corresponding to a great wall of China cutting across an infinite prairie.

This two-dimensional punch, as it is sometimes called, has received considerable attention in the literature. Prandtl [20] showed that for a rigid-perfectly plastic medium, collapse occurs when the applied load is given by

$$L = (2+\pi)\ (2a)\ \tau_M \ , \qquad (4.4)$$

where a is the half-width of the wall and $\tau_M = \kappa / \sqrt{3}$ is the shear strength of the medium. Muskhelishvili [21] supplied the corresponding elastic solution and intimated in the process that his work finds application in the design of foundations. To cite just one modern reference, Lambe and Whitman discuss the full elastoplastic problem in their textbook Soil Mechanics [22] and include some computer results not unlike those reported below.

Despite its popularity, the plane-strain foundation problem suffers from one serious drawback, from the standpoint of engineering applications. Muskhelishvili's analysis shows that the elastic displacements tend logarithmically to infinity in the far field. Thus the plastic

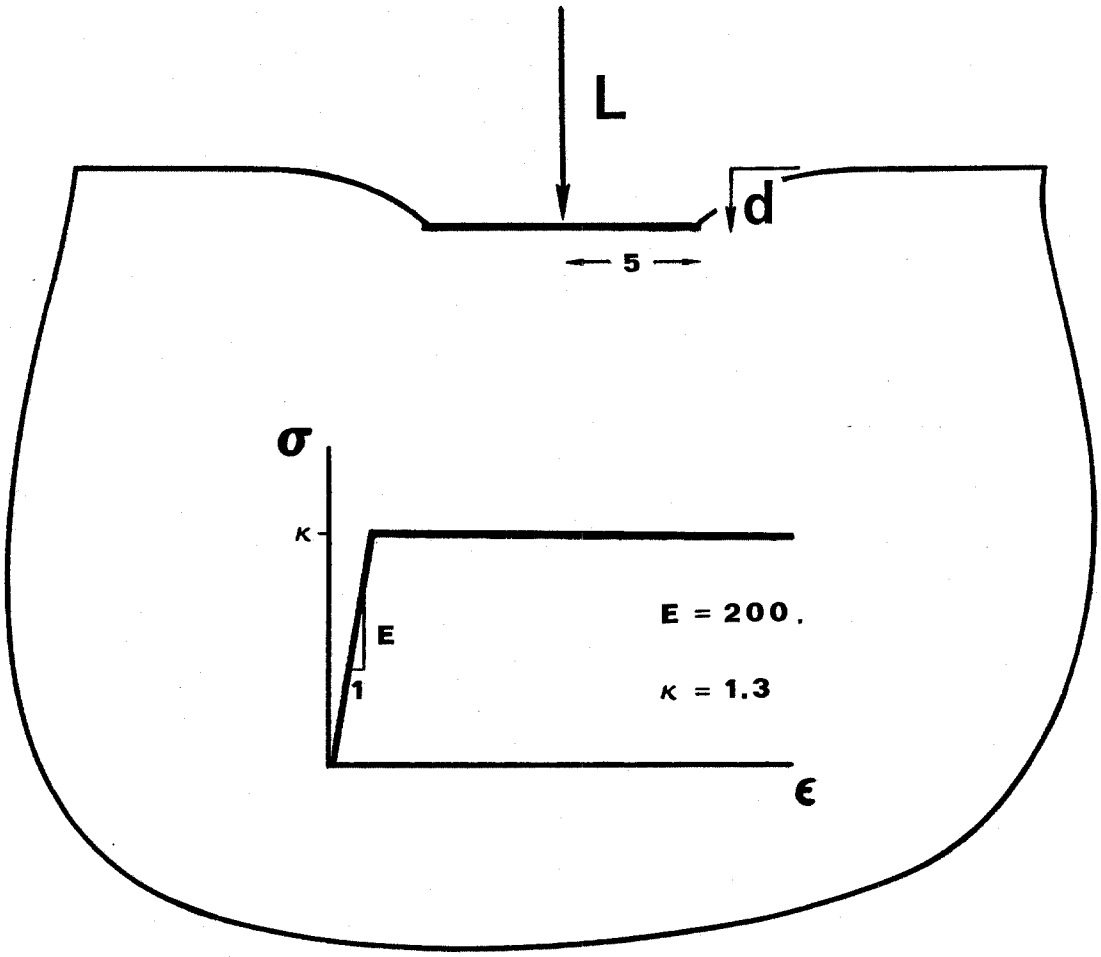

Figure 4.10 The vertically loaded foundation.

collapse, which is supposed to be the focus of attention, is overshadowed by an elastic singularity. This difficulty stems directly from the unphysical assumption of plane strain.

4.2.2 The Computer Implementation

To implement this problem numerically, one must introduce a subtle modification. The finite element method does not lend itself to domains of infinite extent, so the wall has been transplanted, as it were, to a flower trough. Along the sides of the trough, normal displacements are assumed to vanish, as are shear tractions. The problem is symmetric, so only half the domain needs to be discretized. The resulting half-mesh, shown in Figure 4.11, is 30.5 units deep and 36 units wide. Using a finite domain, of course, has the added advantage of avoiding the elastic singularity.

Figures 4.12 and 4.13 present some of the numerical results. The solid lines were obtained with the strain-space constitutive package, while the triangles were generated by Prévost's stress-space algorithm for isotropic plasticity [2,4]. The load-settlement curves, shown in Figure 4.12, agree exceptionally well, both for loading and unloading. However, some discrepancy occurs on the local level, as might be expected. In Figure 4.13, shear stress has been plotted against shear strain for the four elements singled out in Figure 4.11. The uniaxial limit stress used by the Prévost model, which unaccountably strayed from the specified value of 1.3 pressure units, is also given for each of these elements. There appears to be some correlation between the size of the limit stress and the extent to which the corresponding

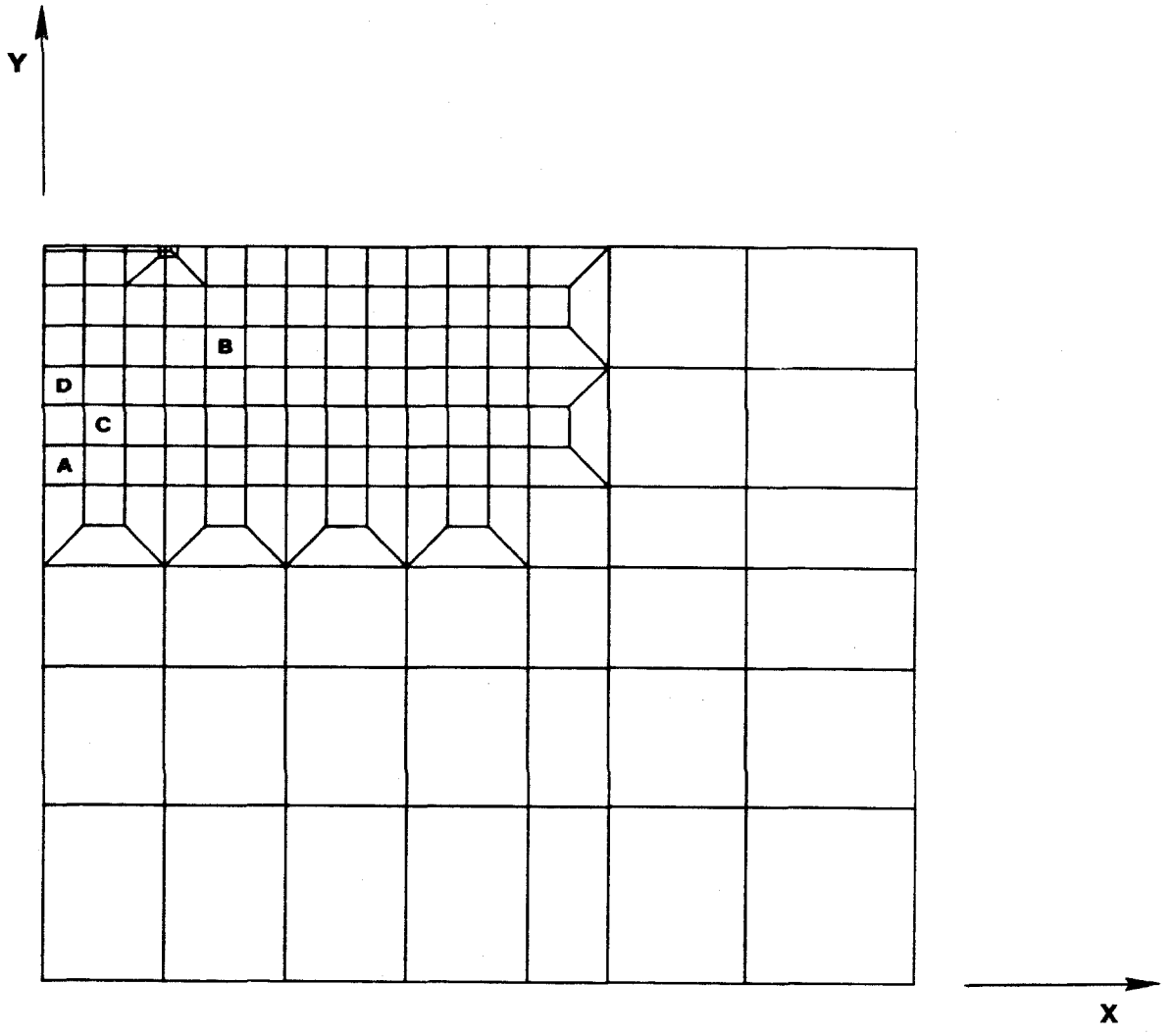

Figure 4.11 The rectangular half-mesh. In figure 4.13 shear stress σ_{xy} is plotted against shear strain ε_{xy} for elements A, B, C, and D.

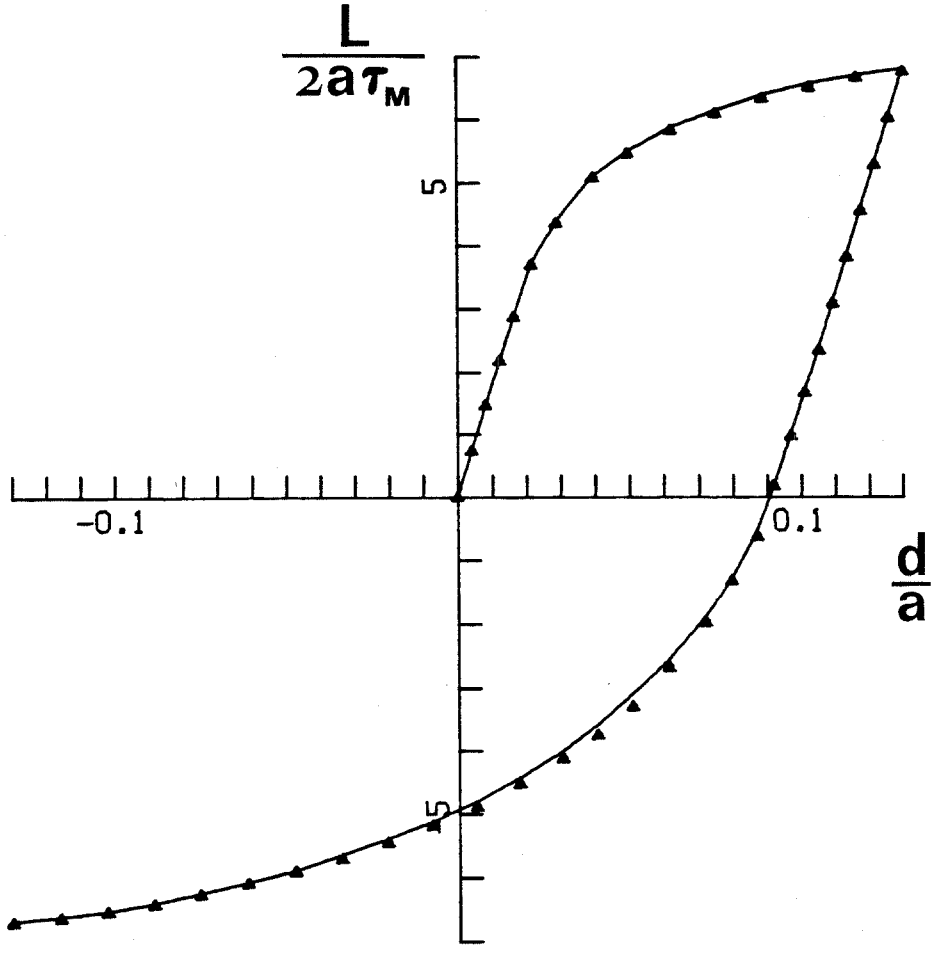

Figure 4.12 The load-settlement curves generated by the strain-space package (solid line) and by Prévost's stress-space model (triangles).

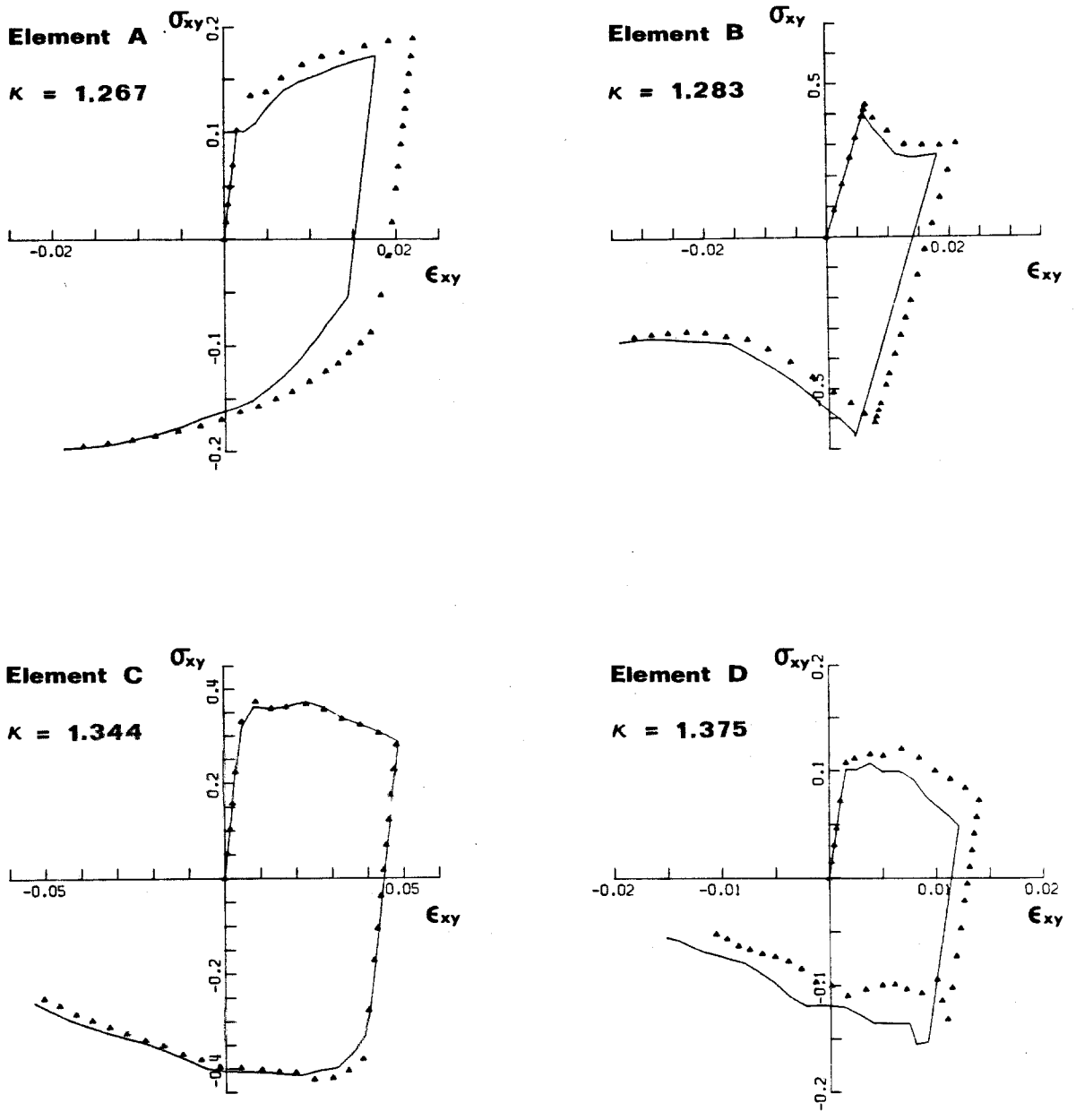

Figure 4.13 Plots of shear stress versus shear strain for the four elements singled out in Figure 4.11. The solid lines were generated by the strain-space package; the triangles correspond to Prévost's model. The κ's denote the uniaxial limit stresses actually used by Prévost's model.

stress-strain curves agree. In any event the curves are at least similar in shape even for the worst cases. This confirms once more that the strain-space formulation is equivalent to traditional plasticity.

4.2.3 Sensitivity of Results to Mesh Characteristics

A word of caution is in order concerning these numerical solutions. The fact is that they depend strongly upon the characteristics of the finite element mesh. To illustrate the point, the problem was worked again, this time just in strain space, using an elliptical half-mesh similar that of Figure 4.18(a). The depth of the soil medium is again 30 units and the half-width is approximately the same this time. The remote boundary is assumed now to be pinned.

The load-settlement curves for the two meshes are shown in Figure 4.14. The elliptical mesh predicts an elastic stiffness 1-1/2 times as great as the rectangular mesh. It is true that the elliptical domain is smaller, but only modestly so. The use of a pinned boundary is also significant, evidently. The plastic solutions differ even more markedly from one another. Although they both overshoot Prandtl's limit load (4.4), the one associated with the elliptical mesh does better. This is apparently because the elliptical mesh is more refined in the region where plastic slippage occurs.

This sensitivity to mesh design cannot be ignored, but neither should it be blown out of perspective. The main point of Section 4.2, after all, was to demonstrate the equivalence of stress- and strain-space plasticity for a model problem. This goal was fully realized.

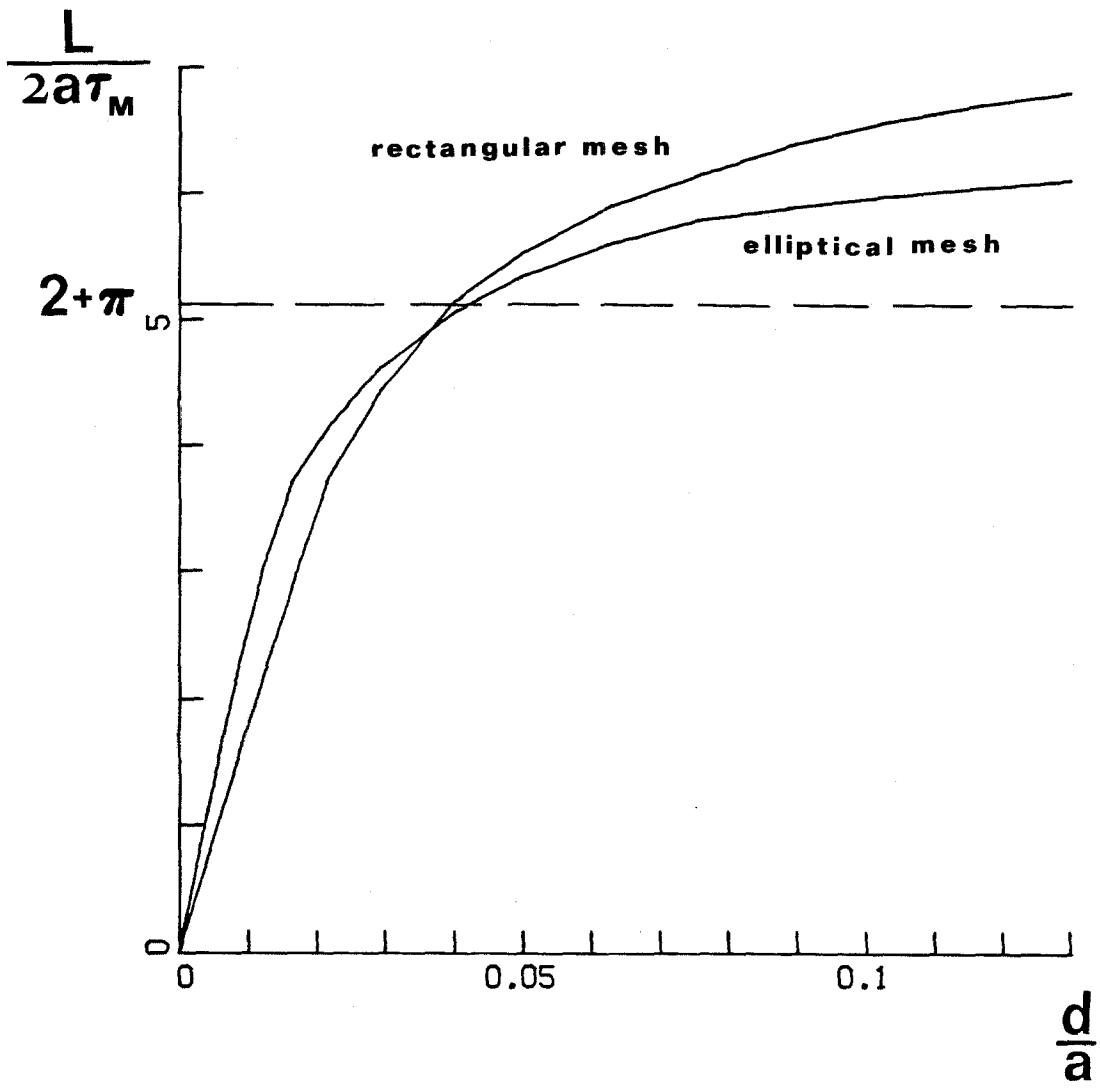

Figure 4.14 Load-settlement curves, generated with two different meshes.

If the elastic solution happens to be sensitive to a remote boundary, so be it. The problem itself is responsible for this difficulty, not the solution technique. The obvious remedy is to turn to a less singular model problem. The spurious limit loads, though, demand more serious consideration. Accordingly, in Section 4.3.3, the question of how finely to subdivide the plastic zone will be reopened.

4.3 An Example Problem: The Rocking Foundation

Consider now the problem of a rocking foundation. One strategy common in the design of tall buildings is to excavate enough soil from under the footings to make the entire structure neutrally buoyant, or nearly so. When such a building is rocked by an earthquake or windstorm, a more or less pure moment is transmitted to the foundation. The effect of gravity is negligible in such a case. Accordingly, throughout this section the foundation problem will be modified to accommodate applied moments but neglect vertical loads. This is depicted schematically in Figure 4.15.

Although the phenomena motivating this investigation are transient by nature, a fully transient analysis would lead to troublesome side issues. To see how this comes about, recall that in the last section it was necessary to replace the infinite domain by a finite one. This gave rise to a somewhat arbitrary, remote boundary. In transient problems such boundaries tend to set up spurious resonances. What one needs is a boundary that will absorb incoming waves rather than reflecting them. Cohen [23] has pursued this idea at considerable length and with some success. However, in the present investigation this issue

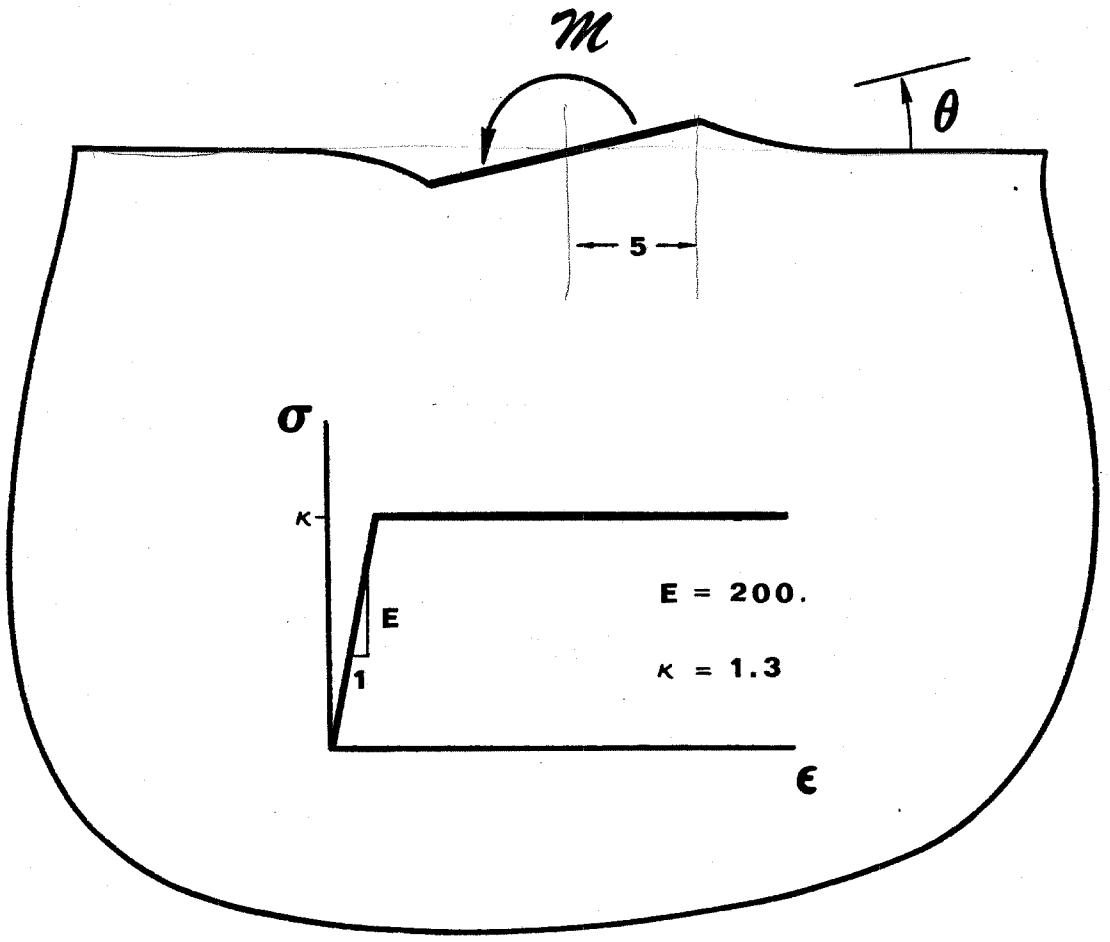

Figure 4.15 The rocking foundation.

will be sidestepped by remaining with quasi-static analysis.

In dealing with the rocking foundation, the first step is to look at relevant analytical solutions. Then, enlisting the help of the finite element program, the next stage is to test the effects of (i) the size of the numerical domain; (ii) the level of mesh refinement; and (iii) the number of yield surfaces used.

4.3.1 Analytical Solutions

Consider first the analytical solution corresponding to an elastic medium. For the rocking foundation the displacements are well-behaved, falling off in the far field as one over the distance from the foundation. Accordingly, Muskhelishvili [21] is able to derive a relation between the applied moment M and the angle of tilt θ. (See his Section 114.) In the incompressible limit this relation simplifies to

$$M = \frac{\pi}{3} E a^2 \theta \tag{4.5}$$

where, again, a is the half-width of the foundation.

Now let the soil be replaced by a rigid-perfectly plastic medium. Although textbooks on plasticity seldom examine this problem, it is easily solved. Let plastic slip be incipient everywhere under the foundation, with one stress state prevailing on the right side and the negative of it on the left. Assume, moreover, that the applied moment arises from normal tractions of magnitude σ. Then,

$$M = 2 \int_0^a \sigma x dx = \sigma a^2 \quad , \tag{4.6}$$

and the slip lines form a fan, as shown in Figure 4.16(a). Part (b) of the figure depicts the Mohr's circles corresponding to the stress at stations 1 and 2. Each circle has radius τ_M, the shear strength of the medium. The slip line running from 1 to 2 turns through an angle of $\frac{\pi}{2}$, so the centers lie a distance $(2)(\tau_M)(\frac{\pi}{2})$ apart. (See, for instance, Calladine [24], section 8.1.) Therefore, as can be seen from Figure 4.16(b),

$$\sigma = (1 + \tfrac{\pi}{2})\tau_M \quad . \tag{4.7}$$

Eliminating σ between (4.6) and (4.7), one concludes that collapse will occur when

$$M = (1 + \tfrac{\pi}{2})a^2 \tau_M \tag{4.8}$$

This result, along with (4.5), gives a basis for evaluating the performance of the plasticity program.

4.3.2 Size of the Domain

In passing from analytical work to numerical, it is necessary to replace the semi-infinite domain indicated in Figure 4.15 by one that is finite. For the sake of economy the domain should be kept as small as possible. It is important to investigate, therefore, how the size of the numerical domain influences the solution.

Let the remote boundary have fixed boundary conditions. The initial slope of the moment-versus-tilt diagram will serve as a global indicator of the elastic response. This parameter is computed for five different domains, using a rectangular mesh similar to the half-mesh

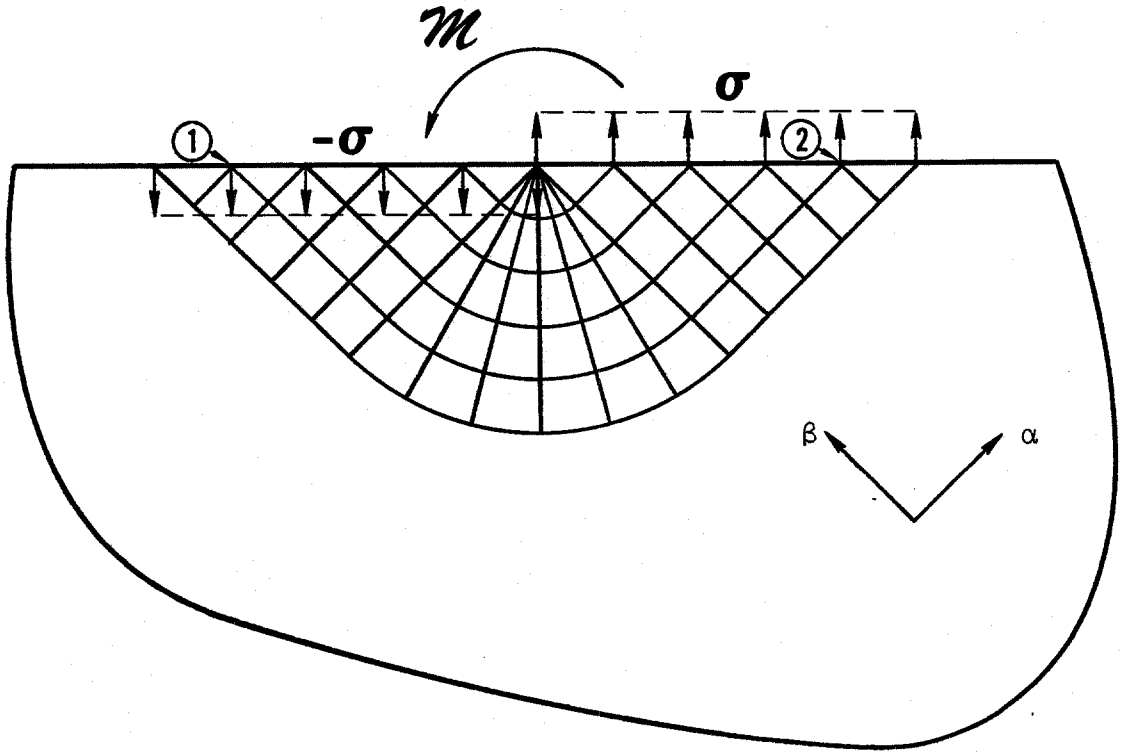

(a) The slip field.

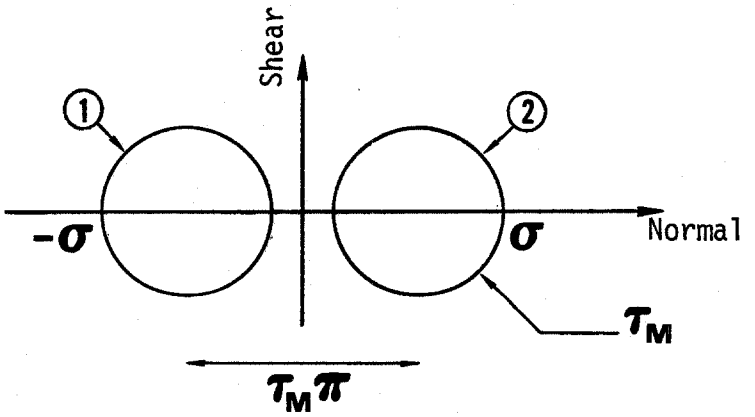

(b) The stress states at stations 1 and 2.

Figure 4.16 Slip-line solution for the rocking foundation.

shown in Figure 4.11. To reduce the size of the active domain, peripheral rows of nodes are simply pinned down. In each case, the horizontal distance from the edge of the foundation out to the boundary is kept roughly equal to the depth. The results are plotted in Figure 4.17, along with some others obtained from the elliptical meshes of Figure 4.18. As the size of the domain increases, the rotary stiffness approaches the value given in (4.5) for the half-space problem. The convergence becomes rather slow, though, once the error drops below ten percent.

The rectangular mesh proves unsatisfactory for plastic analysis because it is too coarse directly under the foundation. Accordingly, the three elliptical meshes shown in Figure 4.18 are introduced. Figure 4.19 shows the corresponding plots of moment versus tilt. Although the curves start off with different slopes, they all reach the same plateau. Evidently, the plastic contribution arises quite locally and is insensitive to the remote boundary.

4.3.3 Mesh Refinement in the Plastic Zone

The level of mesh refinement, though, has a more significant impact upon the plastic behavior. This, at any rate, held true for the vertically loaded foundation. To see whether it remains valid for the present problem, too, consider the three meshes shown in Figure 4.20. (Part (b) of the figure depicts the same mesh as Figure 4.18 (c).) The three have different levels of refinement but all cover the same domain. It was felt that the smallest of the domains from the last section would be adequate since the goal here is to study plastic behavior.

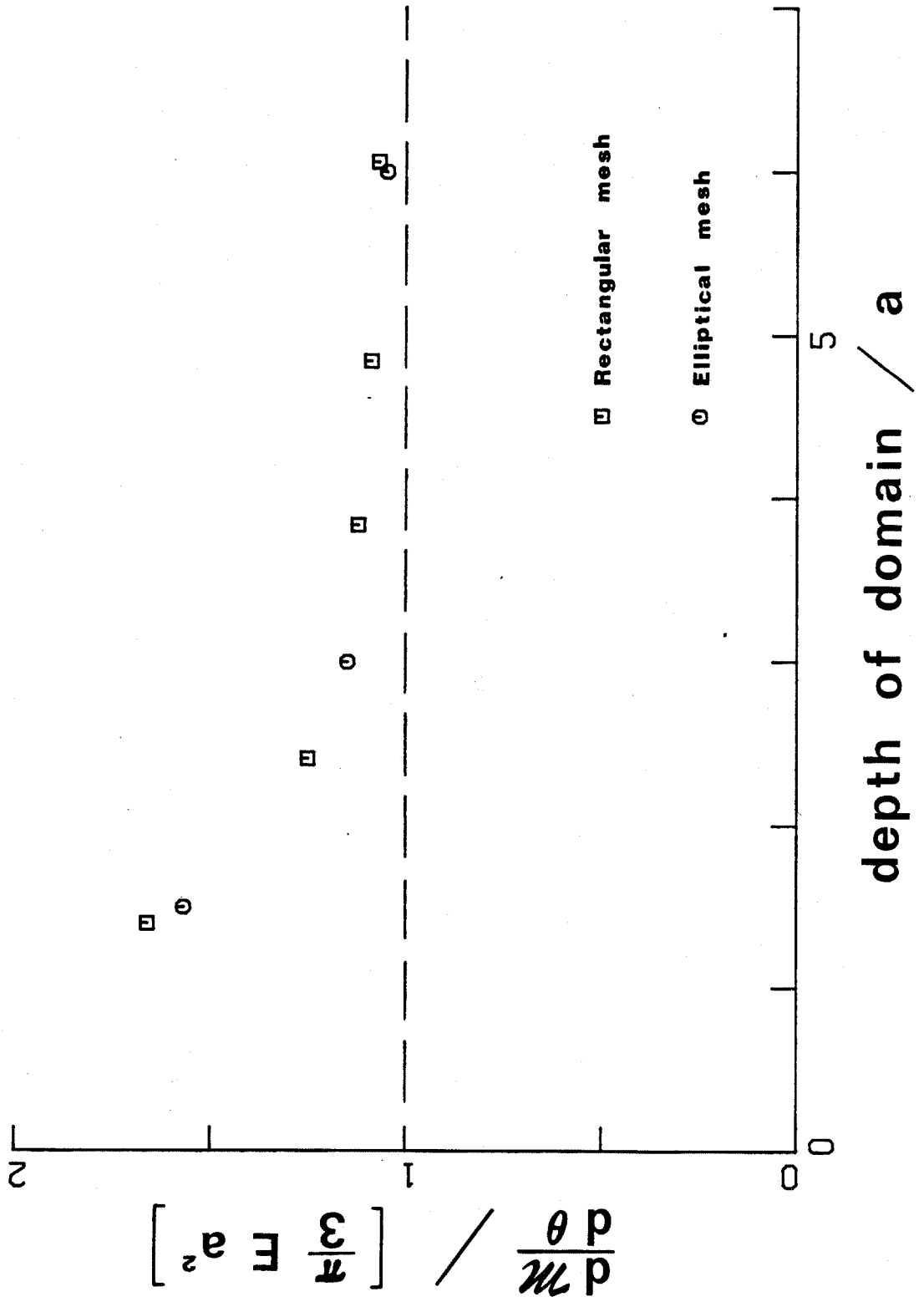

Figure 4.17 Elastic rotary stiffness versus depth of domain.

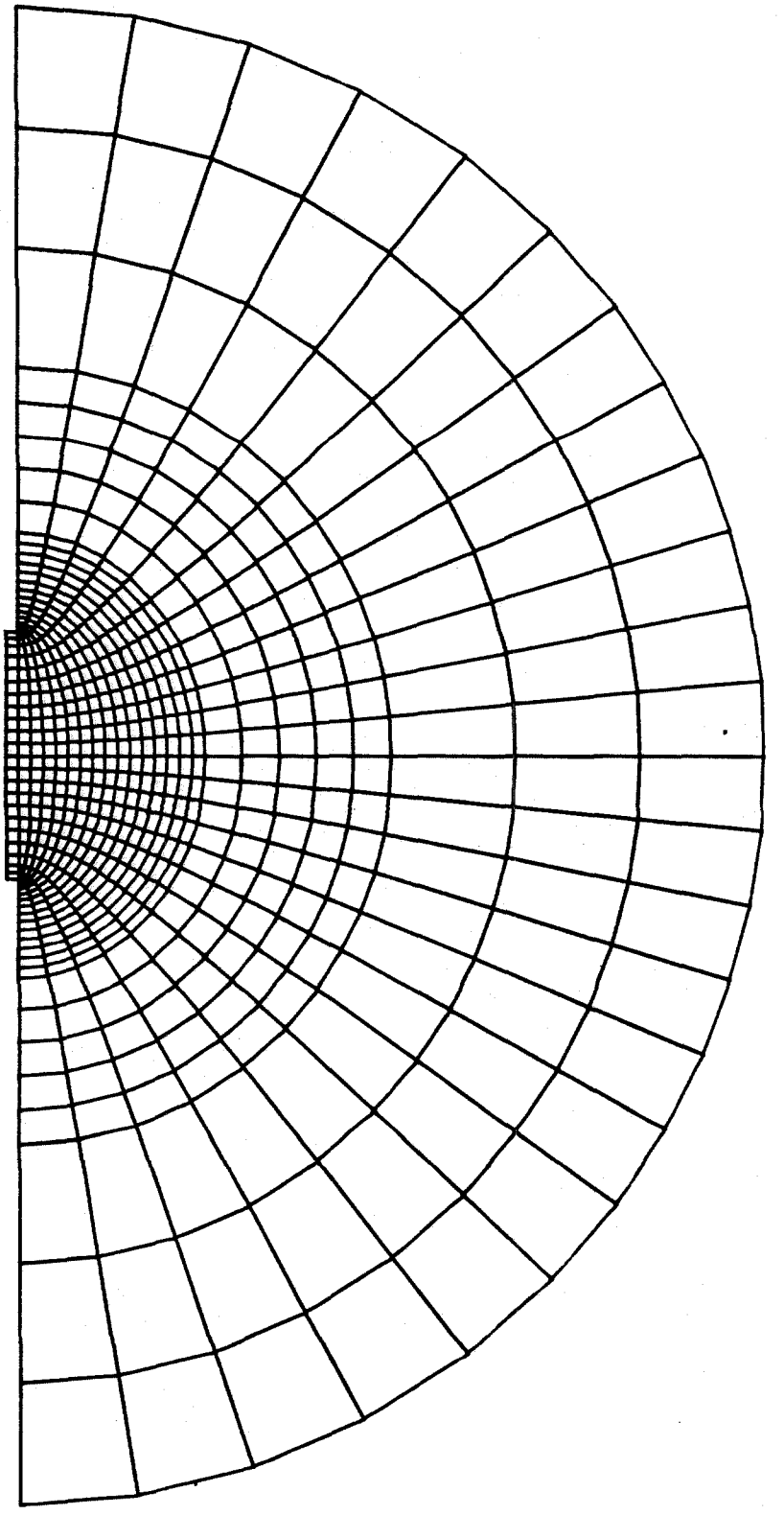

(a) depth = 30

Figure 4.18 Elliptical meshes

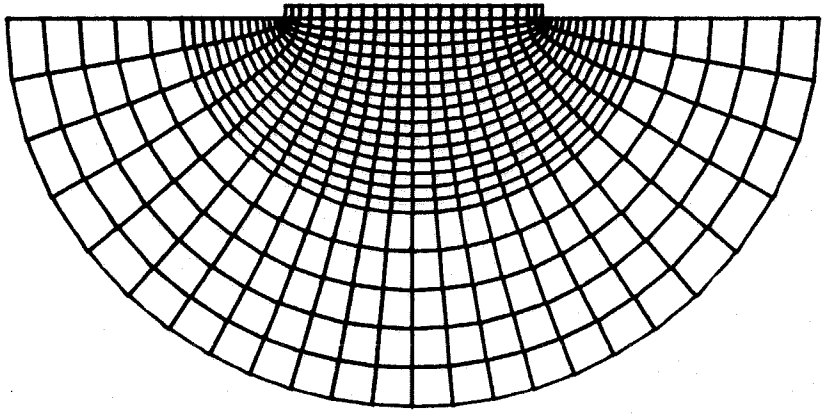

(b) depth = 15

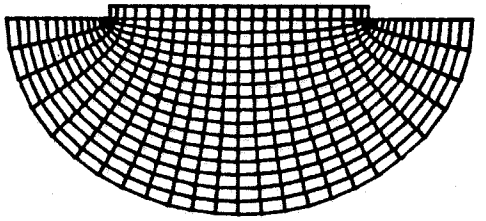

(c) depth = 7.5

Figure 4.18 (Continued) Elliptical meshes.

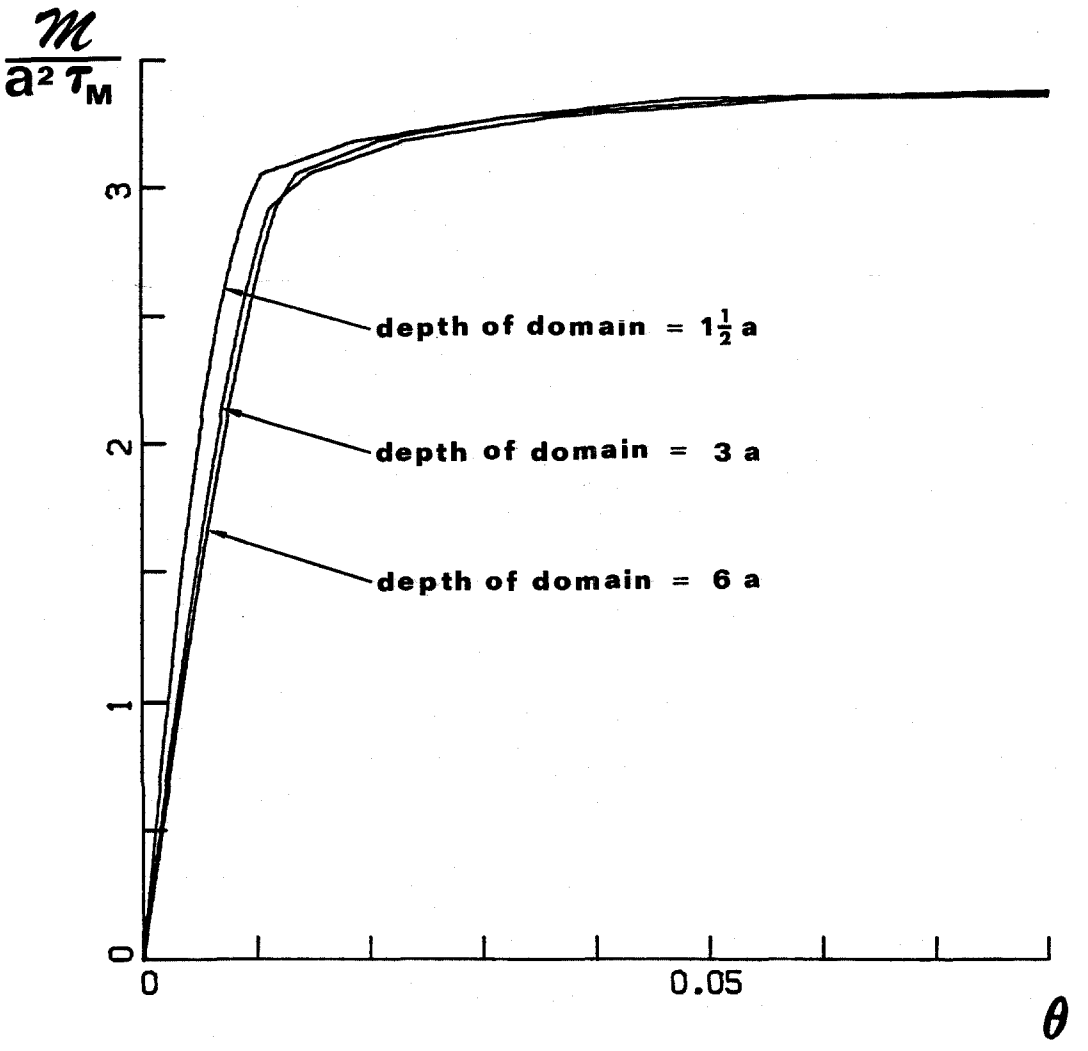

Figure 4.19 Moment-versus-tilt diagrams for three elliptical domains.

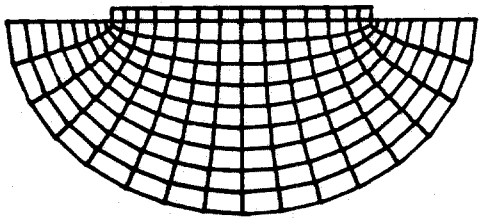

(a) 181 nodes

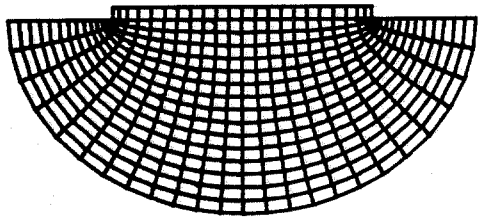

(b) 419 nodes

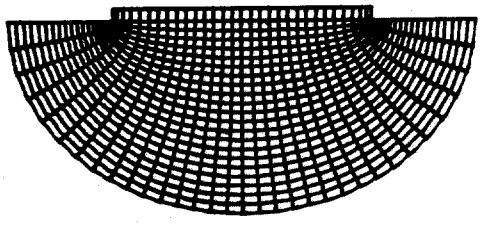

(c) 753 nodes

Figure 4.20 Three levels of refinement for the same domain.

Figure 4.21 gives the corresponding plots of moment versus tilt. It can readily be seen that greater refinement brings results that are closer to the slipline solution (4.8). The trend is in the right direction, but it is discouragingly slow. It would evidently take a very fine mesh to achieve good agreement with the analytical solution.

4.3.4 Multiple Loading Surfaces

One of the significant advantages of strain-space plasticity is that it readily generalizes to accommodate multilinear response curves. Before closing, therefore, it seems appropriate to investigate how significant this added capability might be. Toward this end, a three-surface constitutive model is introduced. As indicated in Figure 4.22, the initial stiffness and ultimate strength are the same as for the bilinear model, but the nonlinearities set in more gradually. Strains of five to ten percent were observed to be quite common in the plastic zone for the bilinear model, and this suggested the shape for the multilinear curve.

The mesh of Figure 4.18(a) was used, and the results are plotted in Figure 4.23. The moment-tilt curve is more rounded for the multilinear material, as could have been expected. Both curves reach plateaus above the slip-line solution, but the curve for the multilinear model comes closer to the mark. This suggests that some of the discrepancy between the curves arises from numerical errors and is spurious. Even so, the difference in global response seems great enough to warrant the use of multilinear models.

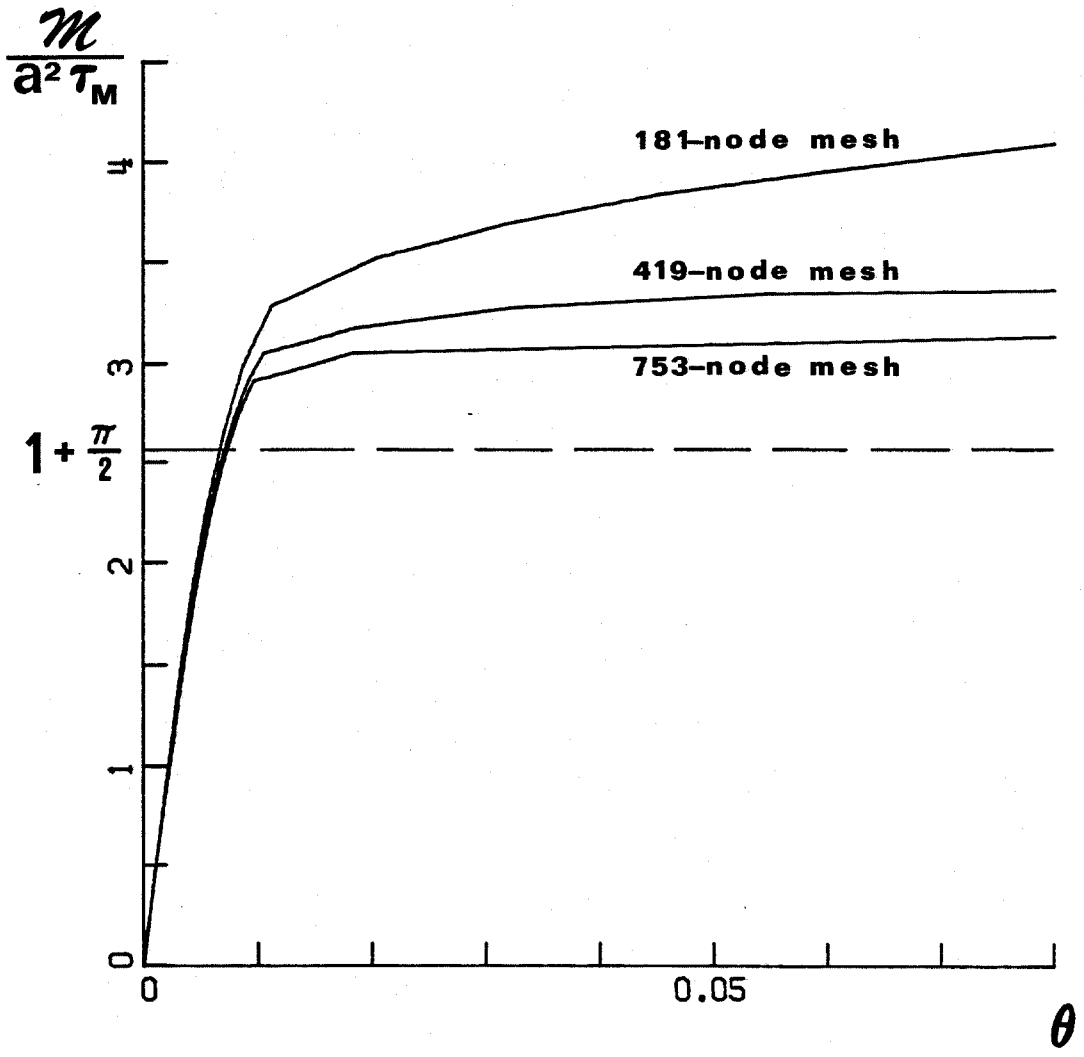

Figure 4.21 Moment-versus-tilt diagrams for three levels of refinement.

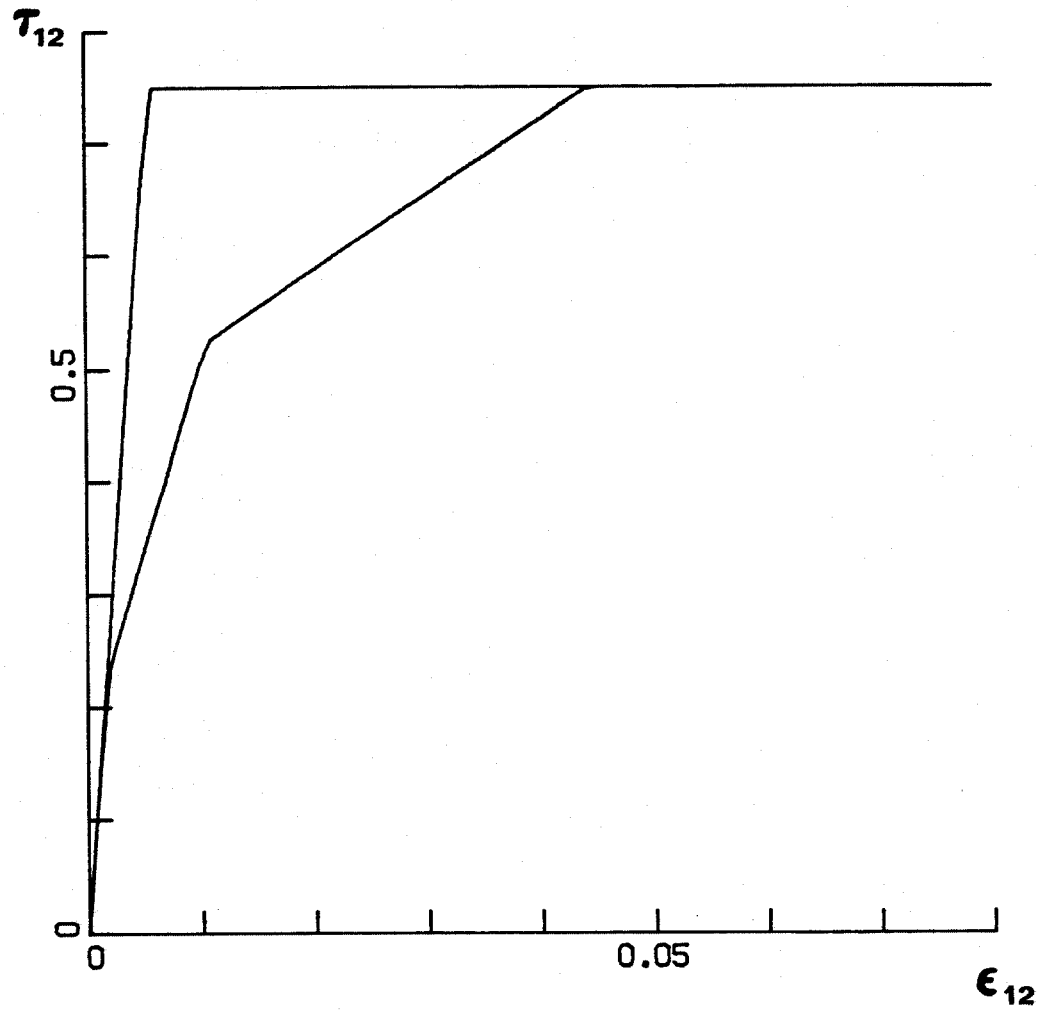

Figure 4.22 Two constitutive models

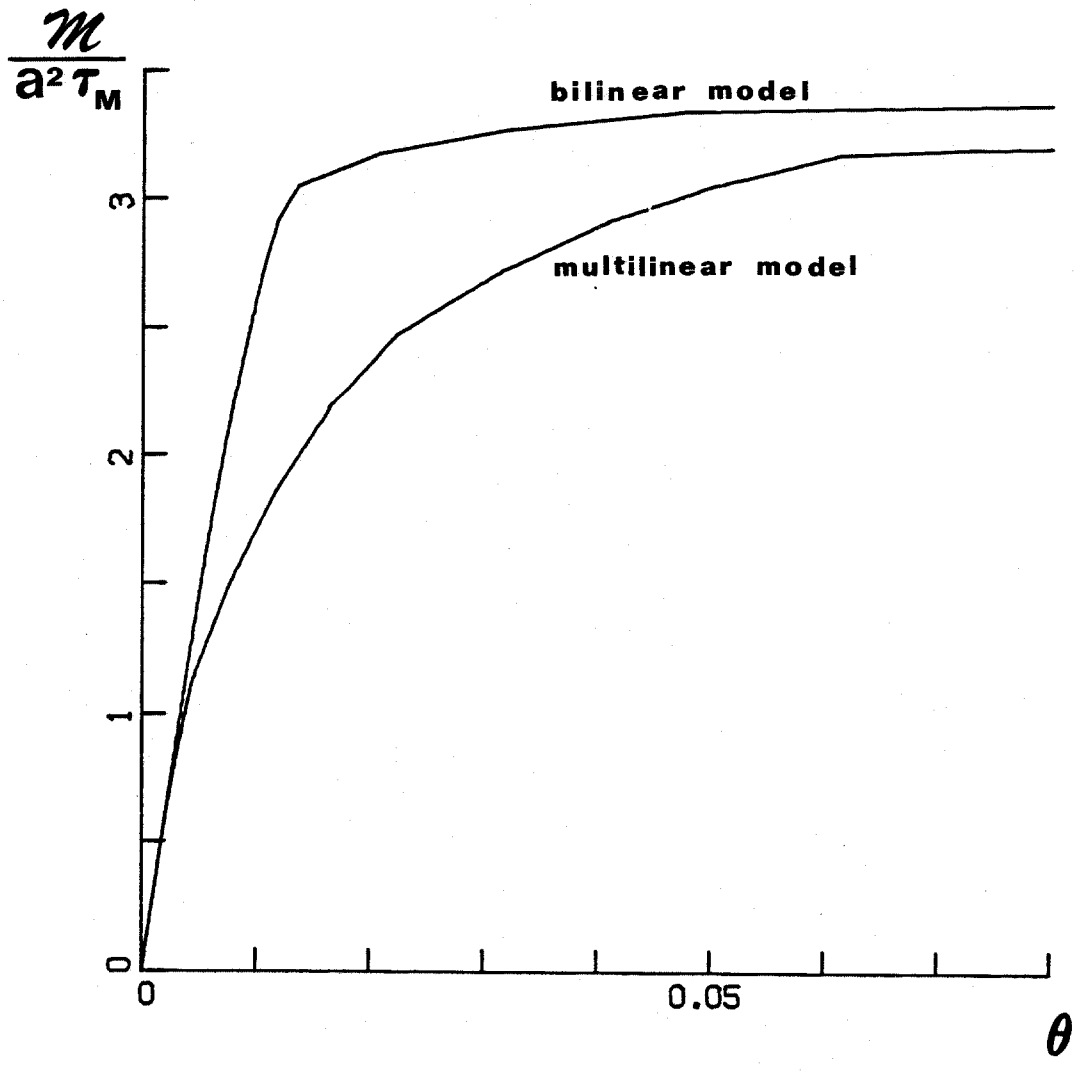

Figure 4.23 Moment-versus-tilt diagrams for two constitutive models.

4.4 Summary and Conclusions

The main objective in Chapter IV has been to demonstrate the potential for using strain-space plasticity in numerical applications. Toward this end, a package of constitutive subroutines was written and tested for accuracy. This package compares favorably with the competing stress-space algorithms. It offers better accuracy when dealing with perfect plasticity, and it generalizes much more readily to multilinear response curves.

The strain-space formulation does not, of course, cure every ailment associated with numerical plasticity. In particular, the limit loads still turn out too large, even when the mesh is quite refined. Evidently, the difficulty stems not from the constitutive subroutines but rather from the finite element method itself. Any system of discretization which entails averaging over finite regions of the domain will be hard pressed to accommodate localized slipping.

Despite this problem, numerical plasticity is widely used in situations where the geometry and the constitutive behavior just do not lend themselves to analytical methods. Thus, even a modest advance in the techniques for implementing plasticity should be welcomed by a wide range of investigators. It is believed that the strain-space subroutines described herein will adapt readily to interface with most any code designed to do nonlinear analysis.

CHAPTER V

CONCLUSIONS

A strain-space version of plasticity theory is herein delineated. It closely resembles the traditional formulation, but with the roles of stress and strain interchanged. Thus, the familiar von Mises and Tresca yield surfaces are replaced by strain-space counterparts which differ from them only in scale. These strain-space surfaces change size and/or position in accordance with hardening laws which likewise parallel the traditional ones from stress space. The loading criteria are identical in form to the conventional ones, but they involve the strain and strain increment in place of the stress and stress increment. Even the normality rule is carried over to strain space. The net result of all of these changes is a constitutive law expressing stress as a functional of strain, the preferred form for dynamics problems.

Somewhat surprisingly, perhaps, this strain-space formulation can be made equivalent to the traditional version. As a matter of fact, a single set of strain-space equations can accommodate the three cases of strain-hardening, ideal, and strain-softening plasticity. This contrasts markedly with the stress-space theory, within which ideal plasticity emerges as a singular case. One is obliged to deal with it specially, and the resulting formulation leads ultimately to numerical difficulties. In strain space, ideal plasticity is characterized by a loading surface that translates in the manner associated with Prager's kinematic hardening law. This model lends itself readily to numerical implementation.

One way to allow for a more general stress-strain curve is to introduce a plurality of loading surfaces. The most convenient approach, from a numerical standpoint, is to use uncoupled, strain-space surfaces. This leads very naturally to a constitutive law expressing stress as a functional of strain. Drucker suggested a model of this sort as early as 1950, and Iwan pondered the possibility while discussing one-dimensional parallel-series models. Yet, for want of a comprehensive treatment of strain-space plasticity, the idea has lain relatively dormant for thirty years.

More common in the literature are models featuring uncoupled, stress-space surfaces. Models of this sort characteristically give strain as a functional of stress and must somehow be inverted. It would be quite convenient if the aforementioned strain-space model turned out to be the desired inverse, as is true for the bilinear analog. However, this is, unfortunately, not the case. To reproduce the results given by a stress-space model with uncoupled surfaces, one would need a bizarre sort of kinematic hardening in strain space where the motion of each surface depends upon the plastic contributions from all the other surfaces. The most prudent course, it would seem, is to work exclusively with the uncoupled strain-space model and thereby avoid the problem of inversion.

Accordingly, it was decided to numerically code the strain-space formulation, incorporating a variable number of uncoupled, von Mises surfaces. This package of constitutive subroutines affords direct numerical confirmation that a strain-space model can match the results

of traditional plasticity. For perfect plasticity, in particular, a test of accuracy shows the strain-space package surpassing all three of the stress-space schemes outlined by Krieg and Krieg. As a further test, a simple boundary-value problem, depicting a gravity-laden foundation on a perfectly plastic earth, is solved via finite elements, using first the strain-space package developed herein and then a stress-space model written by Prévost and Hughes. The two solutions agree very well, both for loading and unloading.

The corresponding problem of a rocking foundation is next addressed. Since practical limitations rule out using a truly semi-infinite domain, it is of interest to see how the size of the elastoplastic medium influences the solution. The ultimate plastic limit turns out to be quite insensitive to domain size. Plastic slip is evidently a localized phenomenon, only mildly influenced by the global elastic solution. The plastic limit does, however, depend strongly upon the level of mesh refinement in the region of plastic slip. As the number of elements increases, the limit drops toward the slip-line solution with a rate of convergence that is frustratingly slow. Finally, the plastic limit is moderately influenced by the choice between a bilinear or multilinear constitutive model. The problem of exceeding the slip-line solution seems to be somewhat less severe for rounded response curves. This lends added significance to the quest for more accurate material models.

It is hoped that the development of multi-linear strain-space plasticity will advance this undertaking. Although infinitesimal deformations have tacitly been assumed throughout this thesis, it may be

useful to point out in this connection that the analytical results remain valid so long as the stress and strain tensors are symmetric. One way to enter the régime of finite deformations, therefore, is to let $\underset{\sim}{\varepsilon}$ be the Lagrangian strain and interpret $\underset{\sim}{\sigma}$ to be the symmetric Piola-Kirchhoff stress, as suggested by Naghdi. Only experiments, of course, can determine how well these assumptions model the behavior of real materials. In any case, the strain-space formulation promises great versatility, and the numerical implementation of it described herein should readily interface with a wide variety of nonlinear analysis programs.

APPENDIX I

THE NORMALITY RULE

Recall that Section 2.3.1 sidestepped mathematical details and offered just a heuristic derivation of the normality condition. It will be shown now that (2.15) follows rigorously from the postulates of that section.

A1.1 Notation

It is convenient in the work which follows to represent symmetric two-tensors by six-vectors. So, for every

$$\underset{\sim}{S} \in \text{sym}(\mathbb{R}) \text{ , having components } S_{ij} \text{ ,}$$

$$\text{let } \{S\} = \begin{Bmatrix} S_1 \\ S_2 \\ S_3 \\ S_4 \\ S_5 \\ S_6 \end{Bmatrix} = \begin{Bmatrix} S_{11} \\ S_{22} \\ S_{33} \\ \sqrt{2}\, S_{23} \\ \sqrt{2}\, S_{31} \\ \sqrt{2}\, S_{12} \end{Bmatrix} \tag{A1.1}$$

In particular (A1.1) will serve to introduce six-vector representations for $\underset{\sim}{t}$, $\overset{+}{\underset{\sim}{t}}$, $\overset{-}{\underset{\sim}{t}}$, $\underset{\sim}{\varepsilon}$, $\overset{+}{\underset{\sim}{\varepsilon}}{}^*$, $\overset{-}{\underset{\sim}{\varepsilon}}{}^*$, $\overset{S}{\underset{\sim}{\varepsilon}}$, $\underset{\sim}{d\sigma}^R$, and $\underset{\sim}{F\varepsilon}$. (The last of these denotes the tensor with components $\partial\hat{F}/\partial\varepsilon_{ij}|(\underset{\sim}{\varepsilon},\underset{\sim}{\sigma}^R,L)$.) Observe that if $\{r\}$ and $\{s\}$ are defined through (A1.1), then

$$r_{ij}s_{ij} = \{r\}^T\{s\} \ . \tag{A1.2}$$

It will be necessary at times to single out one component and treat it differently from the other five.

Lemma A1.1. Let $\hat{F}$ be a relaxation function satisfying (2.11); and let $\underset{\sim}{\sigma}^R \in \text{sym}\,(\mathbb{R}^3)$, $\underset{\sim}{\varepsilon} \in \text{sym}\,(\mathbb{R}^3)$, and $L \in \mathbb{R}$ satisfy

$$\hat{F}(\underset{\sim}{\varepsilon},\underset{\sim}{\sigma}^R,L) = 0 \quad . \quad . \tag{A1.3}$$

Then, there exists an integer I, $1 \leq I \leq 6$, such that

$$F_{\varepsilon I} \neq 0 \quad . \tag{A1.4}$$

Proof. The result follows immediately from (A1.1) and (2.11c). Q.E.D.

Accordingly, let

$$\Omega = \{i \,|\, i \text{ is an integer, } 1 \leq i \leq 6 \text{ , and } i \neq I\} \; ; \tag{A1.5}$$

$$\{S\}_5 = \text{the five-vector of components } S_i \ni i \in \Omega \quad . \tag{A1.6}$$

A1.2 Placing a Strain on the Surface Near $\underset{\sim}{\varepsilon}$

Consider now the implications of placing a strain $\overset{S}{\underset{\sim}{\varepsilon}}$ on the relaxation surface near $\underset{\sim}{\varepsilon}$. As long as $\overset{S}{\underset{\sim}{\varepsilon}}$ lies close enough to $\underset{\sim}{\varepsilon}$, the Implicit Function Theorem applies, and one arrives at

Lemma A1.2. Assume again that the hypotheses of Lemma A1.1 hold, and construct a strain state

$$\overset{S}{\underset{\sim}{\varepsilon}} = \underset{\sim}{\varepsilon} + \underset{\sim}{t} + n\, F\underset{\sim}{\varepsilon} \quad , \tag{A1.7}$$

fixed on the relaxation surface, where $\underset{\sim}{t}$ lies "tangent" to it at $\underset{\sim}{\varepsilon}$:

$$\hat{F}(\underset{\sim}{\varepsilon}^S, \underset{\sim}{\sigma}^R, L) = 0 \quad , \tag{A1.8}$$

$$\{t\}^T\{F_\varepsilon\} = 0 \quad . \tag{A1.9}$$

Let $\{u\}_5$ be any unit five-vector and h be positive and real. Then

$$\text{if} \quad \{t\}_5 = h\{u\}_5 \quad , \tag{A1.10}$$

$$\left.\begin{aligned} t_I &= \sum_{i\in\Omega}\left[-\frac{F_{\varepsilon i}}{F_{\varepsilon I}} + o(1)\right] hu_i \\ n &= o(h) \end{aligned}\right\} \text{as } h \to 0 \quad , \tag{A1.11}$$

where Ω is defined in (A1.5.)

Proof. Restating (A1.8) and (A1.9), with the help of (A1.7), (A1.1), and (A1.6),

$$\begin{aligned} F(\{t\}_5, t_I, n) &\equiv \hat{F}(\underset{\sim}{\varepsilon} + \underset{\sim}{t} + n\underset{\sim}{F_\varepsilon}, \underset{\sim}{\sigma}^R, L) = 0 \\ G(\{t\}_5, t_I, n) &\equiv \{t\}^T\{F_\varepsilon\} = 0 \end{aligned} \tag{i}$$

In view of (A1.3), (i), (A1.1), and (A1.6),

$$\begin{aligned} F(\{0\}_5, 0, 0) &= 0 \\ G(\{0\}_5, 0, 0) &= 0 \end{aligned} \tag{ii}$$

By virtue of (2.11b), (i), (A1.1), and (A1.6),

$$F, G \in C^1(\mathbb{R}^5 \times \mathbb{R} \times \mathbb{R}) \quad . \tag{iii}$$

Finally, by (A1.4), (i), (A1.1), and (A1.6), the Jacobian determinant

$$J = \left.\frac{\partial(F,G)}{\partial(t_I,n)}\right|_{(\{0\}_5,0,0)} = \begin{vmatrix} F_{\varepsilon I} & \{F_\varepsilon\}^T\{F_\varepsilon\} \\ F_{\varepsilon I} & 0 \end{vmatrix} \neq 0 \qquad \text{(iv)}$$

Statements (i), (ii), (iii), and (iv) meet the hypothesis of the Implicit Function Theorem. (The theorem can be found in any advanced calculus book; see, for instance, Taylor [25], Chapter 8.) Therefore, there exists a real constant $A > 0$ such that if

$$\|\{t\}_5\| < A \quad , \qquad \text{(v)}$$

then

$$\begin{aligned} t_I &= f(\{t\}_5) \\ n &= g(\{t\}_5) \end{aligned} \quad , \qquad \text{(vi)}$$

$$\begin{aligned} f(\{0\}_5) &= 0 \\ g(\{0\}_5) &= 0 \end{aligned} \quad , \qquad \text{(vii)}$$

$$f,g \in C^1 \quad , \qquad \text{(viii)}$$

and

$$\left.\frac{\partial f}{\partial t_i}\right|_{\{0\}_5} = -\frac{1}{J}\left.\frac{\partial(F,G)}{\partial(t_i,n)}\right|_{(\{0\}_5,0,0)}$$

$$\left.\frac{\partial g}{\partial t_i}\right|_{\{0\}_5} = -\frac{1}{J}\left.\frac{\partial(F,G)}{\partial(t_I,t_i)}\right|_{(\{0\}_5,0,0)} \qquad \text{(ix)}$$

$$\forall i \in \Omega \quad .$$

In view of (i) and (iv), (ix) yields

$$\left.\frac{\partial f}{\partial t_i}\right|_{\{0\}_5} = -\frac{F_{\varepsilon i}}{F_{\varepsilon I}} \quad , \quad \left.\frac{\partial g}{\partial t_i}\right|_{\{0\}_5} = 0 \quad \forall i \in \Omega \quad . \qquad \text{(x)}$$

Suppose now that (A1.10) holds, with $0 < h < A$, so that (v) is satisfied. Then (vi), (vii), and (viii) imply by Taylor's Theorem that

$$t_I = \sum_{i\in\Omega} \frac{\partial f}{\partial t_i}\bigg|_{\alpha h\{u\}_5} hu_i \quad ,$$

$$n = \sum_{i\in\Omega} \frac{\partial g}{\partial t_i}\bigg|_{\beta h\{u\}_5} hu_i \quad ,$$

where $0 < \alpha,\beta < 1$. By (viii),

$$\left.\begin{aligned} t_I &= \sum_{i\in\Omega}\left[\frac{\partial f}{\partial t_i}\bigg|_{\{0\}_5} + o(1)\right] hu_i \\ n &= \sum_{i\in\Omega}\left[\frac{\partial g}{\partial t_i}\bigg|_{\{0\}_5} + o(1)\right] hu_i \end{aligned}\right\} \text{as } h \to 0 \quad .$$

Substituting in (x), one obtains (A1.11), as required.

A1.3 The Normality Theorem

Recall now the scenario presented in Section 2.3.1. A material specimen is taken from an elastic strain state $\underset{\sim}{\varepsilon}^*$ to a state $\underset{\sim}{\varepsilon}$ lying on the relaxation surface, given a further strain increment $d\underset{\sim}{\varepsilon}$ which produces an increment of stress relaxation $d\underset{\sim}{\sigma}^R$, and then returned by way of $\underset{\sim}{\varepsilon}$ to $\underset{\sim}{\varepsilon}^*$. Three postulates come out of this conceptual experiment:

$$\max|d\varepsilon_{ij}| = O(\delta) \Rightarrow \max|d\sigma^R_{ij}| = O(\delta) \quad \text{as } \delta \to 0 \quad ; \tag{2.12}$$

$$d\underset{\sim}{\sigma}^R \neq f(\underset{\sim}{\varepsilon}^*) \quad ; \tag{2.13}$$

$$(\varepsilon_{ij}-\varepsilon^*_{ij})d\sigma^R_{ij} + O(\delta^2) \geq 0 \quad \text{as } \delta \to 0 \quad . \tag{2.14}$$

As shown in the theorem which follows, these three statements lead rigorously to the normality condition (2.15).

Theorem A1.1. Suppose that, in addition to the hypotheses of Lemma A1.1, statements (2.12), (2.13), and (2.14) hold. Then any stress relaxation increment $d\underset{\sim}{\sigma}^R$ arising at $\underset{\sim}{\varepsilon}$ will satisfy the normality condition (2.15).

Proof. The scheme of the proof is to consider pairs of strain states $\underset{\sim}{\varepsilon}^{*+}$ and $\underset{\sim}{\varepsilon}^{*-}$, which lie just inside the relaxation surface and to opposite sides of $\underset{\sim}{\varepsilon}$. Since the relaxation increment $d\underset{\sim}{\sigma}^R$ is insensitive to the recent elastic history, according to (2.13), statement (2.14) must hold for both members of a given pair. Moreover, the pairs themselves may be chosen rather arbitrarily, and this ultimately implies that $d\underset{\sim}{\sigma}^R$ has to lie normal to the relaxation surface. That $d\underset{\sim}{\sigma}^R$ points outward follows by considering a third $\underset{\sim}{\varepsilon}^*$ lying along the inward normal from $\underset{\sim}{\varepsilon}$.

Begin by choosing a pair of strain states, $\underset{\sim}{\varepsilon}^{*+}$ and $\underset{\sim}{\varepsilon}^{*-}$, just inside the relaxation surface and to opposite sides of $\underset{\sim}{\varepsilon}$. It will suffice, in view of Lemma A1.2, to select an arbitrary unit five-vector and set

$$\{t^{\pm}\}_5 = \pm h\{u\}_5 \quad , \tag{i}$$

$$\left.\begin{aligned} t_I^{\pm} &= \sum_{i\in\Omega}\left[-\frac{F_{\varepsilon i}}{F_{\varepsilon I}} + o(1)\right] t_i^{\pm} \\ n^{\pm} &= o(h) \end{aligned}\right\} \text{ as } h \to 0 \quad , \tag{ii}$$

and

$$\underset{\sim}{\varepsilon}^{*\pm} = \underset{\sim}{\varepsilon} + \underset{\sim}{t}^{\pm} + n^{\pm}\, F\underset{\sim}{\varepsilon} \quad . \tag{iii}$$

Clearly, for all six components

$$\varepsilon_i - \varepsilon_i^{\pm *} = \mp t_i^{+} + o(h) \quad \text{as } h \to 0 \ .$$

Thus, requiring that (2.14) hold for both $\overset{+}{\varepsilon}{}^*$ and $\overset{-}{\varepsilon}{}^*$ leads to

$$\mp \{\overset{+}{t}\}^T \{d\sigma^R\} + o(h\delta) + O(\delta^2) \geq 0$$
$$\text{as } h, \delta \to 0 \ .$$

Suppose, now, that $d\underset{\sim}{\varepsilon}$ (and therefore δ) tends to zero more rapidly than $\underset{\sim}{\overset{+}{t}}$ (and thus h). Then, retaining dominant terms,

$$\{\overset{+}{t}\}^T \{d\sigma^R\} = 0 \ .$$

Substituting from (i) and (ii) into the above and again retaining dominant terms,

$$\sum_{i \in \Omega} \left[- \frac{F_{\varepsilon i}}{F_{\varepsilon I}} d\sigma_I^R + d\sigma_i^R \right] u_i = 0 \ . \qquad \text{(iv)}$$

So far the analysis has singled out one choice for $\{u\}_5$ and worked with the strain states $\underset{\sim}{\overset{+}{\varepsilon}}{}^*$ and $\underset{\sim}{\overset{-}{\varepsilon}}{}^*$ corresponding to it. However, in view of Lemma A1.2 and (2.13), one could choose any unit five-vector for $\{u\}_5$ and still demand that (2.14) hold — and likewise equation (iv). It follows that for some $d\ell \in \mathbb{R}$,

$$d\sigma_{ij}^R = d\ell \left. \frac{\partial \hat{F}}{\partial \varepsilon_{ij}} \right|_{(\underset{\sim}{\varepsilon}, \underset{\sim}{\sigma}^R, L)} \qquad \text{(v)}$$

To resolve the sign of $d\ell$, consider an

$$\underset{\sim}{\varepsilon}^* = \underset{\sim}{\varepsilon} - a\underset{\sim}{F}_{\varepsilon} \quad , \quad a > 0 \quad . \tag{vi}$$

Substitute from (v) and (vi) into (2.14) and retain dominant terms to obtain

$$a \left.\frac{\partial \hat{F}}{\partial \varepsilon_{ij}}\right|_{(\underset{\sim}{\varepsilon},\underset{\sim}{\sigma}^R,L)} d\ell \left.\frac{\partial \hat{F}}{\partial \varepsilon_{ij}}\right|_{(\underset{\sim}{\varepsilon},\underset{\sim}{\sigma}^R,L)} \geq 0 \quad . \tag{vii}$$

In view of (vi) and (2.11c), (viii) establishes that $d\ell > 0$. This completes the proof of (2.15). Q.E.D.

REFERENCES

1. Joyner, W.B., "A Method for Calculating Nonlinear Seismic Response in Two Dimensions," Bulletin of the Seismological Society of America, Vol. 65, no. 5, Oct., 1975, pp. 1337-1357.

2. Hughes, T.J.R., and Prévost, J.H., "DIRT: A Finite Element Program for the Static Analysis of Nonlinear Anisotropic Elastoplastic Hysteretic Continua Subjected to Complicated Loading Paths," California Institute of Technology, May, 1977.

3. Kalev, I., and Gluck, J., "Finite Element Analysis for Cyclic Plasticity," Journal of the Engineering Mechanics Division ASCE, Vol. 103, no. EM1, Feb., 1977, pp. 189-201.

4. Prévost, J.H., "Mathematical Modelling of Monotonic and Cyclic Undrained Clay Behaviour," International Journal for Numerical and Analytical Methods in Geomechanics, Vol. 1, no. 2, Apr.-Jun., 1977, pp. 195-216.

5. Iwan, W.D., "On a Class of Models for the Yielding Behavior of Continuous and Composite Systems," Journal of Applied Mechanics ASME, Vol. 34, no. E3, Sept. 1967, pp. 612-617.

6. Mróz, Z., "On the Description of Anisotropic Workhardening," Journal of the Mechanics and Physics of Solids, Vol. 15, May, 1967, pp. 163-175.

7. Drucker, D.C., "Stress-Strain Relations in the Plastic Range: A Survey of Theory and Experiment," Office of Naval Research Contract N7 onr-358, Brown University, Dec., 1950.

8. Lenskii, V.S., "Analysis of Plastic Behaviour of Metals Under Complex Loading," Plasticity: Proceedings of the Second Symposium on Naval Structural Mechanics (ed. E.H. Lee and P.S. Symonds), Pergamon Press, New York, 1960, pp. 259-278.

9. Palmer, A.C., and Pearce, J.A., "Plasticity Theory Without Yield Surfaces," Proceedings of the Symposium on the Role of Plasticity in Soil Mechanics, Cambridge, 1973, pp. 188-200.

10. Naghdi, P.M., and Trapp, J.A., "The Significance of Formulating Plasticity Theory with Reference to Loading Surfaces in Strain Space," International Journal of Engineering Science, Vol. 13, no. 9/10, Sept./Oct., 1975, pp. 785-797.

11. Naghdi, P.M., "Some Constitutive Restrictions in Plasticity," Constitutive Equations in Viscoplasticity: Computational and Engineering Aspects, AMD, ASME, Vol. 20, 1976, pp. 79-93.

12. Drucker, D.C., "Some implications of Work Hardening and Ideal Plasticity," Quarterly of Applied Mathematics, Vol. 7, no. 4, Jan., 1950, pp. 411-418.

13. Prévost, J.H., "Plasticity Theory for Soil Stress-Strain Behavior," Journal of the Engineering Mechanics Division ASCE, Vol. 104, no. EM5, Oct., 1978, pp. 1177-1194.

14. Prager, W. "An Introduction to the Concepts and Principles of Plasticity," lectures delivered at the Seminar in Applied Mathematics, Boulder, Colorado, July, 1957.

15. Prévost, J.H., and Hughes, T.J.R., "Mathematical Modeling of Cyclic Soil Behavior," ASCE Earthquake Engineering and Soil Dynamics Conference, Pasadena, June, 1978.

16. Krieg, R.D., and Krieg, D.B., "Accuracies of Numerical Solution Methods for the Elastic-Perfectly Plastic Model," Journal of Pressure Vessel Technology ASME, Vol. 99, no. 4, Nov., 1977, pp. 510-515.

17. Christman, D.R., Isbell, W.M., Babcock, S.G., McMillan, A.R., and Green, S.J., "Measurements of Dynamic Properties of Materials, Volume III: 6061-T6 Aluminum," General Motors Technical Center, Warren, Michigan, Defense Nuclear Agency Contract Number DASA01-68-C-0114, 1971.

18. Yoder, P.J., "A Computational Algorithm Based upon Strain-Space Plasticity," Earthquake Engineering Research Laboratory, California Institute of Technology.

19. Maier, G., "Piecewiselinearization of Yield Criteria and Its Role in Structural Plasticity," International Symposium on Discrete Methods in Engineering C.I.S.E., Milan, Italy, Sept., 1974.

20. Prandtl, L., "Über die Härte Plasticher Koerper," Goettinger Nachr., Math. Phys. Kl., 1920. pp. 74-85.

21. Muskhelishvili, N.I., Some Basic Problems of the Mathematical Theory of Elasticity, P. Noordhoff, Ltd., Groningen, The Netherlands, 1963.

22. Lambe, T.W., and Whitman, R.V., Soil Mechanics, John Wiley and Sons, Inc., New York, 1969, pp. 195-196.

23. Cohen, M.F., Development and Study of Silent Boundaries for Dynamic, Soil-Structure Interaction Analysis, Ph.D. thesis, California Institute of Technology, 1981.

24. Calladine, C.R., Engineering Plasticity, Pergamon Press, Oxford, 1969.

25. Taylor, A.E., Advanced Calculus, Ginn and Co., Boston, 1955.